Neonatal and Juvenile Rats with Kaolin-induced Hydrocephalus: Pathogenesis and Treatments

By

Osaama Hassan Khan

A Thesis submitted to the Faculty of Graduate Studies

of the University of Manitoba

in partial fulfillment of the requirements of the degree

of

MASTER OF SCIENCE

Department of Pathology

University of Manitoba

Winnipeg

THE UNIVERSITY OF MANITOBA

FACULTY OF GRADUATE STUDIES

*****

COPYRIGHT PERMISSION

Neonatal and Juvenile Rats with Kaolin-induced Hydrocephalus: Pathogenesis and Treatments

BY

Osaama Hassan Khan

A Thesis/Practicum submitted to the Faculty of Graduate Studies of The University of Manitoba in partial fulfillment of the requirement of the degree

Of

MASTER OF SCIENCE

Abstract

Hydrocephalus is a pathological condition in which an abnormal amount of cerebrospinal fluid (CSF) accumulates in the ventricles of the brain. The goals of the experiments described in this thesis are to investigate the cellular and behavioral changes caused by hydrocephalus and to explore pharmacological interventions for neuroprotection. Several histological, immunological, and behavioral tests were applied to neonatal and juvenile Sprague-Dawley rats subjected to kaolin-induced hydrocephalus. Behavior studies showed signs of developmental delay, impaired gait, and impaired memory. Hydrocephalic animals characteristically had compressed cerebral cortex, decreased myelin content in corpus callosum and marked reactive astroglial change in white matter. Hydrocephalic neonatal rats had evidence of disrupted brain development. Histological evidence of hypoxic injury to oligodendrocytes, neurons and blood vessels suggests ischemia or oxygen radicals as a target for neuroprotection. Magnesium sulfate was mildly protective in the juvenile hydrocephalic rats, however neither it nor nimodipine (a calcium channel blocker) was of benefit in the neonatal pups. The use of adjunctive drug therapy seems to have potential and warrants further attention. These results provide insight regarding the mechanism of injury in the developing brain with concomitant hydrocephalus.

Acknowledgments

I would like to thank my graduate advisory committee, Drs Hugo Bergen and Yvonne Myal for their constructive suggestions and continued support. I gratefully acknowledge financial support from the Manitoba Institute of Child Health, the Manitoba Health Research Council, and the University of Manitoba.

I thank all the members of Dr. Del Bigio's lab from past and the present for their help and support. Very special thanks to Drs. Janani Balasubramaniam and Mengzhou Xue for showing me experimental procedures and for providing unconditional help both in the lab and with my other endeavors. Thanks to Terry Enno for teaching me endless skills in the lab and to Richard Buist for his assistance with the magnetic resonance imaging.

My warmest thanks go out to my supervisor Dr. Marc Del Bigio for accepting me into his lab and for providing the freedom to explore the world of basic medical science. I have always admired his work ethic and will try to implement this into my future career.

My family never hesitated to provide the best opportunities for the progress and success of their children. I am ever so grateful to their never-ending love and support. Daddy, you were defiantly my motivation, and I hope I can do the same for my children. Amera, I could not ask for a more perfect companion.

Table of contents

List of Tables

List of Figures

Chapter 2.3

Chapter 2.5

Abbreviations

ANOVA	analysis of variance
BS	*Bandeiraea* (Griffonia) *simplicifolia*
BSA	bovine serum albumin
° C	degrees Celsius
CBF	cerebral blood flow
CC	corpus callosum
CGalT	ceramide galactosyltransferase
CNP	2,3-cyclic nucleotide phosphodiesterase
CNS	central nervous system
CsA	cyclosporine A
CSF	cerebrospinal fluid
DA	dopamine
DAB	diaminobenzidine
DMSO	dimethyl sulfoxide
DOPAC	dihydroxy-phenylacetic acid
ECM	extracellular matrix
ELISA	enzyme linked immunosorbant assay
GABA	gamma-aminobutyric acid
GFAP	glial fibrillary protein
h	hours
H&E	hematoxylin and eosin

HIF	hypoxia inducible factor
HNE	4-hydroxy-2-nonenal
ICH	intracerebral hemorrhage
IVH	intraventricular hemorrhage
kg	kilogram
MBP	myelin basic protein
MR	magnetic resonance
MRI	magnetic resonance imaging
NE	norepinephrine
NMDA	N-methyl-D-aspartate
NOS	nitric oxide synthase
PBS(T)	phosphate buffered saline (toluene)
PDGF	platelet derived growth factor
PNPP	p-nitrophenylphosphorylcholine phosphocholine phosphodiesterase
RNA	ribonucleic acid
SEZ	subependymal zone
SOD	superoxide dismutase
SVZ	subventricular zone
TGF-beta	transforming growth factor-beta
U	units
UDP	uridine diphosphate galactose
VEGF	vascular endothelial growth factor
5-HT	serotonin

Chapter 1

General Introduction

Chapter 1 General Introduction

1.1 Introduction and definition of Hydrocephalus

Hydrocephalus, derived from the Greek words meaning "water-head", is a pathological condition in which abnormal amounts of cerebrospinal fluid (CSF) accumulate in the ventricles of the brain. The imbalance between CSF production and reabsorption in hydrocephalus is primarily due to obstruction of the subarachnoid space at either sites of CSF outflow (base of the brain) or sites of CSF absorption (subarachnoid granulations or lymphatics outside of the brain).

1.2 Hydrocephalus in the clinical setting

Hydrocephalus is the second most frequent congenital malformation (after spina bifida) of the nervous system, occurring in 5-6/10,000 live births [1]. It also develops in 80% of patients with spina bifida [2], and 15% of premature (<30 weeks) infants following intraventricular hemorrhage [3]. Hydrocephalus can develop later in childhood or adulthood as a consequence of brain tumors, meningitis, brain injury, or subarachnoid hemorrhage. The mainstay of hydrocephalus management is the use of silicone polymer tubes and valves to shunt excess CSF to other body cavities. This technique was commonly used beginning in the early 1960's [4].

1.3 Pathology and Pathogenesis of hydrocephalus

Brain injury due to hydrocephalus is multifactorial. Briefly summarized, the ependyma lining the ventricles is damaged. In the subependymal layer, reactive astrogliosis is almost always observed and mitotic activity occurs among subependymal cells [5]. Hydrocephalus can cause reduction in cerebral blood flow and alterations in oxidative metabolism in subcortical regions [6, 7] where white matter axons and myelin are the main target of damage in hydrocephalus [8, 9]. Many clinical studies demonstrate the presence of ischemia in hydrocephalic patients, however, the mechanism, its role and regional effects on the brain are not well understood. Microglia, the resident macrophages of the central nervous system, also play a role along with astrogliosis in contributing to white matter injury [10]. Imaging studies indicate that the brain is edematous in the periventricular region [11]. Severe hydrocephalus can cause thinning of the cerebral cortex and atrophy of the basal ganglia (2).

There are important differences between adult and pediatric hydrocephalus based upon brain development. The bones in the adult skull have fused at the suture sites and therefore does not allow for substantial increases in head volume compared to the pediatric skull. In humans, myelination in the cerebrum begins shortly after birth and continues until the end of the second decade [12, 13]. Hydrocephalus has been shown to disrupt myelination but is potentially reversible if shunting is instituted prior to axonal injury [14]. Hydrocephalus in preterm or immature brains (equivalent to less than 30 weeks

gestation) has not been well studied. This time period is when the brain has begun to prepare for myelination and glial cells (oligodendrocytes and astrocytes) are in a state of rapid cellular proliferation along the walls of the ventricles of the brain. Ventricular enlargement and gliosis (scarring) could hinder cell proliferation and migration of these important cells. More studies are needed to assess the effect hydrocephalus has on the maturing brain.

1.4 Animal models

To study the pathophysiology of hydrocephalic brain damage (in contrast to the causes of hydrocephalus), the experimental method of induction should cause the ventricles to enlarge but should not directly affect the brain, such as chemical, radiation and viral methods of inducing hydrocephalus. The range of species used includes mouse, rat, guinea pig, rabbit, cat, dog, pig [15], fetal lamb [16], and primates such as the Rhesus monkey (*Macaca mulatta)* [17, 18]. When choosing a model, several factors need to be addressed such as animal availability, the pathological aspects being explored, age, time-course of hydrocephalus, and the methods for assessing physical, behavioral, and/or biochemical changes [19, 20]. Unlike humans, rodents have only narrow layers of periventricular white matter and their brains are lissencephalic (i.e. no gyri), therefore there are limitations in the applicability of rodent models of hydrocephalus.

Animal models of hydrocephalus can be categorized into hereditary and mechanical. Hereditary models include hy3 mouse, hyh mouse, L1 CAM mouse, transforming growth factor -1 mouse, H-Tx rat, and the LEW/Jms rat. Mechanical models require the placement or injection of a foreign material that occludes CSF outflow. These include kaolin, fibroblast growth factor, silicone oil, cyanoacrylic gel, plugs (cotton, cellophane cylinder) and venous occlusion. For a more detailed description of these animal models see the Appendix (Experimental Models of Hydrocephalus), which was published as a book chapter.

1.5 Neuroprotection in hydrocephalus

Pharmacologic intervention

A variety of ineffective agents have been administered to hydrocephalic individuals for centuries (reviewed in [21]). These included purgatives such as rhubarb, jalop and calomel to strong iodine solutions injected into the ventricles. Drug therapy targeting CSF production was attempted in the 1950's. The choroid plexus epithelium releases sodium and bicarbonate to create an osmotic gradient that draws water into the ventricles. Carbonic anhydrase inhibitors (acetazolamide) [22] and furosemide (inhibits sodium reabsorption in renal tubules) [23] have the ability to affect fluid balances in the brain, however, recent randomized controlled trials have shown no benefit in children with post-hemorrhagic hydrocephalus [24, 25]. Isosorbide, an orally absorbed

hyperosmolar agent that is an anhydrate of sorbitol [26] was promoted by Lorber in the 1970's [27]. However, it has not been tested in a randomized controlled trial. Ouabain, a potent inhibitor of the Na^+-K^+-ATPase pump on cell membranes, has not been used for treatment of hydrocephalus because of its systemic toxicity [28]. More sophisticated immunotoxin approaches to choroid plexus destruction have recently been proposed [28].

The role of altered calcium homeostasis as a mechanism of brain injury has been demonstrated in the white matter of hydrocephalic rats [8]. Free calcium ions were detected in the damaged axons of the corpus callosum and proteolytic cleavage of calpain I (a non-lysosomal proteolytic enzyme) supported a role for calcium in the mechanism of axonal injury in hydrocephalus. Many different pathophysiological aspects of cell damage include influx of calcium as a final common pathway of cell injury and cell death. By using drugs that either block or decrease calcium release could potentially decrease cellular injury.

Goals and Hypotheses

Goal 1

To describe the behavioral changes and brain damage in rats with neonatal-onset hydrocephalus.

Hypothesis: Neonatal hydrocephalic rats will demonstrate similar brain injury and behavioral motor and memory deficits as seen in young and adult hydrocephalic rats.

(See Chapter 2.1)

Goal 2

To elucidate the mechanistic issues related to ischemia in neonatal and young hydrocephalic rats.

Hypothesis: Cellular markers of hypoxia will be evident in neonatal and young hydrocephalic rats.

(See Chapter 2.2)

Goal 3

To establish a means of pharmacological protection for neonatal and young rats with hydrocephalus.

Hypothesis: Chronic administration of drugs that affect calcium channels in the brain (magnesium salts, nimodipine, tacrolimus, or calpain inhibitor I) will

ameliorate the behavioral and structural abnormalities associated with severe early-onset hydrocephalus in rats.

(See Chapters 2.3, 2.4 and 2.5)

Chapter 2

Specific Experiments

Chapter 2.1

Brain damage in neonatal rats following kaolin induction of hydrocephalus.

This section was published in Experimental Neurology 2006 August; 200 (2): 311-320

Authors: Osaama H. Khan, Terry L. Enno and Marc R. Del Bigio

Note: Behavioral and immuno-histological experiments completed by Osaama Khan. Biochemical assays were performed by Terry Enno

ABSTRACT

Neonatal and congenital hydrocephalus are common problems in humans. Hydrocephalus was induced in 1-day-old rats by injection of kaolin into the cisterna magna. At 7 and 21 days, magnetic resonance (MR) imaging was used to assess ventricle size, then brains were subjected to histopathological and biochemical analyses. Hydrocephalic pups did not exhibit delays in righting or negative geotaxis reflexes during the first week. At 7 days, there was variable ventricular enlargement with periventricular white matter edema, axon damage, reactive astrogliosis, and accumulation of macrophages in severe but not mild hydrocephalus. Cellular proliferation in the subependymal zone was significantly reduced. The cortical subplate neuron layer was disrupted. In rats allowed to survive to 21 days, weight was significantly lower in severely hydrocephalic rats. They also exhibited impaired memory in the Morris water maze test. Despite abnormal posture, there was minimal quantitative impairment of walking ability on a rotating cylinder. At 21 days, histological studies showed reduced corpus callosum thickness, fewer mature oligodendrocytes, damaged axons, and astroglial/microglial reaction. Reduced myelin basic protein, increased glial fibrillary acidic protein, and stable synaptophysin content were demonstrated by immunochemical methods. In conclusion, impairment in cognition and motor skills corresponds to ventricular enlargement and white matter destruction.

Quantitative measures of weight, memory, ventricle size, and myelin, and glial proteins in this neonatal model of hydrocephalus will be useful tools for assessment of experimental therapeutic interventions.

INTRODUCTION

Hydrocephalus is a common neurological condition of childhood characterized by dilation of the cerebral ventricles, usually caused by obstruction of cerebrospinal fluid (CSF) flow. Axon damage in the periventricular white matter is one of the earliest pathological consequences of ventricular dilation in humans and animals [29] and can account for many of the behavioral deficits [9]. The pathophysiology of hydrocephalus-induced brain damage is multifactorial, with contributions made by gradual physical stretching and compression of brain, ischemia with calcium mediated axoskeletal damage, and possible accumulation of metabolic waste products [29-31]. Infantile hydrocephalus results from congenital brain malformations, intraventricular hemorrhage (IVH), and meningitis. The former can be modeled with H-Tx rats [32] or mutant mice [33]. Post-IVH hydrocephalus can be created by double intraventricular blood injection in 7-day-old rats [34], although in our experience with neonatal rodent models of periventricular hematoma, severe hydrocephalus is a relatively uncommon occurrence [35]. The subarachnoid scarring of post-meningitis or post-hemorrhagic hydrocephalus can be modeled by kaolin injection [20]. The postnatal 21-day rat corresponds roughly to a 6-month human infant with regard to brain development during which time cerebral myelination is developing rapidly [36, 37]. Induction of hydrocephalus at this age is associated with delayed myelination in subsequent 1–4 weeks, which can be prevented by early

diversionary shunting of CSF [14, 38]. The model has been used to test drug protection [39-41]. Most studies of early onset hydrocephalus, corresponding to fetal-onset or premature infant-onset hydrocephalus in humans, have been conducted in the mutant H-Tx rat model, in which the ventricles begin to dilate shortly before birth [32, 42]. Because there remain some uncertainties about the genetic explanations for brain maldevelopment in that model [43-45] and because hydrocephalus in premature human infants is of various etiologies, we wanted to characterize in detail early onset hydrocephalus in neonatal rats using a non-genetic model [20]. Only a few publications concerning this model exist [46-49]. Our goal is to describe in detail the sensorimotor, anatomical, histological, and biochemical alterations with respect to postnatal brain development. We hypothesized that early onset hydrocephalus in rats will be associated with delay in sensorimotor development and white matter damage that is dependent on ventricle size.

METHODS

All animals were treated in accordance with guidelines set forth by the Canadian Council on Animal Care. The local animal use committee approved the experiments. All efforts were made to minimize suffering and the number of animals used.

Animal preparation

Sprague–Dawley rats were bred locally, and 9 litters (10–12 pups per litter) including 98 pups were used. Before kaolin induction, each litter was designated for euthanasia at 7 or 21 days, dictated by tissue needs and availability of the MR imaging system. Rats were placed on aluminum foil over ice for cold anesthesia on postnatal day 1. The neck was wiped with ethanol, and under aseptic conditions, a 28-gauge needle was inserted percutaneously into the cisterna magna (n = 70). Sterile kaolin suspension (0.02 ml; 250 mg/ml in 0.9% saline) was injected slowly to induce hydrocephalus. The pups were returned to their mothers after rewarming. They were housed in standard cages and provided with a normal 12-h day/night lighting schedule with free access to water and pellet food. For identification, numbers were marked on the backs with permanent marker and ear punches were made at 7 days. Along with the hydrocephalics, 8 intact controls and 3 sham-injected rats were studied at 7 days and 12 intact controls and 5 sham-injected rats were studied at 21 days.

Magnetic resonance imaging

Magnetic resonance (MR) studies were performed at 7 or 21 days using a Bruker Biospec/3 MR scanner equipped with a 21-cm bore magnet operating at a field of 7 T (Karlsruhe, Germany) to obtain T2-weighted images of the brain in the

coronal plane (slice thickness 0.5 mm) [14, 38]. When possible, as dictated by availability of the imaging system, rats destined for 21-day survival were also imaged at 7 days. The areas of the lateral ventricles and cerebrum were measured (by computerized planimetry using locally developed software) in the rostral cerebrum at the level of the optic chiasm. Frontal horn size was expressed as a ratio determined by dividing the total area of the ventricles by the area of the cerebrum. Rats were categorized as having either mild or severe ventriculomegaly using a cut-off ratio of 0.25. This value was chosen after analyzing all images because it allowed division into two roughly equal groups for statistical comparisons. For logistical reasons, one 21-day-old pup used for behavioral and biochemical analyses did not have a final MR image, but at brain removal, the ventricles were grossly enlarged. Behavioral assessment

Rats were weighed on days 7, 12, 14, 19, 20, and 21. To study early sensorimotor development, the following outcome measures were examined: ambulatory behavior, righting response, and negative geotactic reactions. These tests were previously validated [50]. The rats were always tested in the same order. Each of these tests was completed in triplicate and averaged. Observing the pups for directed head and forelimb movements on postnatal days 4–7 assessed early ambulatory behavior. Righting response was assessed on day 7 by placing a pup on its back and timing how long it took for it to return to prone position. Negative geotaxis was also assessed on day 7. Pups were placed on a 35° incline plane with head facing down the plane. The maximum time it took for

the pup to turn around 180° so that head was facing up the plane was recorded. On postnatal days 10, 14, 17, and 20, forelimb grip strength was tested by timing the rats' ability to hang from a 1.5-mm diameter wire, elevated 40 cm above a soft sponge. The maximal time allotted was 12 s. Gait agility was assessed on day 20 using a rotating cylinder (diameter 8 cm; Economex, Columbus Instruments) in two separate trials. First, endurance was assessed at a constant speed of 5 revolutions per minute (rpm) for a maximum of 2 min. Second, we measured ability to stay on the cylinder while it accelerated at a rate of 0.1 rpm every second for up to 2 min. The outcome measures and testing protocols for rotating cylinder are the same as those described in juvenile rats with hydrocephalus [39-41]. Finally, on day 20, after each pup had completed the rotating cylinder test, swimming speed was measured in a 20-cm-deep, 1.5-m straight channel; the rats performed three trials, separated by a 30-s rest. Learning and memory were assessed using the modified Morris water maze test in a 90-cm pool filled with 22°C water and containing a 13-cm round hidden platform as previously described [14, 38, 51]. Testing was done in a dimly lit room with a single wall illuminated to provide directional cues. Rats were placed in the center of the pool and allowed to swim until they found the platform. A trial consisted of four attempts to find the platform, each attempt beginning with the rat facing a different quadrant. If the rat failed to complete the task in 60 s, it was given a 30-s rest on the platform before the next attempt. Three trials were performed during the course of the day. The time of the four attempts was

averaged for each trial. We only had sufficient rats in the severe hydrocephalus category for valid statistical analysis.

Histopathological and biochemical studies

Rats were euthanized on day 7 or 21 by overdose with pentobarbital, the vasculature was flushed by transcardiac perfusion with ice-cold 0.1M phosphate-buffered saline and the brains were removed. Samples of the left parietal cerebrum, left frontal cerebrum (both including periventricular tissues), and left hippocampus were dissected and frozen in liquid nitrogen, after which they were stored at −80°C. As described previously in detail [14, 38], frontal cerebrum homogenates were used to biochemically quantify enzymatic activity of 2,3-cyclic nucleotide phosphodiesterase (CNPase, a marker of oligodendroglia and immature myelin) [52], p-Nitrophenylphosphorylcholine phosphocholine phosphodiesterase (PNPP, a marker of myelin and oligodendrocytes) [53, 54], and UDP galactose: ceramide galactosyltransferase (CGalT, a marker of active myelin production by oligodendrocytes) [55, 56]. Enzyme-linked immunosorbent assays (ELISA) developed locally were used to measure the quantity of myelin basic protein (MBP), glial fibrillary acidic protein (GFAP), and synaptophysin. The cerebrum sample was weighed and homogenized in RIPA buffer with proteolytic inhibitors, three times volume to weight. Following two centrifugations at 15,000×g for 30 min at 4°C, the clarified supernatant was frozen in aliquots with

one aliquot used for a protein assay. Wells of 96-well ELISA plates were coated with 100 µl/well of 1 µg/ml polyclonal rabbit anti-human myelin basic protein (MBP) (DAKO, A0623), 1 µg/ml polyclonal rabbit anti-cow glial fibrillary acidic protein (GFAP) (DAKO cat # Z0334), or 4 µg/ml polyclonal rabbit anti-human synaptophysin (DAKO cat #A0010), overnight at 5°C. Washed plates were blocked with 100 µl/well of 5% skim milk powder in PBS for 1 h at room temperature and washed with 0.1 M phosphate-buffered saline with 0.5% Triton (PBST). The bovine MBP standards ranged from 15, 50, 100, 200, 300, 400, to 500 ng/ml (M1891, Sigma). Porcine GFAP standards ranged from 1, 15, 25, 50, 75, 100, to 125 ng/ml (Chemicon AG230). The synaptophysin standards ranged from 0.5, 2.5, 5.0, 10, 20, 30, to 40 ng/ml (recombinant synaptophysin fragment a gift from Dr. Charles White III)[57]. For MBP assay, the samples were diluted to 7.5, 12.5, and 17.5 µg protein/ml, for GFAP assay, the samples were diluted to 5, 15, and 30 µg/ml, and for synaptophysin assay, the samples were diluted to 30, 40, and 50 µg/ml (dilutions were based on pilot experiments to fall within the standard curve). Standards and samples on plates were incubated 1 h at room temperature. Mouse anti-human monoclonal MBP antibody (US Biological, M9758-01) diluted to 1:500, anti-human monoclonal GFAP (Chemicon cat #MAB360) diluted to 1:5000, or anti-human monoclonal synaptophysin (Serotec MCA 1307) diluted to 1:1000 in 5% skim milk/PBST was applied 100 µl/well for 1 h at room temperature. After washing, alkaline-phosphatase-conjugated goat anti-mouse antibody (Cedarlane/Biocan, 115-055-146) diluted to 0.5 µg/ml in 5%

skim milk/PBST was applied 100 µl/well for 1 h at room temperature. Plates were washed again, and phosphatase substrate (100 µl/well, Pierce, 37620) was applied in the dark for 30 min at room temperature. The reaction was stopped with 50 µl/well of 2 N NaOH, and plates were read at 405 nm absorption with a microplate reader (Corona). Controls without antigen were measured to determine the background. Two or three replicated studies were performed to ensure reproducibility and allow meaningful statistical analysis. Western blots for MBP, GFAP, and synaptophysin were performed using the same antibodies.

For histological analysis, the right cerebrum was immersion fixed in 10% buffered formalin. Coronal slices were embedded in paraffin. Sections (6 µm thickness) at the level of the optic chiasm were stained with hematoxylin and eosin as well as solochrome cyanine for visualization of myelin. Corpus callosum thickness was measured in the midline and adjacent to the cingulum. Fluoro-Jade B staining was used to show dying neurons and damaged axons [58] by incubating sections in 0.06% potassium permanganate for 15 min while gently shaking on a rotating platform. Then, 0.001% Fluoro-Jade (Histo-Chem Inc.; Jefferson, AR) staining solution was applied for 30 min followed by washing, drying, and coverslipping. Immunohistochemical methods were used to detect reactive astrocytes (GFAP, 1:500 dilution; DAKO), myelinating immature/mature oligodendrocytes (transferrin, 1:1000; Cappel), intermediate filaments of axons (pan-neurofilament, 1:1000, SMI-32; Sternberger), and proliferating cells in all active phases of cell cycle (Ki-67, 1:500; Novacastra Laboratories Ltd). Microwaving in 0.6 M citric

acid buffer for 20 min facilitated antigen exposure for Ki-67 labeling. Primary antibodies underwent overnight incubation followed by detection with Cy3-conjugated fluorescent secondary antibody. Activated microglia were detected histochemically with lectin from Bandeiraea simplicifolia (BS; 1:100; Sigma). BS was detected with streptavidin horseradish peroxidase followed by diaminobenzidine (DAB). Negative controls were processed without the primary antibody. In seven defined anatomical regions, we counted Ki-67 positive cells at 400× magnification. We then counted the number of bisbenzimide-labeled nuclei in the same area and calculated the proportion of Ki-67 positive cells. The areas included the dorsal cerebral cortex (250×250 μm), corpus callosum (250×50 μm), external capsule (250 × 25 μm), and subependymal zone (SEZ) at four separate sites surrounding the lateral ventricle, specifically the dorsal wall (250×25 μm), the lateral angle (250×50 μm), the dorso-lateral wall (250×25 μm), and the ventro-lateral wall (250×25 μm).

Statistical analysis

Data are presented as mean ± standard error of the mean. Quantitative behavioral, ELISA, and histological data were analyzed to confirm a normal distribution. Statistical analysis then consisted of ANOVA with post hoc Scheffé calculations for intergroup comparisons. For technical reasons, the water maze test performed on postnatal day 20 had an insufficient number of mildly

hydrocephalic rats, therefore only control and severely hydrocephalic rats were compared using Student's t test. Statistical significance was defined as $P<0.05$. Software used was StatView 5 (SAS Institute; Cary NC).

RESULTS

There were no differences between sham and intact rats; therefore, the results are combined into single control groups for each age. Of the 70 rats that were injected with kaolin, 24 died shortly after the injection (usually respiratory failure, less often failure to regain consciousness) or were euthanized within the first 3 days because of failure to gain weight or inability to move due to spinal cord damage. Ten rats showed no evidence of ventricular enlargement on the first MR image (that is, there was no difference from control rat brains). The remaining 36 rats that developed ventricular enlargement were euthanized on day 7 (n = 15) or day 21 (n = 21). Ventricular enlargement was associated with a dome-shaped head and/or persistent fontanel, which could be seen as early as 4 days and persisted to 21 days (Fig. 1). Hydrocephalic rats had an abnormal broad-based gait with tiptoed stepping, hunched back, and lethargic pace. Severely hydrocephalic rats had less weight apparent by day 7 and which was statistically significant at 19 days (Fig. 2).

Magnetic resonance imaging

MR imaging showed that the ventricles, as well as the subarachnoid space especially around the hindbrain, were variably enlarged at 7 days and 21 days (Figs. 3 and 4). To assess the progression of ventricular enlargement, 12 pups were imaged on both 7 and 21 days. There was a strong correlation between ventricle size at 7 days and 21 days ($r = 0.956$, $P<0.0001$, Fisher's r to z test), indicating that initially mild hydrocephalus did not convert to severe hydrocephalus and vice versa. There was an increase of 90±27% (mean±SEM) in the ventricle proportion among these hydrocephalic rats. Periventricular white matter was edematous in the hydrocephalic 7-day pups. Severe ventriculomegaly was associated with destruction of the external capsule so that the caudatoputamen remained attached only ventrally. Behavioral assessment There was no statistically significant evidence that mildly or severely hydrocephalic rats were impaired in early ambulation, righting response, negative geotaxis reflex, wire hanging duration, or performance on continuous and accelerating rotating rods despite the qualitatively abnormal gait (data not shown). In the straight water trough, 20-day-old severely hydrocephalic rats swam more slowly. In contrast to controls, there was also statistically significant evidence that severely hydrocephalic rats failed to improve their ability to find the hidden platform in the water maze during successive tests through the day. This suggests that an impairment of memory exists (Fig. 5).

Anatomical and histological assessments

Following sacrifice, kaolin could be identified on the ventral surface of the brainstem and as far as the middle cerebral arteries and olfactory tracts. Yellow hemosiderin deposits were occasionally visible on the dorsal surfaces of the frontal and parietal lobes where thinning was severe. Bloody discoloration of the CSF was rarely seen. In the severely hydrocephalic rats, the brains collapsed promptly upon opening of the skull; therefore, all quantitative assessment of the ventricles is based on the MR imaging. The following histologic descriptions highlight the abnormalities at the two time points studied. Where quantitative assessments were not made, the abnormalities described were apparent predominantly in the severely hydrocephalic rats. At 7 days, there was negligible myelin staining in cerebral white matter in control rats. The corpus callosum was expanded with edema fluid such that axons were surrounded by large extracellular spaces. Hydrocephalic brains exhibited enlarged ventricles with rarefaction or shredding of the frontal periventricular white matter (Figs. 6A, B). There was severe loss of ependyma, buried ependymal rosettes along the ventricle wall, rare clusters of hemosiderin-laden macrophages, and scattered apoptotic nuclei in the white matter. Subplate neurons, which were apparent as a regular band in the deep cortex of controls, were lost in a patchy manner in the severely hydrocephalic rats (Figs. 6E, F). Cell proliferation, as judged by Ki67 immunoreactivity, was significantly reduced in the subependymal zone of

severely hydrocephalic rats only (Figs. 6G, H; 7). In the white matter and cerebral cortex where there were far fewer Ki67 positive cells, there was no significant differences (not shown). Neurofilament immunolabeling demonstrated varicosities along damaged axons in the shredded white matter (Fig. 6K). Transferrin immunolabeling of myelinating oligodendrocytes was rare in control and hydrocephalic animals; this was expected because myelination has not yet begun around the lateral ventricles at 7 days [36]. BS lectin demonstrated more macrophages (round shape) than reactive microglia (bipolar cells with delicate processes) in the white matter (Fig. 6Q). At 21 days, control animals had small ventricles and prominent staining of myelin in the periventricular white matter. The corpus callosum of severely hydrocephalic animals was very atrophic (0.34±0.03 mm in controls vs. 0.15±0.04 mm in severely hydrocephalic; $P<0.05$, ANOVA) and stained weakly with solochrome cyanine (Figs. 6C, D). In some severely hydrocephalic rats, the periventricular white matter was completely absent. Dorsal cortical gray matter was thin in the severely hydrocephalic rats. The subependymal zone was much thinner in 21-day control rats than 7-day rats but remained an active proliferation site as judged by Ki67-immunoreactive cells. However, the proportion of Ki67 positive cells was significantly reduced in both the mild and severe hydrocephalics as compared to controls (Figs. 6I, J; 7). Fluoro-Jade staining and neurofilament immunostaining showed damaged axons with varicosities, however, because the white matter atrophy was so severe in the severely hydrocephalic rats, there were subjectively fewer than at 7 days

(Fig. 6L). Immunohistochemical detection of GFAP revealed hypertrophic reactive astrocytes in the periventricular white matter (Figs. 6M, N). Transferrin-immunoreactive mature oligodendroglia were abundant in white matter of controls and fewer in hydrocephalics (Figs. 6O, P). BS lectin staining showed abundant periventricular microglia with delicate processes (Fig. 6R).

Biochemical studies

ELISA measurements (Table 1) showed that MBP content in the frontal cerebrum was lower in severely hydrocephalic rats at 7 and 21 days, and GFAP content was higher in severely hydrocephalic rats at 7 and 21 days. Synaptophysin content was not significantly altered by hydrocephalus. Western blots corroborated these findings (Fig. 8). In contrast to the MBP finding, PNPP and CNPase enzyme activities, considered to be present in myelin and oligodendrocytes [53, 54], showed no consistent alteration in hydrocephalic rats (Table 1). CGalT activity, a marker of actively myelinating oligodendrocytes, tended to be lower in the 7-day hydrocephalic rats.

DISCUSSION

The neonatal rats used in this experiment were chosen because their brains are comparable to those of 24–26 gestational week humans [59, 60]. Humans of this age are potentially affected by congenital fetal-onset hydrocephalus or post-hemorrhagic hydrocephalus after premature birth. The kaolin model is inexpensive and simple. Large quantities of animals with varying severity of ventricular enlargement can be produced for study of short- and long-term effects of progressive injury on behavior and the process of brain maturation. In general, our hypothesis that behavior and brain changes, both destructive and reactive, are dependent on the severity of hydrocephalus is supported. Our goal was to provide a more complete description of behavioral and histological changes in the kaolin model of hydrocephalus and to determine which quantitative parameters might be useful for further studies of pharmacological interventions in neonatal hydrocephalus [39-41]. It has been long recognized that kaolin is an effective tool for producing hydrocephalus but that the result is variable and somewhat unpredictable. We had hoped that measures of early behavior such as ambulation and reflexes [50] would be useful in showing which neonates were developing severe hydrocephalus, however, none of these tests was sufficiently sensitive. A lag in weight gain was more predictive. In an individual animal at 7 days, MR imaging was the only reliable way of assessing severity of hydrocephalus. At later ages, although we observed

a clear qualitative difference in the gait and posture, quantifiable gait performance on a rotating cylinder was not substantially impaired at 20 days, despite severe brain damage. Apparently, the rats learn to accommodate to their disability quite well. Perhaps a more demanding test such as a balance beam or a variable rung ladder would be a more sensitive indicator of motor disability. We did, however, show memory deficits in the severely hydrocephalic pups by postnatal day 20 using a modified Morris water maze test. We have previously shown that this is due to destruction of the fimbria/fornix connections rather than a direct effect on the hippocampus [9]. Brain damage must be assessed after sacrifice. Because the brain collapses upon removal, MR imaging is much more reliable for determining ventricle size than any gross anatomic or histologic method. Although there are many progressive destructive changes evident histologically, because of profound tissue distortions, they can be difficult to quantify. We found that whole cerebrum assay of myelin basic protein (MBP) and glial fibrillary acidic protein (GFAP) using the ELISA method was easier and more reliable than immunohistochemistry for measuring myelin content and reactive astroglial change respectively. Our other bioenzymatic assays of myelin and oligodendrocytes were less reliable, perhaps because the enzymes are not restricted to myelin. With respect to alterations in postnatal brain development due to hydrocephalus in rodents, Miyan and coworkers have studied cell proliferation in the subependymal zone of H-Tx rats. Around the time of birth, H-Tx rat brain cells seem to be arrested in the S phase of cell cycle. An inhibitory

factor appears to be present in the CSF [61, 62]. We confirmed that neonatal-onset hydrocephalus can cause suppression of cell proliferation in the subependymal zone. However, it should be noted that, by postnatal day 1 when we injected the kaolin to induce hydrocephalus, most neurons have already been generated. Oligodendrocyte progenitors are produced during the first postnatal week in the subependymal zone lining the lateral ventricles [63, 64]. Therefore, suppressed proliferation could have an impact on the ultimate capacity for white matter myelination, perhaps even after treatment by shunting. Another abnormal developmental feature we observed was disorganization in the subplate neuron layer of 7-day hydrocephalic rats. These cells form a temporary circuit that initiates both afferent and efferent connections between cerebral cortex and thalamus. In rats, they undergo regressive changes after the second postnatal week [65, 66]. Recent studies also suggest that these neurons can be altered in human hydrocephalus [67]. Thalamic neurons are known to degenerate in the postnatal H-Tx rat [68]. This could contribute to the higher cortical deficits that complicate the lives of hydrocephalic infants. White matter destruction was evident as early as postnatal day 7 in rats with neonatally induced hydrocephalus. It is similar to that observed in neonatal kittens with early white matter edema, axonal swelling, karyorrhectic cells, and delayed myelination [30]. In addition, oligodendroglial hypoplasia was seen at 21 days. This may be due to interruption of the normal maturation of oligodendrocytes, which occurs at 7–21 days [69]. Hydrocephalus might cause death of mature oligodendrocytes

through ischemia [14, 38] or it might prevent oligodendrocyte progenitor differentiation and migration. A consequence of hydrocephalus is that surviving oligodendrocytes produce less myelin [14, 38] and the association with neighboring axons is lost [70]. Reactive astroglial and microglial changes in the shredded white matter were clearly shown in this study, as has been observed in most hydrocephalic conditions [31]. The prominence of macrophages at 7 days suggests that there is considerable destruction of white matter in the early phases of ventricular dilatation [71]. Most descriptions of brain changes in rodents with neonatal onset hydrocephalus are derived from the H-Tx mutant rat. The H-Tx trait appears to be a multiple gene interaction that exhibits autosomal recessive inheritance with incomplete penetrance [45]. Ventricle dilatation in the H-Tx model begins at around 18–20 days gestation, likely as a consequence of cerebral aqueduct occlusion [32]. Jones and coworkers as well as others have published morphological [42, 72-74] and metabolic details [75] concerning the HTx rat. Studies of spatial learning and memory showed cognitive deficits in the H-Tx hydrocephalic pups [72, 73]. It should be noted that non-hydrocephalic H-Tx control rats also showed impairments when compared to Sprague–Dawley rats [76]. The kaolin induced neonatal hydrocephalic rat model has been described only rarely in the literature. Intracranial pressure and cerebral blood flow (using transcranial Doppler) were assessed in rats that received kaolin injections at 2–3 days age. The intracranial pressure was elevated at 15 days, and it declined to normal by 2 months [47, 77]. McAllister and coworkers showed

using Golgi impregnation neurons that pyramidal neurons of the cerebral cortex have decreased number and length of dendrites at postnatal 10–12 days [49]. In another publication, changes in norepinephrine (NE), dopamine (DA), 3,4-dihydroxy-phenylacetic acid (DOPAC), and serotonin (5-HT) were documented in several brain regions 11 days after induction of hydrocephalus using high performance liquid chromatography [46]. Hydrocephalus induction with kaolin in 7-day Wistar rats was associated with changes among choline acetyltransferase and tyrosine hydroxylase immunoreactive neurons in 14- to 28-day and 56-day hydrocephalic rats [48]. In summary, the rat model of hydrocephalus induced by cisternal injection of kaolin on postnatal day 1 adequately mimics some aspects of the pathology of hydrocephalus in fetuses and premature infants [29, 30]. The behavioral changes reflect to some extent the severity of damage. Quantitative measurements of ventricle size, memory, histologic features, and protein content used in combination can distinguish mild from severe degrees of hydrocephalus. Future studies will assess the ability of pharmacological interventions to reduce brain damage caused by ventricle enlargement. The altered development of brain in the context of hydrocephalus remains an underappreciated phenomenon also in need of further investigation.

Table 1
Measurements of brain proteins and myelin-associated enzyme activities in control, mildly, and severely hydrocephalic rat brains

	7-day control	7-day mild	7-day severe	21-day control	21-day mild	21-day severe
GFAP (μg/mg brain)	0.33 ± 0.13	0.58 ± 0.18	1.41 ± 0.27 *P = 0.034	0.42 ± 0.20	0.64 ± 0.19	3.40 ± 1.08 *P = 0.033
MBP (μg/mg brain)	0.251 ± 0.002	0.246 ± 0.002	0.025 ± 0.001	0.886 ± 0.147	0.988 ± 0.092	0.411 ± 0.063 *P = 0.040
Synaptophysin (μg/mg brain)	0.020 ± 0.004	0.014 ± 0.001	0.027 ± 0.010	0.124 ± 0.014	0.123 ± 0.005	0.119 ± 0.011
PNPP activity (nmol/mg protein/h)	13.4 ± 0.5	19.0 ± 0.8 *P = 0.027	13.9 ± 0.7	24.3 ± 1.3	21.1 ± 1.2	30.6 ± 1.7
CGalT activity (nmol/mg protein/h)	1.17 ± 0.20	0.84 ± 0.16	0.88 ± 0.03	7.73 ± 1.35	9.93 ± 1.05	7.77 ± 1.14
CNPase activity (nmol/mg protein/h)	0.50 ± 0.04	0.29 ± 0.01	0.31 ± 0.10	0.67 ± 0.04	0.60 ± 0.09	0.97 ± 0.07

All data are expressed as mean ± standard error of the mean. Statistical comparisons were made using ANOVA followed by Scheffé test for intergroup comparisons. Significant P values are shown for comparisons to control values. MBP, synaptophysin, PNPP, CGalT, and CNPase all exhibited a significant age-related effect when the control values were compared.

Note: From Khan et. al; Experimental Neurology 2006 August; 200 (2): 311-320.

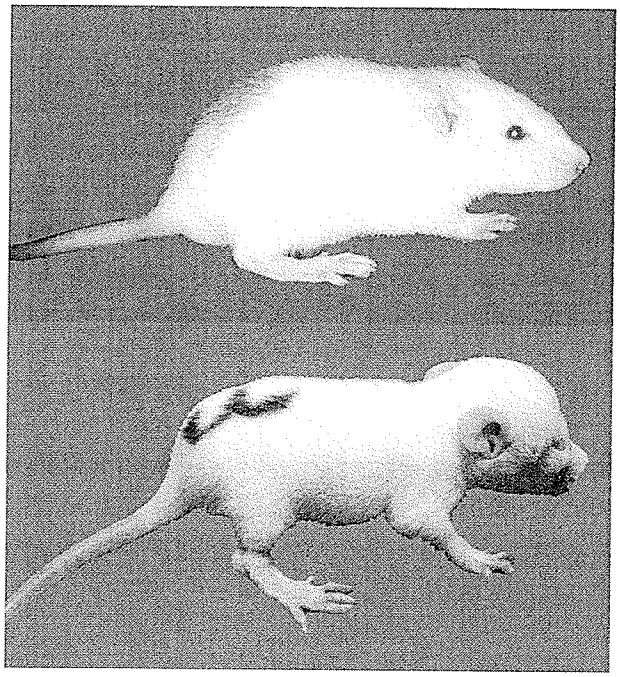

Figure 1. Control (upper panel) and severely hydrocephalic (lower panel) Sprague–Dawley rats at postnatal day 21. Hydrocephalic rats have a dome-shaped head, thin body, hunched back, and abnormal broad-based stance and gait.

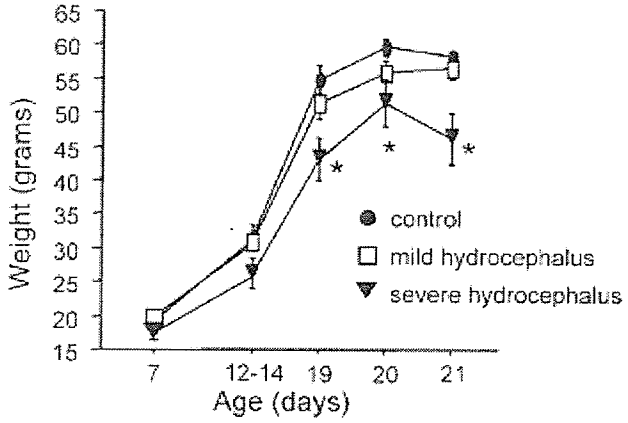

Figure 2. Line graph showing weight (mean ± SEM) in control and hydrocephalic rats. The severely hydrocephalic rats exhibit significantly lower body weights by 19 days (*P < 0.04, ANOVA).

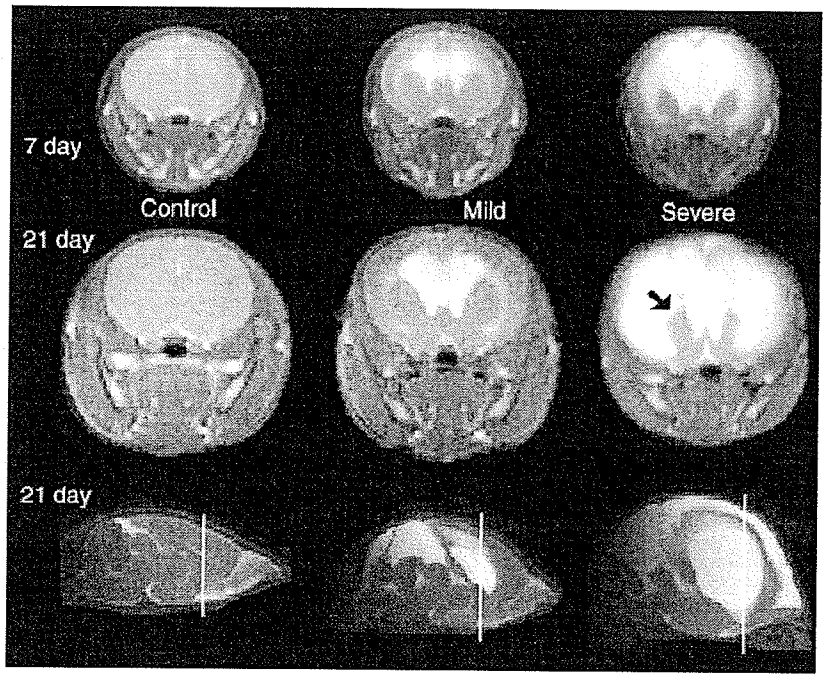

Figure 3. Magnetic resonance (MR) coronal T2-weighted images of control, mild, and severe hydrocephaly in postnatal day 7 (upper row) and 21 rats (middle row). Hydrocephalic pups have progressive enlargement of the ventricles with white matter edema (bright signal intensity) in the corpus callosum and external capsule. At 21 days, the severely hydrocephalic rats exhibit destruction of the external capsule with a disconnected putamen that is anchored ventrally (arrow). CSF accumulates in the subarachnoid space dorsal to the cerebellum and brainstem in all cases and dorsal to the cerebrum in severe cases (shown on sagittal slices in lower row). The vertical white bars on the sagittal images indicate the level of the corresponding coronal slice above. For purposes of comparison to Figure 4, the ventricle to brain area ratios for control, mild, and severe are: 0.001, 0.075, and 0.549 at 7 days and 0.001, 0.225, and 0.584 at 21 days.

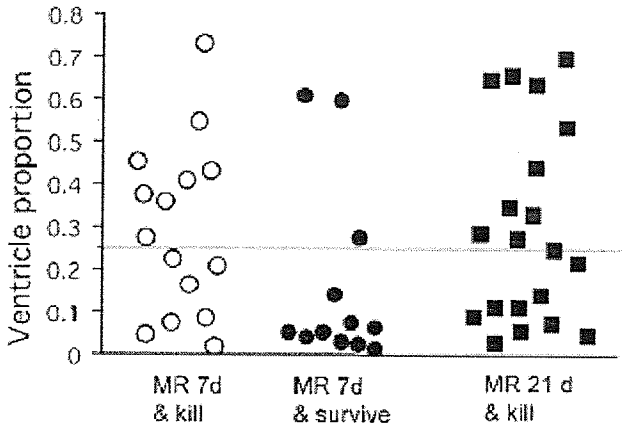

Figure 4. Scattergram plot showing ventricle/brain area proportion as assessed on MR images obtained postnatal days 7 and 21. The open circles show data for rats imaged at 7 days that were then killed. The filled circles show data for rats that were imaged at 7 days and allowed to survive until 21 days. The rats were categorized as having either mild or severe ventriculomegaly using a dividing value of 0.25. All control rats had values of <0.005 (not shown on plot).

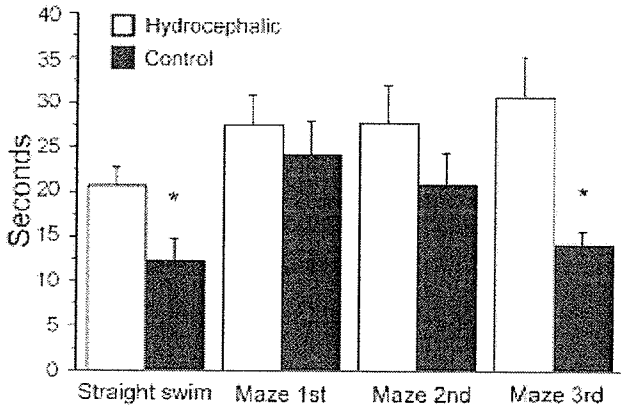

Figure 5. Bar chart of showing times (mean ± SEM) to swim in the straight trough and to find the hidden platform in the water maze on three successive trials on day 20. Severely hydrocephalic rats swam more slowly in the straight trough (*P = 0.0248, unpaired Student's t test). Unlike control rats, which found the hidden platform more quickly on successive trials, hydrocephalic rats failed to improve (3rd maze trial, *P = 0.026).

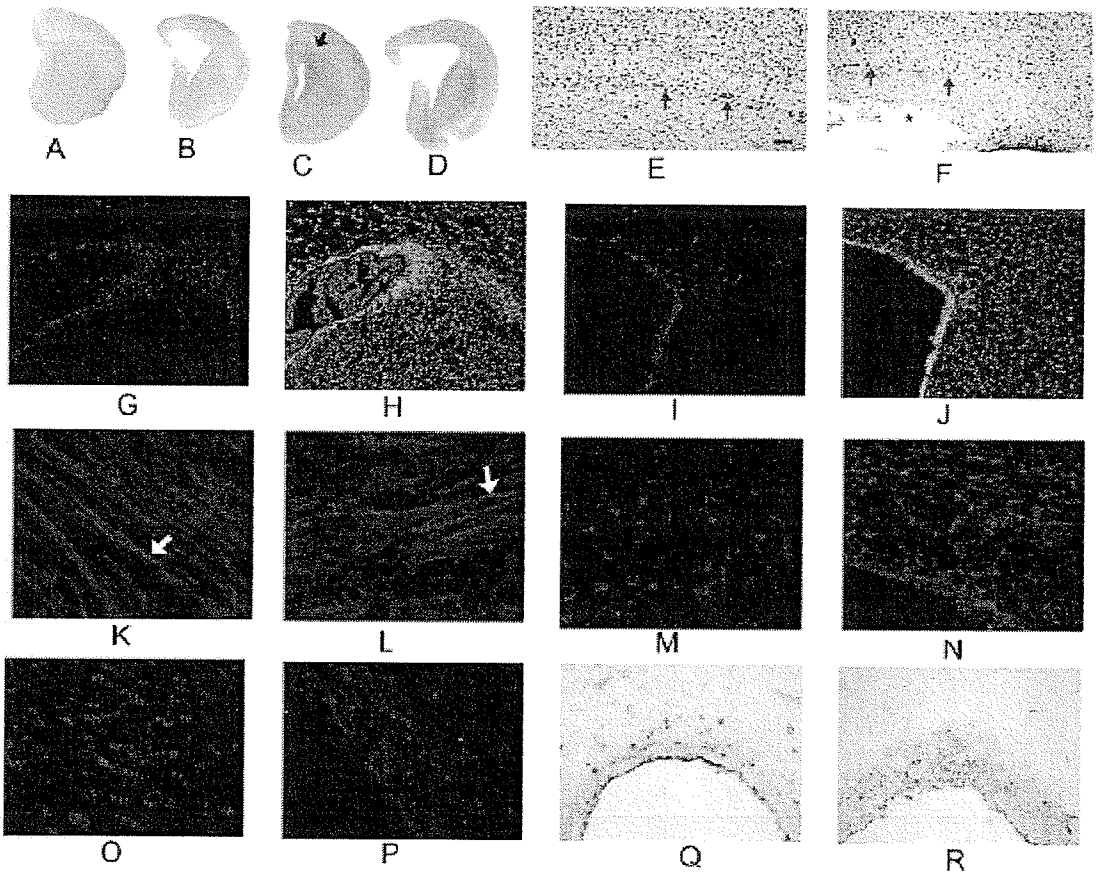

Figure 6. Histologic studies on 7-day and 21-day control and hydrocephalic rats. Coronal slices stained with solochrome cyanine to demonstrate myelin show negligible myelin deposition in 7-day control brains (A) and ventricular dilatation with white matter rarefaction in 7-day hydrocephalic brains (B). In 21-day controls, myelin staining is evident in the corpus callosum and external capsule (C, arrow). The 21-day hydrocephalic brain is severely distorted with enlarged ventricles, atrophic white matter, and thin cerebral cortex (D). Hematoxylin and eosin-stained sections at 7 days show a distinct row of subplate neurons in the deep cortex of controls (E, arrows), whereas the subplate in hydrocephalic rats is disrupted (F, arrows) and the adjacent white matter is fragmented (*). Ki67

immunolabeled cells are abundant at the lateral angle of the frontal horn in 7-day control rats (G; bisbenzimide double stain shown in panel H) but are reduced in severely hydrocephalic rats (I; bisbenzimide double stain shown in panel J). Neurofilament immunolabeling shows damaged axons with irregularities and varicosities (arrows) in corpus callosum of 7-day (K) and 21-day (L) hydrocephalic rats. GFAP immunolabeling in the periventricular white matter of 21-day control rats shows perivascular astrocytes (M). GFAP expression is increased in reactive astrocytes of 21-day hydrocephalic rats (N). Transferrin immunolabeling in 21-day control corpus callosum shows an abundance of oligodendrocytes (O), while in hydrocephalic brains the cells are smaller and fewer. BS lectin labeling shows round macrophages in the periventricular white mater of 7-day hydrocephalic rats (Q), whereas in 21-day severely hydrocephalic rats the labeling shows a network of delicate interwoven processes due to microglial activation (R). Bar shown on panel E is 200 μm for G–J, 100 μm for E, F, M–R, and 50 μm for K, L.

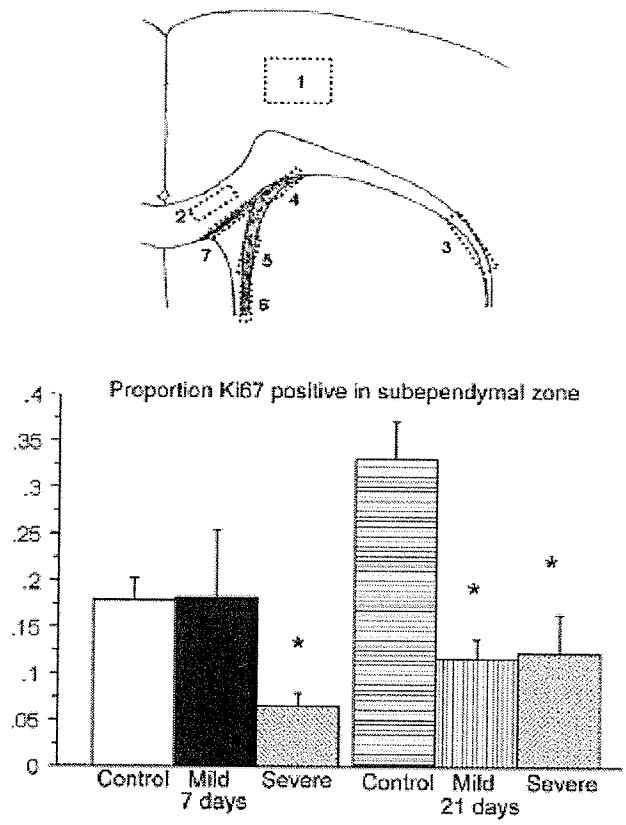

Figure 7. Upper panel shows the anatomical areas selected for Ki67/bisbenzimide cell counting. 1—dorsal gray matter 2—medial white matter/corpus callosum; 3—lateral white matter/external capsule; 4—subependymal zone (SEZ) at angle of lateral ventricle; 5—lateral SEZ; 6—ventral SEZ; 7—dorsal SEZ. The lower panel shows a bar chart comparing cell proliferation in subependymal zone for control, mild, and severe hydrocephalic pups at 7 and 21 days. Data are expressed as the proportion of Ki67 positive nuclei/total bisbenzimide-stained nuclei (mean ± SEM). Two-way ANOVA showed a statistically significance effect of ventricle size ($P = 0.0006$) but not age. Note that the higher proportion of positive cells in the SEZ of 21-day rats

compared to 7-day rats is an artifactual effect of the analysis being proportionate. The meaningful analyses are within the age groups only. Post hoc Scheffé calculations for intergroup comparisons showed statistically significant reductions in cell proliferation associated with hydrocephalus (*$P < 0.005$). Two-way ANOVA performed on data from white matter revealed an age-related effect $P = 0.035$, but no effect of hydrocephalus. In the cortex, there were no significant differences (data not shown).

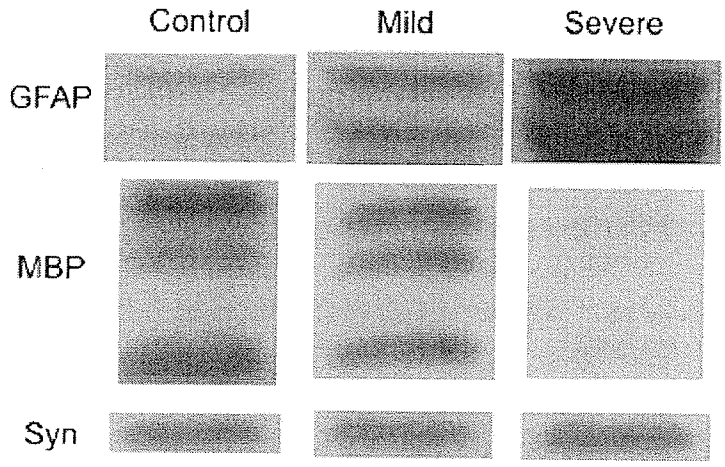

Figure 8. Photograph showing selected Western blot findings from cerebrum homogenates. Multiple bands reflect the presence of multiple isoforms of the proteins. Increased glial fibrillary acidic protein (GFAP) indicates the presence of reactive astroglial change in hydrocephalic rats at 21 days. Severe hydrocephalus was associated with reduced myelin basic protein (MBP), indicative of impaired myelination. Synaptophysin was not altered in hydrocephalic rat brains. These results corroborate the quantitative findings in the ELISA measurements (see Table 1).

Chapter 2.2

Cerebral white matter hypoxia in young rats with kaolin-induced hydrocephalus.

This section will be submitted for peer review to a neuroscience-oriented journal to be determined.

Authors: Osaama H. Khan, Packiasamy A.R Juliet, and Marc R. Del Bigio

Note: Behavioral and immuno-histological experiments completed by Osaama Khan. Biochemical assays were performed by Terry Enno. P.A.R. Juliet performed antioxidant enzyme assays.

ABSTRACT

Hydrocephalus is associated with reduced blood flow in periventricular white matter. We hypothesized that the brains of young rats with hydrocephalus would exhibit evidence of hypoxic and oxidative brain damage, as well as protective responses. Hydrocephalus was induced by injection of kaolin into the cisterna magna of 1-day and 21-day-old Sprague-Dawley rats. Ventricle size was assessed by magnetic resonance imaging (MRI). In situ evidence of tissue hypoxia was shown by pimonidazole hydrochloride binding in periventricular glial and endothelial cells. Biochemical assay of nitrite suggested increased nitric oxide production and nitrotyrosine was detected by immunohistochemistry in white matter. Biochemical assay of thiobarbituric acid reaction and immunohistochemical detection of 4-hydroxy-2-nonenal in white matter indicate presence of lipid peroxidation. Neither catalase nor glutathione peroxidase activities were increased. We did not detect a change in hypoxia inducible factor 1α by quantitative RT-PCR. Global vascular endothelial growth factor (VEGF) expression determined by quantitative RT-PCR and ELISA was not changed, although VEGF immunoreactivity was increased in reactive astrocytes of hydrocephalic white matter. We conclude that in this model of neonatal kaolin induced hydrocephalus, hypoxia in white matter might contribute to the destructive vascular changes and that the cellular compensatory mechanisms might not be adequate.

INTRODUCTION

Hydrocephalus is characterized by obstruction of cerebrospinal fluid (CSF) flow and enlargement of the cerebral ventricles. It is associated with destruction of periventricular axons and neurons due to a combination of mechanical injury (stretch), accumulation of waste products in the CSF, and impaired blood flow [29]. As in stroke and trauma, calcium mediated axonal damage plays a role [8]. Reduction in cerebral blood flow as a result of hydrocephalus, especially in the white matter, is well described in human and animal literature [29, 78-81]. Tissue ischemia can lead to generation of oxygen free radicals, which can damage lipids, proteins, and nucleic acids of cells and mitochondria potentially causing cell death [82]. Increased production of Nitric oxide (NO) can occur in these circumstances [83] and can form peroxynitrite, which can modify amino acids that can be detected immunohistochemically using an antibody to nitrotyrosine [84]. Oxidation of lipids can be detected using biochemical assay or by immunohistochemical detection of 4-hydroxy-2-nonenal (HNE) [85]. The 2-nitroimidazole hypoxia marker, 1-[(2-hydroxy-3-piperidinyl) propyl]-2-nitroimidazole hydrochloride (pimonidazole hydrochloride) readily traverses cell membranes in its oxidized form, and at PO2 <10 mmHg, it forms irreversible covalent adducts with thiol groups in proteins, peptides, and amino acids that can be detected immunohistochemically [86].

Protective reactions can occur following ischemic and hypoxic stresses. Superoxide dismutase, glutathione peroxidase and catalase are regulated intracellular antioxidant enzymes that serve to decrease oxygen free radicals [87]. Hypoxia inducible factors (especially HIF-1α) are key regulators of hypoxia-induced gene expression such as vascular endothelial growth factor (VEGF). VEGF is an angiogenic growth factor and an endothelial cell-specific mitogen [88, 89]. Global hypoxia induces transient accumulation of the oxygen-regulated HIF-1α and upregulation of VEGF expression in the rat brain [90]. We hypothesized that the brains of young rats with hydrocephalus would exhibit evidence of hypoxic and oxidative brain damage, as well as protective responses.

METHODS

Animal preparation

All animals were treated in accordance with guidelines set forth by the Canadian Council on Animal Care and experiments were approved by the local animal use committee. All efforts were made to minimize suffering and the number of animals used. Sprague-Dawley rats were bred locally. Sterile kaolin (aluminum silicate) suspension (20-30µl of 25% suspension in 0.9% saline) was injected into the cisterna magna under isoflurane anesthesia and aseptic conditions to induce hydrocephalus at 1 or 21 days. After kaolin injection the pups were returned to their mothers and were housed in standard cages and

provided with a normal 12-hour day/night lighting schedule with free access to water and pellet food. For identification, numbers were marked on the backs with indelible ink or the ears were punched. Three different categories of hydrocephalic (and age-matched control) rats were studied: Neonatal with early hydrocephalus (postnatal day 7), infantile with moderate to severe hydrocephalus (postnatal day 14-21), and juvenile with moderate to severe hydrocephalus (postnatal day 42 – 49) (see Table 1 for summary of assays done in different age categories and sample sizes; see Figure 1 for example MR images). Our primary focus was on the infantile stage, but when assays were done at multiple stages, potential age and / or stage related differences can be considered.

Magnetic resonance imaging.

Magnetic resonance (MR) studies were performed within 24 hours of sacrifice using a Bruker Biospec/3 MR scanner equipped with a 21-cm bore magnet operating at a field of 7 T (Karlsruhe, Germany) to obtain T2-weighted images of the brain in the coronal plane. The areas of the lateral ventricles and cerebrum were measured at the level immediately anterior to the third ventricle. Frontal horn size was expressed as a ratio determined by dividing the total area of the ventricles by the area of the cerebrum.

Euthanasia and tissue dissection

Rats were euthanized by overdose with pentobarbital, the vasculature was flushed by transcardiac perfusion with ice-cold 0.1M phosphate-buffered saline

and the brains were removed. Samples of the left parietal cerebrum, left frontal cerebrum (both including periventricular white matter), and left hippocampus were dissected and homogenized immediately for enzyme assays, or frozen in liquid nitrogen and stored at -80 °C. The right cerebrum was placed in 10% formalin for fixation then coronal slices were embedded in paraffin.

Biochemical assays

Nitric oxide (NO), which is synthesized by nitric oxide synthase, has an extremely short half-life (<10 seconds), which makes it difficult to study directly. Because NO is metabolized to nitrite and nitrate, quantitation of these stable anions can be used to indirectly determine the amount of NO originally present. We used a colorimetric assay kit for nitrate / nitrite (Cayman Chemical #760871; Ann Arbor, MI). Infantile rats were euthanized and the left half brain, from which the brainstem and cerebellum had been removed, was immediately homogenized in PBS and centrifuged as directed by the manufacturer. Nitrate was reduced into nitrite by nitrate reductase, lactate dehydrogenase was used to degrade excess NADPH, then the Griess reagent was used to convert nitrite into a purple azo compound, which was quantified by spectrophotometry at 540μm. Nitrite was assayed in triplicate and concentrations were calculated from a standard curve. Results are recorded as nitrite concentration (μM mean ± SEM).

For lipid peroxidation and antioxidative enzyme assays, infantile rats from a single litter were studied. The left cerebrum dorsal to the lateral ventricle was

mechanically homogenized for 1 minute in ice-cold Tris-EDTA buffer (pH 7.4; 0.1 M Tris-HCl and 1 mM EDTA; 10% w/v). Lipid peroxidation was measured using the thiobarbituric acid reaction [91, 92]. Catalase [93] and glutathione peroxidase [94] activities were assayed using well-documented methods. Samples were run in triplicate. Previously frozen samples of fronto-parietal cerebrum from neonatal and infantile rats were used for quantification of VEGF protein using enzyme linked immunosorbent assay (ELISA) (mouse anti-rat VEGF, R&D Systems, Minneapolis MN). Samples were run in triplicate.

Pimonidazole administration

Pimonidazole binds to protein in hypoxic environments and can be detected by immunohistochemistry. Pimonidazole (Hypoxyprobe-1 kit; Chemicon International, Temecula, CA) was used for detection of tissue hypoxia according to supplier's instructions in two separate experiments. Infantile rats received a single dose of pimonidazole (60 mg/kg intraperitoneal) 90 minutes prior to sacrifice. Juvenile rats received two doses 90 and 30 minutes prior to sacrifice. Three additional hydrocephalic rats received sham injection of saline rather than pimonidazole. The rats were euthanized by CO_2 overdose, then perfused transcardially with 10% formalin. Fixed brains were sliced in the coronal plane and embedded in paraffin then sectioned at 5μm thickness. Antibodies to localize pimonidazole were used at a dilution of 1/25 with secondary detection by peroxidase-conjugated antibody followed by diaminobenzidine. Pimonidazole

labeling was semiquantitatively graded in white matter and gray matter (cerebral cortex and striatum) separately as: 0 (no labeling), 1 (rare cells detected; <1 in any 200x microscopic field), 2 (scattered cells throughout region or clusters). Sections were assessed blindly with respect to pimonidazole injection status.

Histological studies

Brain slices from neonatal, infantile, and juvenile rats collected from previous experiments were used for histological analysis. Peroxynitrite modification of amino acids can be detected immunohistochemically using an antibody to nitrotyrosine [84]. Oxidation of lipids can be detected using immunohistochemical detection of 4-hydroxy-2-nonenal (HNE) [85, 95]. Paraffin sections (6 μm thickness) of the right cerebrum were taken at the level of the optic chiasm. Immunohistochemical methods were used to detect nitrated proteins (nitrotyrosine clone HM11, 1:100 dilution; Zymed Laboratories Inc. San Francisco, CA), lipid peroxidation (4-hydroxy-2-nonenal (HNE)), 1:500, Calbiochem, San Diego, CA), hypoxia inducible factor (HIF-1α, Novus Biologicals, Littleton, CO), and vascular endothelial growth factor (VEGF, 1:500, Abcam Ltd., Cambridge, MA). Antigen exposure for nitrotyrosine detection was accomplished by microwaving in 0.6 M citric acid buffer. Primary antibodies underwent overnight incubation followed by detection with Cy3-conjugated fluorescent secondary antibody. Hematoxylin was used as a counterstain. Negative controls were processed without the primary antibody.

Statistical Analysis

Data are presented as mean ± standard error of the mean. Quantitative data were analyzed to confirm a normal distribution. Statistical analysis then consisted of ANOVA with post-hoc Scheffé calculations for inter-group comparisons, or unpaired t test for two group comparisions. Non-parametric score data were analyzed with Mann-Whitney U test or Kruskal-Wallis test for two or three groups respectively. Statistical significance was defined as $p<0.05$. Software used was StatView 5 (SAS Institute; Cary NC).

RESULTS

Rats that received kaolin injections shortly after birth developed grossly enlarged heads by 10 – 14 days, gained body weight at a lower rate than controls, and had unsteady gait. Magnetic resonance imaging showed a range of ventricle enlargement (Figure 1). Kaolin injected rats with negligible ventricle enlargement were omitted from the experiment. In general, the ventricles enlarge progressively with thinning of the dorsal cerebrum and complete destruction of the periventricular white matter and external capsule by 21 days. The behavioral, biochemical and histopathological features of this model have been described in detail in a recent publication [96]. Rats injected with kaolin on day 21 after birth had similar characteristics with severe cerebral thinning by 42 days age; they have been described in detail previously [5, 14, 38].

Evidence for hypoxic and oxidative changes

Hypoxic changes in proteins were demonstrated by immunohistochemical detection of pimonidazole binding. The infantile non-hydrocephalic rats that received pimonidazole exhibited rare cortical and striatal neurons (based on morphology) with nuclear labeling, but there was no white matter labeling. In the hydrocephalic rats, pimonidazole was detectable in scattered neuronal nuclei throughout the striatum and cerebral cortex (especially layers III, IV,V) (Figure 2). In the white matter clusters of glial cells and endothelial cells had cytoplasmic and nuclear labeling. Some of the glial cells had nuclear changes characteristic of apoptosis. The identity of the glial cells was not obvious, but most had round nuclei suggestive of oligodendroglial lineage. There was no linear labeling indicative of axonal protein hypoxia. Frequent capillary profiles were labeled. Statistical comparison of the grading showed that pimonidazole labeling was more apparent in the white and gray matter of hydrocephalic rats in comparison to controls ($p=0.011$ gray, $p=0.049$ white; Mann-Whitney U test). Examination of the juvenile control rats showed no labeling in any region of the brain. Among the 6 hydrocephalic rats, in the white matter there was no labeling in 2 rats, rare cells in 2, and clusters of cells in 2. In the gray matter, 4 rats had no labeling and 2 rats had scattered or small clusters of neurons labeled (not shown). Omission of the primary antibody or injection of saline rather than pimonidazole was associated with no labeling. Nitrite assay of brain homogenates indicated that

moderate to severe hydrocephalus was associated with increased NO production in the cerebrum (control 2.7±0.6 μM vs. hydrocephalic 5.6±0.9 μM; p=0.027). However, in situ tissue detection of NO was inconclusive. There was no evidence for protein nitration (nitrotyrosine immunoreactivity) in control rats at any age (Figure 3). In neonatal hydrocephalic rats, nitrotyrosine immunolabeling was present around capillaries in the periventricular white matter, but absent in gray matter. In infantile hydrocephalic rats, nitrotyrosine immunolabeling was evident in cytoplasm of white matter glial cells. The round nuclei and blunt processes suggest that these were oligodendrocytes. Juvenile hydrocephalic rats had negligible nitrotyrosine immunolabeling. Oxidative changes in lipids were assessed biochemically and immunohistochemically. Thiobarbituric acid reaction showed that hydrocephalus in infantile rats was associated with a 38% increase in brain lipid peroxidation (control 6.53±0.14 nmol/g vs. hydrocephalic 9.03±0.57 nmol/g wet tissue; p=0.0138). Pimonidazole binding to hypoxic adducts in the same rats was moderately correlated to thiobarbituric acid reaction detection of lipid peroxidation (r=0.63). As expected, there was no in situ evidence for lipid peroxidation (HNE immunoreactivity) in control pups at any age (Figure 4). Lipid peroxidation was noted in the white matter only in infantile hydrocephalic rats, particularly in regions with severe fragmentation. The labeled cells were generally fusiform with comma-shaped nuclei characteristic of microglia.

Evidence for protective responses

There was no significant change in antioxidative enzyme activity as a consequence of hydrocephalus in infantile rats. Catalase remained stable (control 0.200±0.003 vs. hydrocephalic 0.019±0.002 K / g protein; p=0.96) and glutathione peroxidase was not significantly different between control and hydrocephalic rats (control 0.994±0.218 vs. hydrocephalic 1.487±0.317 U / mg protein; p=0.47). HIF-1α immunoreactivity was not detectible in any control or hydrocephalic group. ELISA quantification showed that VEGF content in frontal cerebrum (combined gray and white matter) was higher in the 7-day control (25.3 ± 2.9 ng/g) than in the 21-day control (15.4 ± 1.1 ng/g) brains. In comparison to controls, there was no significant difference in the 7-day hydrocephalic (29.2 ± 1.6 ng/g; p = 0.249) or the 21-day hydrocephalic (15.2 ± 2.0 ng/g; p = 0.941) brains. With respect to localization, 7-day, 21-day and 42-day control brains had minimal immunoreactivity for VEGF in cortical neurons and none in white matter (Figure 5). Hydrocephalic brains at all 3 ages had more prominent VEGF immunoreactivity in cortical neurons and in hypertrophic astrocytes in the white matter. Subjectively, this was greater in rat brains with severe hydrocephalus.

DISCUSSION

Brain injury in hydrocephalus is a multifactorial process marked by ventricular enlargement leading to stretching of axons with concomitant cortical

compression. We have previously demonstrated decreases in progenitor cell proliferation, oligodendrocyte generation, and myelination as a consequence of hydrocephalus in neonatal and young rat brains [14, 96, 97]. Reduction in cerebral blood flow, especially in the white matter, is well described in hydrocephalic brains [29, 79, 80, 98]. The periventricular white matter is susceptible to injury in part because terminal arteries supply it. The focus of these experiments was to characterize the response between hypoxic damage and the protective response in brains of young hydrocephalic rats. The results suggest that white matter proteins and lipids are subjected to hypoxia, that they suffer oxidative damage, that nitric oxide (NO) production might play a role in the damage, and that protective responses in the form of upregulated "anti-oxidative" enzymes or VEGF production are minimal (summarized in Figure 6).

To identify hypoxic cells in young hydrocephalic rats we used pimonidazole hydrochloride, an exogenous hypoxia marker. We observed binding in cortical and striatal neurons, periventricular blood vessels, and glial cells, some of which were undergoing apoptosis. Oligodendroglial apoptosis has previously been demonstrated in young hydrocephalic rats [5, 14]. Free radical generation is a well-accepted outcome of hypoxia and/or ischemia. Reactive oxygen species (ROS) (e.g.superoxide, peroxide, and hydroxyl radicals) and reactive nitrogen species (e.g. peroxynitrite) are natural byproducts of oxygen/nitrogen metabolism and can accumulate in states of environmental stress. These reactive species can damage DNA, lipids, and proteins. Through

biochemical assay using the thiobarbituric acid reaction and using immunohistochemical detection of 4-hydroxy-2-nonenal (HNE), we observed evidence of lipid peroxidation in white matter of hydrocephalic pups. Some of this appeared to be in microglia, which are known to become reactive and phagocytose cell and myelin debris in hydrocephalus. The lipid peroxidation by-product 4-hydroxynonenal has been shown to be toxic to axons and oligodendrocytes [99] and has been shown to inhibit neurite outgrowth and disruption of axon microtubules in vitro [100]. Nitric oxide production during hypoxia with continuing blood flow can lead to peroxynitrite formation, which then nitrates tyrosine residues in proteins [101]. We showed indirectly though tissue assay that NO content is increased in hydrocephalic brain and that nitrotyrosine immunoreactivity is present in blood vessels and glial cells (possibly oligodendrocytes) of hydrocephalic rat brains. We are not aware of any studies that have sought evidence for DNA damage in hydrocephalus. An expression study showed upregulation of mRNA related to DNA repair in brains of H-Tx rats [102].

There are discrepant data in the literature concerning nitric oxide synthase (NOS) in hydrocephalus. NOS is activated by Ca^{++} [103, 104], and we have previously shown that Ca^{++} is increased in hydrocephalic white matter [8]. Using NADPH-diaphorase histochemistry, young hydrocephalic H-Tx rat brains appear to have reduced NOS activity in neurons [105]. Adult rats with kaolin-hydrocephalus appear to have increased neuronal NOS content in cortical and

hippocampal neurons, based upon immunoreactivity [106, 107]. The mRNA for an inhibitor of neuronal nitric oxide synthase was upregulated in young but not in adult hydrocephalic rats [108]. Other forms of NOS (endothelial and inducible) have not been studied directly in hydrocephalus.

Antioxidant enzymes such as superoxide dismutase (SOD), catalase, and glutathione peroxidase can be upregulated in tissues as a defense against oxidative damage. We did not observe an increase in glutathione peroxidase or catalase activity. In an immunohistochemical study on brains from WIC-Hyd rats with congenital hydrocephalus, the amount of Cu-Zn SOD was reduced in comparison to controls [109]. In young and adult rats with kaolin-induced hydrocephalus, we observed no change in SOD mRNA expression [108]. Similarly, there was either no change or a reduction in Cu-Zn SOD, Mn-SOD, and catalase mRNA expression in H-Tx rats [102]. Therefore, it appears that the response of antioxidant enzymes in hydrocephalic rat brains suggest that it is inconsequential.

Angiogenesis is an alternate protective mechanism through which oxygen, glucose and essential nutrients can be brought to tissues undergoing hypoxic stress [110]. HIF-1α is an upstream transcription factor that undergoes oxygen-dependent hydroxylation leading to changes in gene expression, including regulation of the angiogenesis pathway [111]. Global hypoxia induces transient accumulation of the oxygen-regulated HIF-1α and upregulation of VEGF expression in the rat brain [90]. VEGF, the production of which is activated by

HIF-1α, is involved in angiogenesis. In the young brain, VEGF is expressed by endothelial cells, neurons and astroglia [112, 113]. We observed an increase in VEGF immunoreactive cells, probably reactive astrocytes, in the white matter of hydrocephalic rat brains. From a quantitative standpoint, the VEGF ELISA measurements did not reveal a statistically significant increase; nevertheless, it is possible that real localized increases in white mater could be missed in homogenates of the cerebrum. Clinically it has been shown that VEGF content is increased in the CSF of infants with posthemorrhagic hydrocephalus [114, 115]. The few studies that have attempted to quantify capillary density in hydrocephalic brains usually reveal a decrease compared to controls. This includes the periventricular area of hydrocephalic premature human fetuses [71], H-Tx rats [74], and adult rabbits with silicone oil-induced hydrocephalus [78]. One exception is a study in adult dogs; capillary density initially decreased in the cortex but was increased after 12 weeks [116]. In that experimental model, immunoreactivity for VEGF receptor 2 was increased in neurons of hypoglossal and vagal nuclei [117], as well as in neurons and glia of the hippocampus [118]; however, it should be noted that those data have not been published in detail. It should also be noted that anti-angiogenic isoforms of VEGF have been reported [119] and therefore simple detection of VEGF does not necessarily equate to angiogenesis. No one has directly examined endothelial cell proliferation in hydrocephalus.

Although we have provided numerous pieces of evidence to support our hypothesis that hypoxic mechanisms play a role in hydrocephalic brain damage, there are a few shortcomings that need to be considered. First, not all of the assays have been done at all stages of hydrocephalus and therefore we cannot be certain of the specific sequence of changes. Second, for technical reasons related to some of the assays, the tissue samples are not necessarily exactly comparable between experiments; therefore direct correlations are not possible. Third, because hydrocephalus is a chronic disorder with gradual progressive changes, any of the assays might miss transient changes, for example in gene expression. Finally, we must highlight the limitations of comparing assays on homogenized tissue with immunohistochemical studies; the former are generally more reliable as quantitative methods, however they can miss regional changes observable only with the latter.

In summary, in young rats with kaolin-induced hydrocephalus, multiple approaches indicate that hypoxia and NO production are associated with cellular changes, especially in periventricular white matter. These correlate well with the sites of damage and predicted mechanisms of brain cell injury. Protective responses at the cellular level appear to be minimal and inadequate. Using the single outcome measure of malondialdehyde concentration in brains of adult rats with kaolin-induced hydrocephalus, the oxygen radical scavenger N-acetylcysteine and the antioxidant epigallocatechin gallate were reported to be

mildly protective [120, 121]. Further studies are needed to address how pharmacological intervention can aid the protective responses in the hydrocephalic brain.

Table 1. Biochemical and histologic assays performed on hydrocephalic rats

	Neonatal (1 week)	Infantile (2-3 weeks)	Juvenile (6 weeks)
Biochemical assays on cerebrum			
Nitrite		C6, H11	
Thiobarbituric acid reaction		C5, H6	
Catalase / glutathione peroxidase		C5, H6	
VEGF ELISA	C6, H7	C6, H8	
VEGF / HIF1α qRT-PCR		C3, H3	C3, H3
Histologic assessments			
Pimonidazole (hypoxia)		C5, H6	C2, H6
DAF-2A (nitric oxide)		C3, H6	
Nitrotyrosine, HNE, VEGF, HIF1α immunohistochemistry	C8, H5	C10, H7	C10, H7

Age categories are defined in the Methods section. The number of control (C) and hydrocephalic (H) rats are indicated for each type of assessment

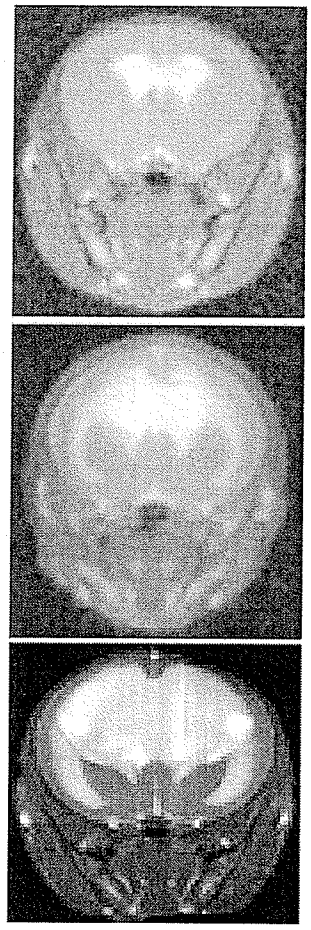

Figure 1. Examples of magnetic resonance (MR) coronal T2-weighted images showing rat brain with early neonatal hydrocephalus at postnatal day 7 (upper), severe infantile hydrocephalus on postnatal day 21 (center), and severe juvenile hydrocephalus on postnatal day 42 (lower).

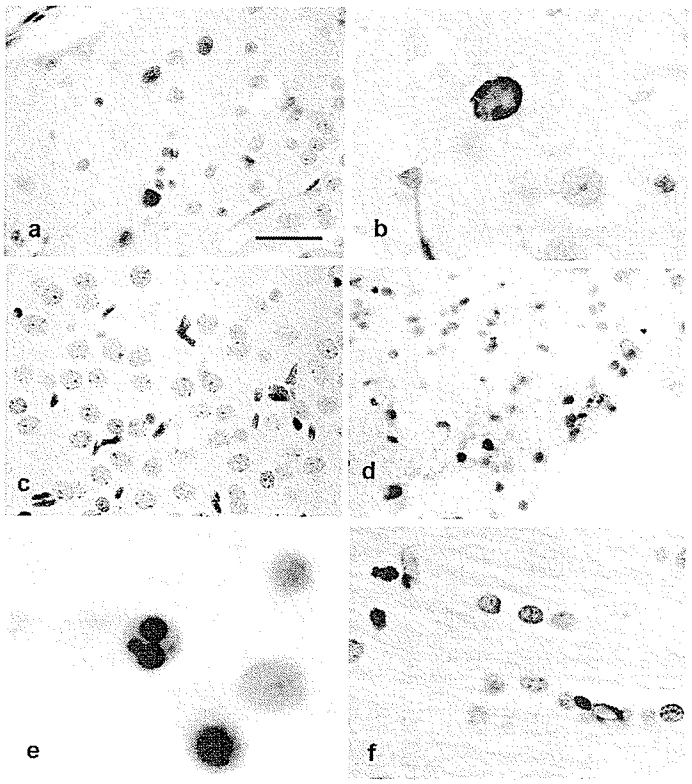

Figure 2. Photomontage showing pimonidazole immunolabeling in hydrocephalic rat brain. Diaminobenzidine reaction product (brown) indicates presence of hypoxic adducts; sections are counterstained with hematoxylin (blue). Labeling is apparent among neurons in cortical layer 5 of a 2-week hydrocephalic rat (a and b). Similar but less frequent labeling was seen in age-matched controls (not shown). Omission of the primary antibody was associated with absence of reaction product (c). In damaged white matter, but not in normal white matter, clusters of labeled cells were present (d). They tended to have round nuclei and rarely appeared among chains of nuclei, suggesting that they are oligodendrocytes. Some labeled cells had nuclear fragmentation (e) suggestive of apoptotic cell death. Also in white matter, capillary profiles were frequently labeled (f). Scale bar (shown in panel a) is 50 μm for panels a, c, d, 25μm for panels d and f, and 12μm for panel e.

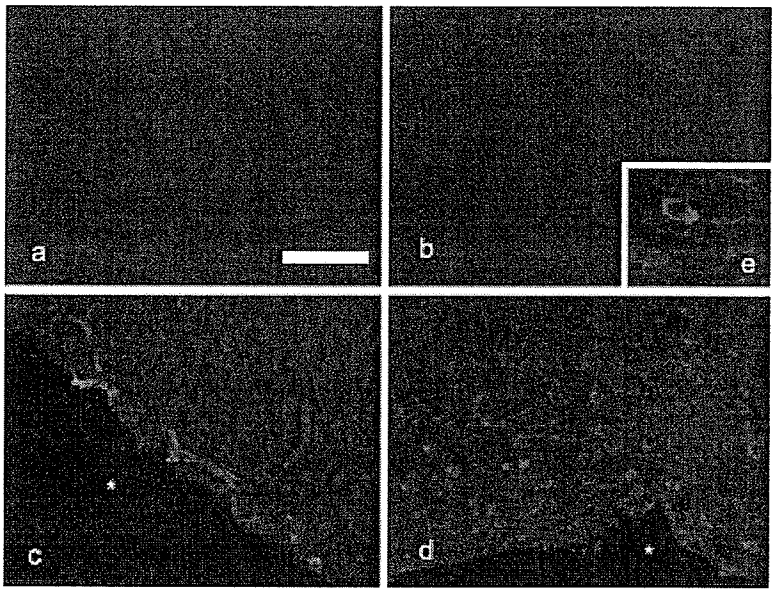

Figure 3. Nitrotyrosine immunofluorescence labeling in hydrocephalic rat brain. Omission of the primary antibody is associated with no labeling in the periventricular white matter or cortex (a). There is no nitrotyrosine labeling in brains of control rats (b; neonatal in this example). In the periventricular white matter of neonatal hydrocephalic brains, cells with morphology of endothelial cells were labeled (c). In the infantile period, nitrotyrosine immunolabeling was present in glial cells in the white matter of hydrocephalic rats (d). The round nuclei and blunt processes are characteristics of oligodendrocytes (e; positive labelling in hydrocephalic pups at all ages). Bar = 100μm for a, b, d and 50μm for c, e. Asterisk (*) represents the lateral ventricle.

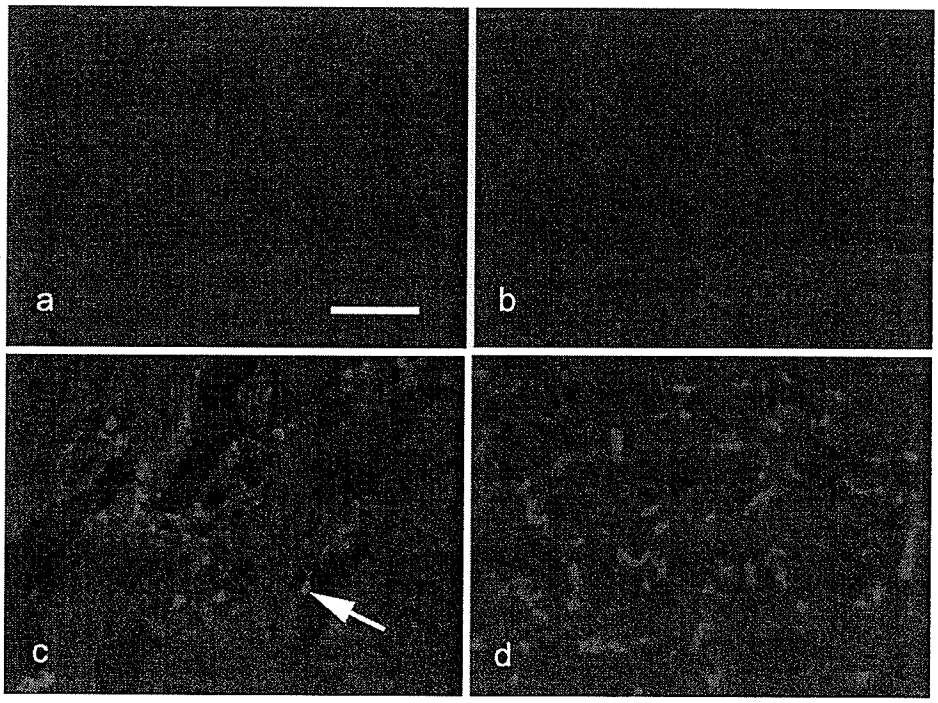

Figure 4. Lipid peroxidation products demonstrated by 4-hydroxy-2-nonenal (HNE) immunofluorescence labeling. Omission of the primary antibody is associated with no labeling in the periventricular white matter or cortex (a). There was no labeling in brains of control rats (b, 21 days in this example). Hydrocephalic neonatal and infantile rats had HNE immunolabeling in the shredded white matter near the dorsolateral angles of the lateral angles (c; 21 days in this example). In the juvenile period, HNE immunolabeled cells were abundant in periventricular white matter (d); based upon their fusiform morphology with few processes, they are likely microglia. Bar = 1003 μm for a, b, c and 503 μm for d.

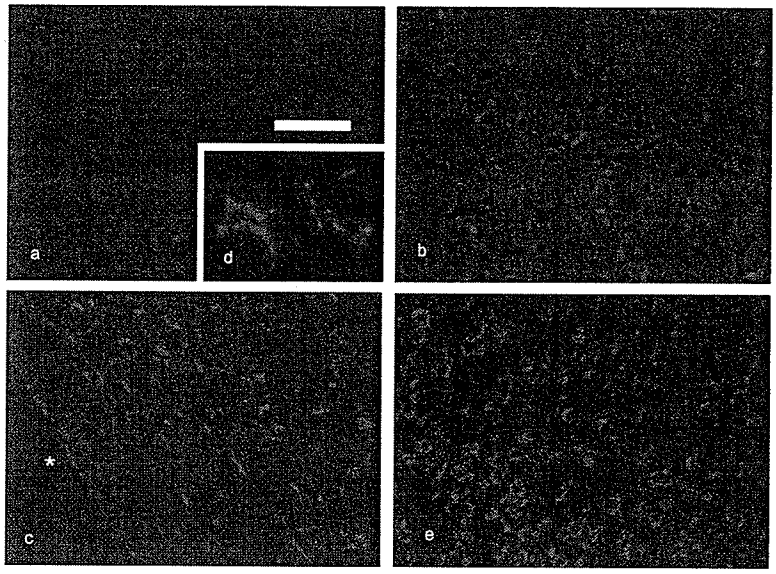

Figure 5. Vascular endothelial growth factor (VEGF) immunofluorescence labeling in rat brain. Omission of the primary antibody was associated with no fluorescence in the periventricular white matter or cortex (a). Control gray matter at 7, 21, and 42 days (b; 42 days in this example) exhibited weak immunolabeling in the cytoplasm of cortical neurons (b). There was no immunoreactivity in white matter of control rats at any age. In hydrocephalic brains VEGF immunoreactivity in white matter was apparent at 7, 21, and 42 days (c). In the latter, the white matter was extremely atrophic. The cells were stellate (d) and their morphology was similar to that of GFAP immunoreactive astrocytes on adjacent sections (not shown). The cytoplasm of cortical neurons remained immunoreactive in hydrocephalic rats at all ages studied (e). Subjectively, this was more intense than in control brains. Bar = 1003 μm for a and b, 503 μm for c and e, and 25 μm for d.

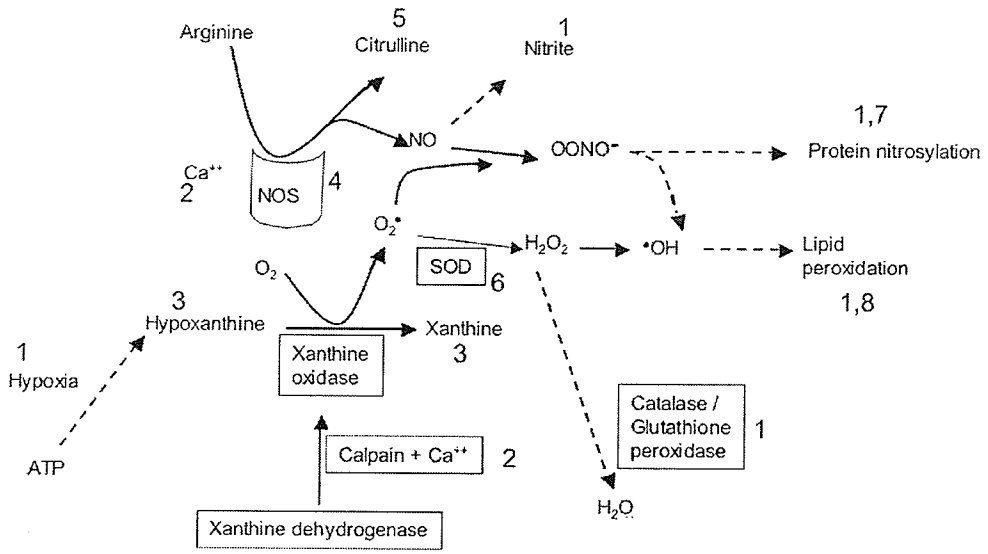

Hypoxia-mediated brain damage in hydrocephalus

Figure 6. Flow chart showing possible sequence of hypoxia-mediated damage in white matter of hydrocephalic brains. The biochemical outline is based upon well-recognized principles. The numbers indicate the references where evidence for each step has been provided. Note that the data do not support upregulation of the antioxidant enzymes superoxide dismutase, catalase, or glutathione peroxidase. Abbreviations: NOS – nitric oxide synthase; SOD – superoxide dismutase. References: 1 – this paper; 2 - (Del Bigio 2000); 3- (Bejar et al. 1983; Levin et al. 1984); 4 - (Klinge et al. 2002); 5 - (Perez-Neri et al. 2007); 6 - (Mori et al. 1993); 7 - (Chow et al. 2005); 8 - (Fersten et al. 2004; Socci et al. 1999)

Chapter 2.3

Magnesium sulfate therapy is of mild benefit to young rats with kaolin-induced hydrocephalus.

This section was published in Pediatric Research 2003 June; 53 (6): 970-976.

Authors: Osaama H. Khan, Terry Enno and Marc R. Del Bigio

Note: Behavioral and immuno-histological experiments completed by Osaama Khan. Biochemical assays were performed by Terry Enno.

ABSTRACT

Hydrocephalus causes damage to periventricular white matter at least in part through chronic ischemia. Magnesium sulfate (MgSO4) has been shown to be protective in various models of neurological injury. We hypothesized that this agent would ameliorate the effects of experimental childhood-onset hydrocephalus. Hydrocephalus was induced in 3- and 4-wk-old rats by injection of kaolin into the cisterna magna. Tests of cognitive and motor function were performed on a weekly basis. In a blinded and randomized manner, MgSO4 was administered in two separate experiments (s.c. injection 0.85, 4.1, or 8.2 mM/kg/d), supplemented by osmotic minipump infusion (0.03 mM/d) to prevent low trough levels for 2 wk, beginning 2 wk after induction of hydrocephalus. The brains were then subjected to histopathological and biochemical analyses. With the 4.1 mM/kg/d dose, serum Mg++ levels were elevated transiently from 1.3 to approximately 7 mM/L. We observed statistically significant improvement in gait performance and reduced astroglial reaction. There was also a trend to improved memory performance, but no evidence of increased myelin or synaptic protein content. The 8.2 mM/kg/d dose was associated with sedation and there was no evidence of improvement in any parameter. We conclude that MgSO4 might be mildly protective in experimental hydrocephalus.

INTRODUCTION

Hydrocephalus is a common neurological condition characterized by pathologic dilation of the cerebral ventricles. It is usually caused by obstruction of cerebrospinal fluid (CSF) flow. Axon damage in the periventricular white matter is one of the earliest pathologic consequences of ventricular dilation in humans and animals [29]. The pathophysiology of hydrocephalus-induced brain damage is multifactorial, with contributions made by gradual physical stretching, compression, ischemia and possible accumulation of metabolic waste products [31]. It has been postulated that physical trauma and ischemic injury to axons combine to alter membrane permeability leading to local influx of calcium and activation of calpains, which can cause proteolytic damage to the axonal cytoskeleton [8]. Magnesium is a calcium antagonist that blocks NMDA channel receptors in a voltage dependent manner, as well as voltage and receptor-operated calcium channels [122, 123]. Magnesium sulfate therapy reduces lipid peroxidation after experimental spinal cord injury [124], long-term hypoxic-ischemic brain damage in 7-d-old rat [125], and the volume of traumatic brain lesions [126]. It also facilitates recovery of function following electrolytic cortical injury [127]. Magnesium may act as a cerebral vasodilator thereby improving the cerebral circulation [128] and preventing cell damage. Clinically, magnesium sulfate is used for seizure prophylaxis in the management of pregnant women with eclampsia. Some reports suggest that this treatment

is associated with reduced incidence of cerebral palsy in low birth weight infants [129].

In an experimental model of hydrocephalus induced by injection of kaolin into the cisterna magna of immature rats we have previously demonstrated the presence of abnormal quantities of soluble ionic calcium and activated calpains in the periventricular white matter [8]. Diminished blood flow has been demonstrated in the white matter of hydrocephalic rats [130]. We hypothesized that administration of magnesium sulfate to young rats could ameliorate the abnormalities associated with moderate to severe early onset hydrocephalus.

METHODS

All animals were treated in accordance with guidelines set forth by the Canadian Council on Animal Care. The experiments were approved by the local animal use committee. All efforts were made to minimize suffering and the number of animals used. The experimental protocol is summarized in Fig. 1 and detailed below.

Animal preparation.

Sprague Dawley rats were bred locally and 62 males were delivered after weaning at age 3 wk (weight 39–63 g). In the 1st experiment behavior testing was done before hydrocephalus induction. In the 2nd experiment rats were injected with kaolin immediately upon arrival, effectively 1 wk earlier than in the first experiment. Anesthesia was induced by intramuscular injection of ketamine/xylazine (90/5 mg/kg). The neck was shaved and, under aseptic conditions, a 27-gauge needle was inserted percutaneously into the cisterna magna. Sterile kaolin suspension (0.04 mL; 250 mg/mL in 0.9% saline) was injected slowly to induce hydrocephalus. In response to this quantity of kaolin, young rats experience gross enlargement of the cerebral ventricles and head and typically die within 6 wk. Controls received a sham injection with needle insertion only. Blood samples were taken from the tip of the rat's tail under anesthesia before kaolin injection to obtain a baseline serum magnesium level (using Hitachi 737 Clinical Chemistry Autoanalyzer). Two to three rats were housed in standard cages and provided with a normal 12-h day/night lighting schedule with free access to water and pelleted food. As the rats became impaired, moistened food and water were provided on the cage floors.

Magnetic resonance imaging and assignment to treatment group.

Magnetic resonance (MR) studies were performed using a Bruker Biospec/3 MR scanner equipped with a 21-cm bore magnet operating at a field of

7 T (Karlsruhe, Germany) to obtain T2-weighted images of the brain in the coronal plane. The widths of the lateral ventricles and cerebrum were measured in the rostral cerebrum immediately anterior to the third ventricle. Frontal horn size was expressed as a ratio determined by dividing the total width of the ventricles by the width of the cerebrum. These methods have been previously described in detail [38, 39]. Rats underwent MR imaging no more than 24 h before commencement of drug treatments. After imaging (Fig. 2), the rats were stratified according to ventricle size index and assigned alternatively to drug treatment or control groups. Rats underwent MR imaging 2 wk later, no more than 24 h before sacrifice.

Preparation and administration of MgSO4.

In previously published work, short-term administration of 2.2–2.5 mM/kg/d MgSO4 benefited young rats with hypoxic-ischemic brain injury [125, 131] and 2.2–5.0 mM/kg/d benefited adult rats with quinolinate or hypoglycemia-induced brain injury [132-134]. Magnesium sulfate has a short half-life after bolus administration therefore we wanted to prevent low trough levels by continuous administration *via* osmotic minipumps. Sterile solutions of high (2.4 mM, saturated) and low dose (0.5 mM) MgSO4 and saline control (2.4 mM) were prepared. Osmotic minipumps (Alzet model 2002, rated at 12.5 _L/d _ 14 d;

DURECT Corp., Cupertino CA, U.S.A.) delivered the high dose solution at 0.03 mM/d. Assuming body weights of ~160g at the onset of treatment, this equals 0.2 mM/kg/d. Osmotic minipumps were preloaded by the senior author and provided to the animal handlers in a blinded manner. The rats were anesthetized with ketamine/xylazine and pumps were implanted s.c. on the back under aseptic conditions. The treatment code was not broken until all behavioral, structural, and biochemical analyses were complete. To achieve doses comparable to those therapeutic in other studies, we needed to add supplemental boluses daily. Using the same solutions, syringes were loaded in a blinded manner and 0.85 or 4.1 mM/kg/d was injected s.c. every morning. Tail blood was obtained various times after injection at the time of sacrifice to determine roughly the kinetics of magnesium in blood. In experiment 1 a single daily bolus did not keep serum magnesium trough levels elevated. Because the results showed a potential dose dependent benefit, a second experiment was performed with two groups; high dose infusion (2.4 mM) combined with 2 daily injections of MgSO4 (total dose 8.2 mM/kg/d) compared with saline infusion/bolus control. The rats in this experiment were injected with kaolin 1 wk earlier (average weight 52.7g) than in the first experiment.

Behavioral testing.

The outcome measures and testing protocols are the same as those described in prior drug treatments of young rats with hydrocephalus [39]. All testing was done in a blinded manner. The rats were weighed twice per week. On a weekly basis, beginning before kaolin injection in experiment 1, or after kaolin injection in experiment 2, several specific behavioral tests were performed. The rats were always tested in the same order and a given rat was tested at the same time of the day from week to week. On the first testing day of each week, swimming speed was tested in a 20-cm-deep 15-cm-wide water trough by measuring the time to swim 150 cm. Memory was then assessed in a modified water maze test using a 90-cm pool (filled with 22°C opacified water) that contained a 13-cm-round hidden platform 1 cm below the water surface as previously described [38, 51]. Testing took place in a dimly lit room with a single wall illuminated to provide directional cues. The rats were placed in the center of the pool and allowed to swim until they found the platform. A trial consisted of four attempts to find the platform, each attempt beginning with the rat facing a different quadrant. If the rat failed to complete the task in 60 s, it was given a 30-s rest period before the next attempt. Three trials were performed during the course of the day; each was separated by a 3-h interval. The times of the 4 attempts were averaged for each trial.

On the second testing day of each week, the rats were observed in an open field situation for a period of 1 min to assess arousal, grooming, and gait by using a previously validated set of parameters [135]. Quantitative monitoring of

spontaneous activity was then performed for 10 min in a square enclosure (43 _ 43 cm) with 15 infrared beams (spaced every 3 cm) along the floor in each of two horizontal directions and a third set of similarly spaced beams 8.5 cm above the floor (Opto-Varimex; Columbus Instruments, Columbus OH, U.S.A.). Vertical, total, and ambulatory beam breaks were counted, the latter being defined as an interruption in a series of adjacent beams. Finally, gait agility was assessed using a rotating cylinder (7-cm diameter) (Economex, Columbus Instruments) in 2 separate trials. First, endurance at a constant speed of 5 rpm was assessed for a maximum of 2 min. Second, we measured the ability to stay on the cylinder, which accelerated beginning at 2.5 rpm and increasing at a rate of 0.1 rpm every second for up to 2 min. The time was recorded from the moment the rat was placed on the rotating cylinder until it fell off. The rotating cylinder test is complex and involves proprioceptive, tactile, vestibular, and motor functions.

Histopathological and biochemical studies of brains following drug treatments.

At the end of the 2-wk drug treatment period and following the final MR imaging session, the rats were given an overdose of ketamine/xylazine (90:5 mg/kg), blood was drawn for magnesium level analysis, the vascular system cleared by transcardiac perfusion with ice-cold 0.1M PBS, and the brains were removed quickly. The cerebral hemispheres were spread apart to facilitate

dissection of the corpus callosum from one side. Samples of the corpus callosum, parietal and frontal cerebrum, hippocampus, and cerebellum were dissected and frozen in liquid nitrogen, after which they were stored at _80°C. The remaining pieces were immersion fixed in 10% buffered formalin. The anterior cerebrum, cut coronally at the level of the optic chiasm, was embedded in paraffin. Sections (6 _m thickness) were stained with solochrome cyanine for visualization of myelin. Corpus callosum thickness was measured in the midline and adjacent to the cingulum. As described previously in detail [5, 14], frontal cerebrum homogenates were used to quantify glial fibrillary acidic protein (GFAP), synaptophysin, and myelin basic protein (MBP) by using Western blots. Corpus callosum homogenates were used to assay the myelin related enzyme *p*-nitrophenylphosphorylcholine phosphocholine phosphodiesterase (PNPP), and the oligodendrocyte-related enzyme ceramide galactosyltransferase (CGalT) by biochemical means. Two or three replicated studies were performed to ensure reproducibility and allow meaningful statistical analysis.

Statistical analysis.

Data are presented as mean ± SEM. For Western blots, the densitometric values were normalized to those of control values and percent changes relative to control are indicated. They were analyzed by nonparametric methods, either Mann-Whitney test or Kruskall-Wallis test as appropriate for the number of

groups. Quantitative behavioral data were analyzed to confirm a normal distribution. Statistical analysis then consisted of two-tailed *t* test or ANOVA with posthoc Fisher least square difference calculations for inter-group comparisons, as appropriate. To take into consideration multiple tests, statistical significance was defined as p _ 0.03. Software used was StatView 5 (SAS Institute; Cary NC, U.S.A.). Power was calculated using the online Power Calculator tool (http://ebook.stat.ucla.edu/calculators/powercalc/).

RESULTS

Experiment 1.

For the final analysis 24 rats were used (8 saline, 8 low dose, 8 high dose). Excluded from the analysis were 1 rat that died during kaolin injection, 5 that died of uncertain cause, and 1 that was euthanized during drug treatment because of severe neurologic deficits. There was no obvious adverse effect of the MgSO4 in these rats. The average pretreatment serum Mg^{++} level was 1.13 _ 0.01 mM/L. Samples taken the day of sacrifice showed that Mg^{++} levels were high (>7 mM/L) for only the first 120 min (Fig. 3). Morphologic and biochemical analysis of brains from hydrocephalic rats at the end of the experiment revealed no statistically significant difference between the groups for body weight, ventricle size, PNPP, CGalT, MBP, and synaptophysin (Table 1). The high dose group (4.1 mM/kg/d) performed better on the accelerating rotating cylinder (p = 0.0248) and tended to perform better on the continuous speed cylinder and in the

water maze test (Figs. 4 and 5). Corpus callosum thickness showed a trend in improvement. The power of these tests is in the range of 0.25–0.30; to increase the power to 0.80 would require sample size of ~35 per group. There was a statistically significant reduction in reactive gliosis as indicated by GFAP content in the frontal cerebrum ($p < 0.02$).

Experiment 2.

We conducted the second experiment to determine whether higher MgSO4 doses (8.2 mM/kg/d) could protect rats more effectively. For the final analysis 21 rats were used (4 nonhydrocephalic control, 10 saline, 7 high dose). Excluded from this experiment were 2 rats that died during kaolin injections, 1 that died of unknown cause during drug treatment, 3 that were euthanized before drug treatment, and 3 that were euthanized during drug treatment due to severe neurologic deficits. Also, 2 rats that we thought were likely to die due to severe early neurologic deficits were treated in an unblinded manner with high dose MgSO4. One of these rats survived until the end of the experiment, however, neither are included in the final analysis. The high dose MgSO4 injections were associated with profound lethargy and sedation for 1–2 h after the boluses. In contrast to experiment 1, serum Mg^{++} levels were significantly elevated ($p < 0.02$) in the treated group in the early trough phase, 3–6 h after the bolus.

Morphologic and biochemical analysis of brains from hydrocephalic rats at the end of the experiment revealed no statistically significant difference between the groups for any of the parameters tested (Table 2). The treated group had a tendency to perform worse on the rotating cylinder; the sedative effect of the MgSO4 likely played a role. The GFAP protein quantity tended to decrease in the high dose MgSO4 group.

DISCUSSION

These experiments using young rats with kaolin-induced hydrocephalus show that MgSO4 treatment, in a dose dependent manner, has a mild protective effect, but that high doses are associated with adverse effects, particularly sedation. The serum concentrations of Mg^{++} achieved here have previously been shown to be associated with increased levels of Mg^{++} in brain tissue [136]. MgSO4 treatment can inhibit the intracellular Ca^{++} increase following experimental head trauma [137] and can protect the traumatized brain when administered as late as 24 h after the injury [138, 139]. We have previously shown that calcium-activated proteolysis (activated calpain) is associated with the axonal injury in experimental hydrocephalus [8]. Therefore Mg^{++} might prevent activation of calpains by antagonizing Ca^{++} movements into damaged axons. Alternately, like nimodipine, which is protective to a greater degree than MgSO4 in this experiment [39], Mg^{++} might enhance cerebral blood flow [128],

thereby reducing the white matter damage caused by hydrocephalus. In both trials, MgSO4 treated hydrocephalic rats had reduced GFAP content in the cerebrum, suggesting that there was less reactive astroglial change due to hydrocephalus [29]. It is possible that this is due to a reduced axon injury stimulus, or perhaps it reflects a direct effect of Mg^{++} on astrocytes; in culture Mg^{++} causes increased proliferation of glial precursors but not mature astrocytes [140], and Mg^{++} can modulate amino acid fluxes in astrocytes [141]. An obvious shortcoming of this experiment was that MgSO4 at high doses caused sedation in the rats. This may have obscured a protective effect on behavior. However, we did not observe structural or biochemical protection therefore this dose was likely without benefit. We do not know if the protection conferred by MgSO4 is permanent. It would be useful to determine the effect by extending the experiment following discontinuation of the drug; however, because hydrocephalus is progressive new damage would be incurred. The reverse experiment, in which hydrocephalic rats are deprived of dietary Mg^{++} would also be of use for understanding interactions with Ca^{++}. Direct measurements of brain Mg^{++} would help interpretation of all these experiments. In conclusion, we find that MgSO4 provides mild protection against brain damage in a rat model of childhood-onset hydrocephalus. However, we cannot recommend this for therapy in humans at this time. It should be noted that a recent study showed antenatal MgSO4 in preterm labor was associated with adverse neurologic outcome, in contrast to expectations [142]. We will continue to explore

pharmacological approaches that might be used as a supplement to shunt treatment of hydrocephalus.

Table 1. *Results of magnesium sulfate treatment in hydrocephalic rats (experiment 1)*

	Control saline (4.1 mM/kg/day)	Low $MgSO_4$ (0.85 mM/kg/day)	High $MgSO_4$ (4.1 mM/kg/day)
Sample size	8	8	8
Ventricle area index (pre-treatment)	0.215 ± 0.045	0.229 ± 0.044	0.195 ± 0.016
Ventricle area index (post-treatment)	0.344 ± 0.062	0.302 ± 0.074	0.291 ± 0.042
Body weight (g) (pre-treatment)	156 ± 10	179 ± 9	174 ± 8
Body weight (g) (post-treatment)	240 ± 13	269 ± 13	256 ± 8
Swim time (s) 150 cm (post-treatment)	15.3 ± 1.5	13.3 ± 2.7	10.2 ± 1.2
Modified water maze test (post-treatment, 1st trial) (s)	25.9 ± 9.6	18.9 ± 10.6	11.9 ± 7.9
Modified water maze test (post-treatment, 3rd trial) (s)	15.6 ± 6.7	18.8 ± 10.7	5.43 ± 3.2
Ambulatory activity (post-treatment) (beam breaks in 15 min)	1670 ± 464	1472 ± 429	1022 ± 238
Endurance on roller (continuous speed, post-treatment) (s)	48.7 ± 16.5	76.7 ± 21.2	75.6 ± 21.4
Endurance on roller (accelerating speed, post-treatment) (s)	13.6 ± 7.7	28.6 ± 9.2	51.6 ± 14.8*
Corpus callosum thickness (μm)	134 ± 39	222 ± 49	225 ± 54
CGalT activity corpus callosum (nM/mg protein/h)	1.25 ± 0.27	1.16 ± 0.11	1.41 ± .27
PNPP activity corpus callosum (nM/mg protein/h)	82.1 ± 9.0	76.9 ± 5.0	99.3 ± 17.8
MBP frontal cerebrum (arbitrary densitometric units)	1.00 ± 0.14	1.01 ± 0.15	0.84 ± 0.13
Synaptophysin frontal cerebrum (arbitrary densitometric units)	1.00 ± 0.02	1.09 ± 0.06	1.06 ± 0.088
GFAP frontal cerebrum (arbitrary densitometric units)	1.00 ± 0.08	0.76 ± 0.09	0.69 ± 0.10†

All data are expressed as mean ± standard error of the mean.
* $p = 0.0248$ high dose vs. control. ANOVA with post hoc Fisher least square difference test for intergroup comparisons.
† $p = 0.0213$ high dose vs. control hydrocephalic, Kruskall-Wallis test for nonparametric data.
Pre-treatment—data obtained immediately before starting drug treatment, 2 weeks after kaolin injection ~ 6 weeks age.
Post-treatment—data obtained immediately before starting drug treatments, 4 weeks after kaolin injection at ~ 8 weeks age.

Table 2. *Results of magnesium sulfate treatment on hydrocephalic rats (experiment 2)*

	Control saline (4.1 mM/kg twice/day)	$MgSO_4$ (4.1 mM/kg twice/day)	Nonhydrocephalic controls
Sample size	10	7	4
Ventricle area index (pre-treatment)	0.199 ± 0.029	0.206 ± 0.023	–
Ventricle area index (post-treatment)	0.213 ± 0.023	0.198 ± 0.022	0.001 ± 0.0001
Body weight (g) (pre-treatment)	127 ± 4	131 ± 5	148 ± 11
Body weight (g) (post-treatment)	221 ± 9	231 ± 11	281 ± 16
Swim time (s) 150 cm (post-treatment)	15.9 ± 1.7	19.0 ± 3.2	14.0 ± 2.0
Modified water maze test (post-treatment, 1st trial) (s)	5.3 ± 1.3	8.7 ± 3.6	4.9 ± 1.1
Modified water maze test (post-treatment, 3rd trial) (s)	2.8 ± 0.4	3.4 ± 0.4	2.1 ± 0.1
Ambulatory activity (post-treatment) (beam breaks in 15 min)	922 ± 117	592 ± 240	1128 ± 300
Endurance on roller (continuous speed, post-treatment) (s)	120 ± 0.0	67.1 ± 18.9	119.3 ± 0.75
Endurance on roller (accelerating speed, post-treatment) (s)	75.3 ± 11.3	55.8 ± 18.7	90.3 ± 13.2
Corpus callosum thickness (μm)	313 ± 28	296 ± 25	390 ± 74
CGalT activity corpus callosum (nM/mg protein/h)	2.77 ± 0.14	2.90 ± 0.12	2.52 ± 0.13
PNPP activity corpus callosum (nM/mg protein/h)	69.3 ± 4.1	80.6 ± 4.3	83.9 ± 1.1
MBP frontal cerebrum (arbitrary densitometric units)	1.00 ± 0.12	0.85 ± 0.22	1.07 ± 0.16
Synaptophysin frontal cerebrum (arbitrary densitometric units)	1.00 ± 0.07	0.94 ± 0.08	0.93 ± 0.08
GFAP frontal cerebrum (arbitrary densitometric units)	1.00 ± 0.11	0.75 ± 0.09	0.59 ± 0.10
Serum magnesium (mM/L)†	1.3 ± 0.2	1.6 ± 0.06‡	1.2 ± 0.3

All data are expressed as mean ± standard error of the mean.
* $p < 0.0001$ normal rats vs. both hydrocephalic groups. ANOVA with post hoc Fisher least square difference test for intergroup comparisons.
† 300 min following last bolus.
‡ $p < 0.02$ high dose $MgSO_4$ vs. control hydrocephalic. Student t test.

Note: From Khan et. al; Pediatric Research 2003 June; 53 (6): 970-976.

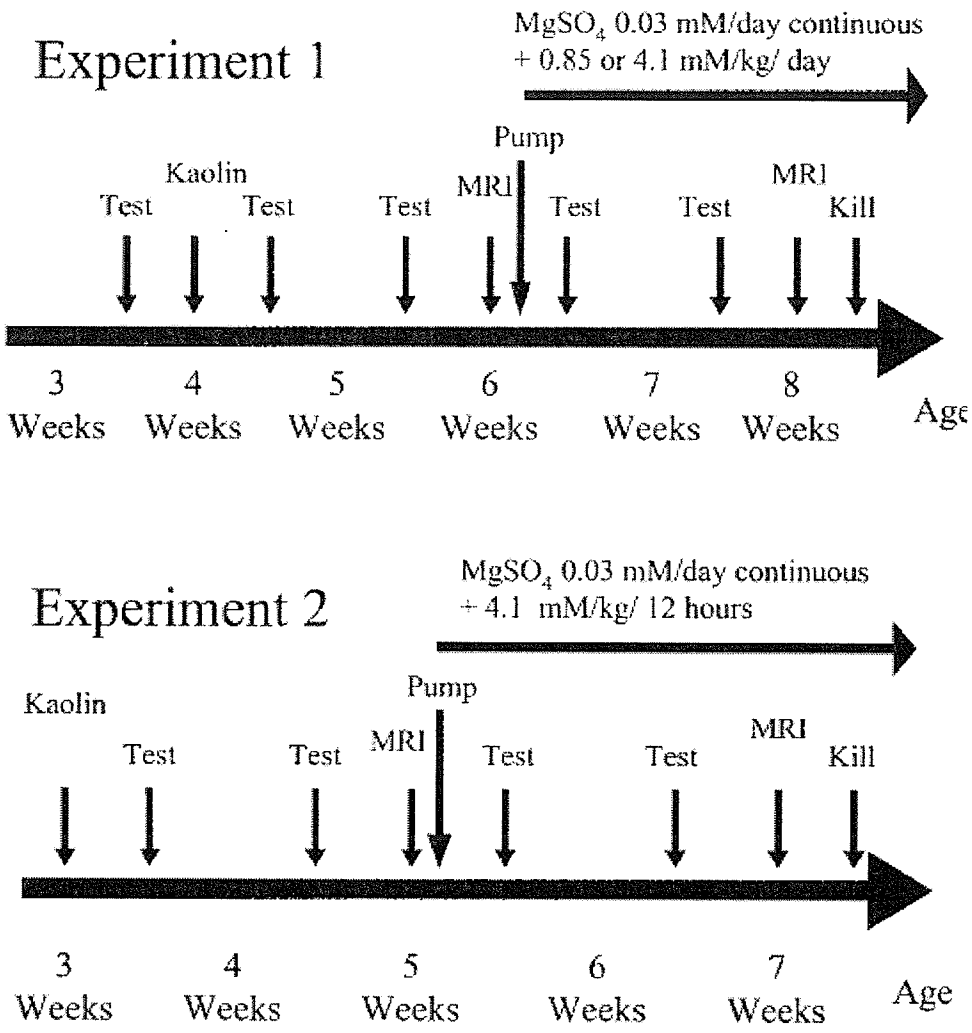

Figure 1. Line diagrams showing experimental design for MgSO4 treatment of hydrocephalic rats. The age of the rats is shown below the line and the drug dose is shown above the upper arrow. In experiment 1, weekly behavior testing (Test) was started before kaolin injection (Kaolin) whereas in experiment 2 kaolin was injected soon after weaning. Magnetic resonance imaging (MRI) was done before implantation of infusion pumps (Pump) and treatment onset. The final MRI was done no more than 24 h before sacrifice (Kill).

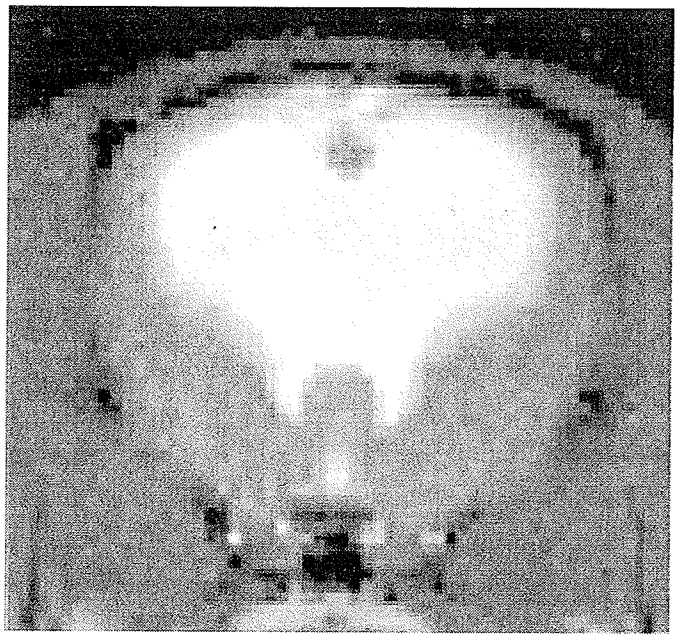

Figure 2. A typical magnetic resonance image (T2-weighted) through the frontal cerebrum (coronal slice) of a hydrocephalic rat at the end of experiment 2. Moderately severe ventricular enlargement is apparent.

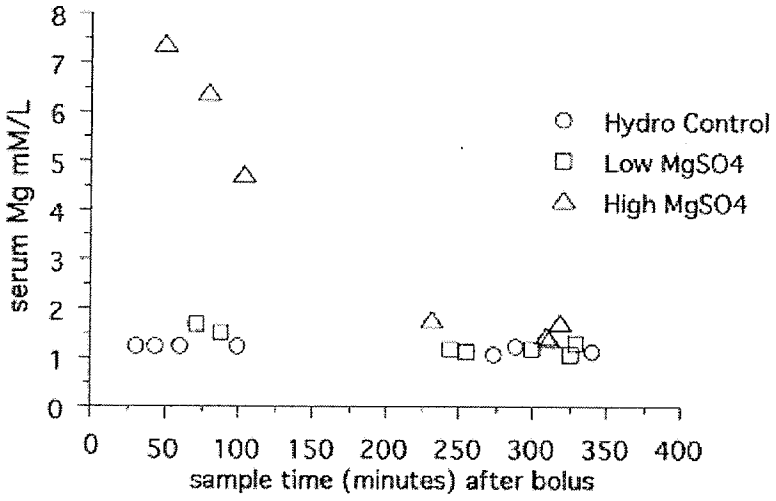

Figure 3. Scatter plot showing serum Mg levels taken at different times after last injection of MgSO4 or vehicle control in experiment 1. Mg levels were substantially elevated for 120 min, and returned to normal levels by 230 min.

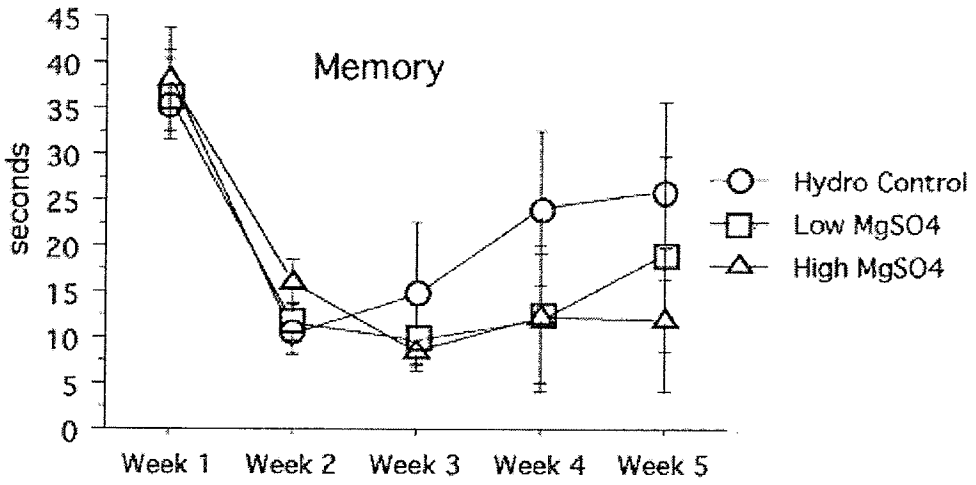

Figure 4. Line graph showing latency times (in seconds) to finding the hidden platform in the water maze test on the first (morning) trial of each weekly assessment in experiment 1. Week 2 and week 3 correspond to the period of hydrocephalus onset. Drug treatment was administered during week 4 and week 5. At the end of week 5, the high dose MgSO4 group tended to perform better than the untreated hydrocephalic controls (p = 0.3065).

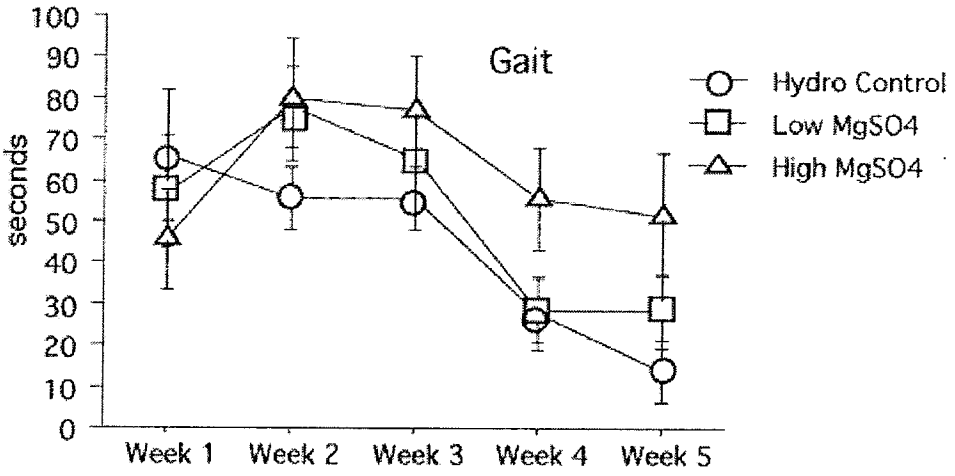

Figure 5. Line graph showing time (in seconds) spent on the accelerating rotating cylinder of each weekly assessment in experiment 1. In the final week the high dose MgSO4 group performed better than untreated hydrocephalic controls (p= 0.0248).

Chapter 2.4

Tacrolimus and cyclosporine A are of no benefit to young rats with kaolin-induced hydrocephalus.

This section was published in Pediatric Neurosurgery 2003 December; 39 (6):309-313.

Authors: Osaama H Khan, Terry Enno and Marc R. Del Bigio

Note: Behavioral and immuno-histological experiments completed by Osaama Khan. Biochemical assays were performed by Terry Enno.

ABSTRACT

Hydrocephalus causes damage to periventricular axons. Tacrolimus, cyclosporine A (CsA) and calpain inhibitors have been shown to protect axons in rat models of acute traumatic brain injury. We hypothesized that these agents would ameliorate the axon damage and behavioral effects in experimental hydrocephalus. Hydrocephalus was induced in 3-week-old rats by injection of kaolin into the cisterna magna. Tests of cognitive and motor function were performed on a weekly basis. In a blinded and randomized manner, tacrolimus (FK506; 3.6 mg/kg body weight) or CsA (10 mg/kg) was administered once daily by subcutaneous injection for 2 weeks, beginning 2 weeks after induction of hydrocephalus. In a separate experiment, calpain inhibitor I (10 mg/kg/day) was administered by continuous subcutaneous infusion. The brains were subjected to histopathological and biochemical analyses after 2 weeks of treatment. There was no statistically significant protection in regard to behavior, brain structure or brain composition in any of the experiments. However, there was biochemical and histological evidence of renal injury following chronic tacrolimus and CsA administration. Calcineurin inhibition does not offer significant protection in this rat model of hydrocephalus.

INTRODUCTION

Hydrocephalus is a common neurological condition characterized by pathological dilation of the cerebral ventricles due to obstruction of cerebrospinal fluid flow. Axon damage in the periventricular white matter is one of the earliest pathological consequences of ventricular dilation [29]. It has been postulated that physical trauma and ischemic injury to axons combine to alter membrane permeability leading to local influx of calcium and activation of calpains, which can cause proteolytic damage to the axonal cytoskeleton [8]. Tacrolimus (FK506) and cyclosporine A (CsA) are immunophilin ligands used clinically for the prevention of allograft rejection. Their potential role in nervous system injury arose from the observation that immunophilins are more abundant in brain cells than in immune cells. They inhibit calcineurin, a calcium-dependent phosphatase that regulates entry of transcription factors into the nucleus [143]. Cain, an endogenous inhibitor of calcineurin, can be cleaved by calpain; loss of inhibition activates calcineurin to mediate calcium-triggered cell death [144]. Tacrolimus and CsA administered by daily intraperitoneal injections reduce the white matter injury in a rat model of chronic brain ischemia [145, 146]. Tacrolimus protects against axonal injury in rats following brain impact-acceleration [147] and increases survival of neurons in rats with transient global cerebral ischemia [148] and focal ischemia [149]. It also improves axon survival in rats after spinal cord injury [150]. CsA, but not tacrolimus, additionally blocks the mitochondrial permeability transition pore, which is considered to be an important mediator of

apoptosis and necrosis [151, 152]. CsA has been shown to significantly ameliorate axonal damage in a controlled cortical impact model of traumatic brain injury [153], possibly through prevention of calpain activation [154]. Calpain inhibitors, following central and peripheral administration, can reduce brain damage in a variety of animal models [155-157]. Because calcium-mediated axonal damage occurs in hydrocephalus, and calpains or calcineurin might play a role, we hypothesized that chronic administration of tacrolimus, CsA or calpain inhibitor I could ameliorate the behavioral and structural abnormalities associated with severe early-onset hydrocephalus in rats. Drug treatment for infantile hydrocephalus might be a useful supplement to shunting when shunting cannot be performed immediately. Because the axon damage is gradual in hydrocephalus, we predicted that chronic administration of the agents would be necessary for protection, as we have shown in prior experiments [39, 41]. We selected doses based upon the experiments of others in which the agents were shown to protect brain when administered intraperitoneally or subcutaneously [145, 146, 157].

METHODS

Animal Preparation

All animals were treated in accordance with guidelines put forth by the Canadian Council on Animal Care. The experiments were approved by the local

animal use committee. Male Sprague-Dawley rats (total n = 80) were bred locally and delivered after weaning at the age of 3 weeks (weight 45–55 g). Anesthesia was induced by intramuscular injection of ketamine-xylazine (90 and 5 mg/kg, respectively). The neck was shaved and, under aseptic conditions, a 27-gauge needle was inserted percutaneously into the cisterna magna. Sterile kaolin suspension (0.04 ml, 250 mg/ml in 0.9% saline) was injected slowly. Nonhydrocephalic controls received a sham injection with needle insertion only. In response to this quantity of kaolin, young rats experience gross enlargement of the cerebral ventricles and head and die within 6 weeks. Two or three rats were housed in standard cages with a 12-hour day/night lighting schedule and free access to water and pelleted food. As the rats became impaired, moistened food and water were provided on the cage floors.

Magnetic Resonance Imaging and Assignment to Treatment Group

Magnetic resonance (MR) studies were performed using a Bruker Biospec/3 MR scanner equipped with a 21-cm bore magnet operating at a field of 7 T (Karlsruhe, Germany) to obtain T2-weighted images of the brain in the coronal plane. The widths of the lateral ventricles and cerebrum were measured in the rostral cerebrum immediately anterior to the third ventricle. Frontal horn size was expressed as a ratio determined by dividing the total width of the

ventricles by the width of the cerebrum. These methods have been previously described in detail [39]. Rats underwent MR imaging no more than 24 h before commencement of drug treatments. After imaging, the rats were stratified according to ventricle size index and assigned alternately to drug treatment or control groups. The treatment code was not broken until all behavioral, structural and biochemical analyses were complete. Rats underwent MR imaging 2 weeks later, no more than 24 h prior to sacrifice.

Drug Preparation and Administration

Tacrolimus (Fujisawa Canada Inc.) was dissolved in a Cremophor RH 60 (BASF Corporation). In a preliminary 5-week experiment (33 rats), we injected 0.5 (11 rats) or 3.0 (12 rats) mg/kg/day of tacrolimus subcutaneously. We did not observe a statistically significant benefit in comparison to controls (10 rats) (data not shown). Therefore, we conducted this experiment with a higher dose of 3.6 mg/kg/day. Using the same vehicle, CsA (Novartis Pharma Canada Inc.) was dissolved for administration at a dose of 10 mg/kg/day. Drugs and vehicle controls were prepared by the senior author, loaded into syringes and supplied in a blinded manner for subcutaneous injection. In a separate experiment, calpain inhibitor I (N-acetyl-*L*-leucyl-*L*-leucyl-*L*-norleucinol; Sigma) was dissolved in 70% ethanol-30% water and loaded into Alzet mini-osmotic pumps (Model 2ML2, DURECT Corp., Cupertino, Calif., USA) for subcutaneous implantation and

administration at a starting dose of 10 mg/kg. These rats (n = 7) were compared to control rats that received vehicle infusion only (n = 7). Blood samples were taken from the tip of the tail before kaolin injection to obtain baseline blood urea nitrogen and creatinine levels (using Hitachi 737 Clinical Chemistry Autoanalyzer).

Behavioral Testing

On a weekly basis, several specific behavioral tests were performed as previously described [39, 158]. On the first day of the week, swimming speed and memory were assessed in a modified water maze test. On the second testing day, rats were observed in an open area field where arousal, grooming and gait were assessed using a previously validated set of parameters [135]. Quantitative monitoring of spontaneous activity was then performed for 10 min; vertical, total and ambulatory beam breaks were counted (Opto-Varimex, Columbus Instruments, Columbus, Ohio, USA). Gait agility was assessed by the ability to stay on a rotating cylinder (Economex, Columbus Instruments) in 2 separate trials. First, endurance was assessed at a constant speed of 5 rpm for a maximum of 2 min. Second, we recorded the time on the cylinder as it accelerated for up to 2 min. The rats were weighed twice a week and were always tested in the same order.

Histopathological and Biochemical Studies of Brains following Drug Treatments

At the end of the 2-week drug treatment period and following the final MR imaging session, rats were given an overdose of pentobarbital, and blood was drawn for urea nitrogen, creatinine, bilirubin and lactate dehydrogenase level analysis as well as complete blood count. The vascular system was cleared by transcardiac perfusion with icecold .1 *M* phosphate-buffered saline and the brains were removed quickly. The cerebral hemispheres were spread apart to facilitate dissection of the corpus callosum. Samples of the frontal corpus callosum, parietal cerebrum and hippocampus were dissected and frozen in liquid nitrogen. They were stored at –80° C. The remaining brain pieces, along with kidney and liver from 11 rats (5 control, 2 tacrolimus, 1 cyclosporine, 3 calpain inhibitor), were immersion fixed in 10% buffered formalin. The anterior cerebrum, cut coronally at the level of the optic chiasm, was embedded in paraffin. Brain sections (6-Ìm thickness) were stained with solochrome cyanine for visualization of myelin. Corpus callosum thickness was measured in the midline and adjacent to the cingulum. As described previously in detail [14, 39], cerebrum homogenates were used to quantify glial fibrillary acidic protein (GFAP), synaptophysin and myelin basic protein (MBP) by using Western blots. Corpus callosum homogenates were used to assay the myelin-related enzyme p-

nitrophenylphosphorylcholine phosphocholine phosphodiesterase (PNPP) and the oligodendrocyte-related enzyme ceramide galactosyltransferase (CGalT) by biochemical means. Two or three replicated studies were performed to ensure reproducibility and allow meaningful statistical analysis.

Statistical Analysis

Data are presented as mean ± standard error of the mean. For Western blots, the densitometric values were normalized to those of control values, and percentage changes relative to control are indicated. They were analyzed by the nonparametric Kruskal-Wallis test or Mann-Whitney U test. Quantitative behavioral data, ventricle size data and biochemical assay were analyzed to confirm a normal distribution. Statistical analysis then consisted of ANOVA with post hoc Scheffé calculations for intergroup comparisons or unpaired Student t tests. Statistical significance was defined as $p < 0.05$. Software used was StatView 5 (SAS Institute, Cary, N.C., USA).

RESULTS

The rats tolerated the procedures reasonably well. In the calcineurin inhibition experiment, 22 hydrocephalic rats (7 vehicle control, 7 tacrolimus and 8 CsA) were used for the final analysis. Excluded from the analysis were 3 rats that died during kaolin injection, 1 that died of an uncertain cause and 3 that were

euthanized during the drug treatment phase because of severe neurological deficits. An additional 4 rats that did not receive kaolin injections were subjected to the behavioral testing, drug injections and biochemical assays as a further control. There were no obvious adverse effects of the drugs in these rats.

In hydrocephalic rats, there was biochemical evidence of damage to myelin (PNPP and MBP), a decrease in synaptophysin and an increase in reactive astrogliosis measured by GFAP in parietal cerebrum compared to normal controls (Table 1). The tacrolimus-treated hydrocephalic rats tended to exhibit less progression of ventricle enlargement and performed slightly better on the roller test but this was not statistically significant. There was no statistically significant difference between the three groups in measures of white matter integrity including CGalT activity, MBP content and corpus callosum thickness (Table 1). Tacrolimus renal toxicity was evident in the form of increased blood urea and creatinine levels. Microscopic examination of kidneys from tacrolimus- and CsA treated rats revealed basophilic concretions in renal tubules at the interface between the cortex and medulla. In the calpain inhibitor I experiment, 1 untreated hydrocephalic rat was euthanized prior to the end of the experiment because of severe neurological deficits. The blood tests and histologic examinations demonstrated no evidence of kidney, liver or marrow toxicity. In comparison to untreated hydrocephalic rats, there was no significant difference in the progression of ventricle size, corpus callosum thickness, weight gain, behavioral tests or biochemical assays of brain tissue (data not shown).

DISCUSSION

These experiments using young rats with kaolin induced hydrocephalus show that neither tacrolimus, CsA nor calpain inhibitor I had a significant protective effect on the function, structure or composition of the brain when administered chronically. We used doses previously shown to be protective in rat models of brain injury. We have also previously shown that all of the parameters measured in the experimental paradigm are potentially protectable by drug intervention, for example by nimodipine [39] and magnesium sulfate [41]. It should be noted that tacrolimus and CsA can inhibit L-type Ca^{2+} channels in a manner similar to nimodipine [159]. Most successful neurological protection studies with tacrolimus and CsA have been on adult rodents. It is possible that the immature brain is less amenable to the effect of these drugs. However, newborn rats show a favorable energy metabolism response to tacrolimus at doses lower than those used here [160]. Furthermore, FK506 binding protein, which complexes with tacrolimus, exhibits no change in avidity from 3 weeks to 24 months in rat brains [161]. Although there are many reports of efficacy, FK506 is not effective in all models of axon injury; for example, it failed to influence optic nerve regeneration in rats [162]. In comparison to the calcineurin inhibitors, which are used in humans for purposes other than brain protection, calpain inhibitors have so far been restricted to experimental situations [163, 164].

This experiment has several shortcomings. The behavioral change due to hydrocephalus was mild despite significant ventricle enlargement and biochemical evidence of brain damage. A study of rats with more severe hydrocephalus might increase the likelihood of detecting behavioral protection. Concerning the administration route, the issue of blood-brain barrier penetration arises. CsA does not seem to cross the intact blood-brain barrier [165]. When delivered by intravenous or intraperitoneal injection, CsA enters the brain after fluid percussion injury, but prior to injury, brain levels are much lower [166]. Some calpain inhibitors cross the blood-brain barrier [167], but the extent to which calpain inhibitor I does so is not clear. The degree to which the blood-brain barrier is altered by hydrocephalus is unknown [31]. Because we did not measure drug levels in brain, we must consider the possibility that drug delivery was not adequate in this experiment. Higher doses of CsA and tacrolimus might be feasible, although there was histologic evidence of kidney damage even at the doses used in this experiment. Continuous rather than pulsed administration might reduce the toxicity of these agents [168]. In this regard, we had considered several options following the preliminary experiment but decided against them for various reasons. Continuous parenteral delivery would require impractically large osmotic minipumps or replacement of minipumps, which would require additional anesthetics and surgical procedures. We were not confident that we could achieve the necessary doses using oral delivery by gavage. Furthermore,

both CsA and tacrolimus have the potential to cause damage to the blood-brain barrier and white matter [169]; therefore, they might not, for hypothetical reasons, be a good choice for treatment of hydrocephalus.

In conclusion, we found no evidence that tacrolimus, CsA or calpain inhibitor I are of significant benefit to young rats with moderately severe hydrocephalus. Toxicity and/or drug delivery to brain might be limiting factors. In our laboratory, we have done a number experiments to assess the feasibility of drug protection in hydrocephalus. We have found that drugs capable of increasing cerebral blood flow (e.g. nimodipine [39] and $MgSO_4$ [41]) can reduce hydrocephalus-associated brain injury. Drugs with direct neuroprotective or axon-protective effects do not (e.g. mexiletine, riluzole [158], CsA, tacrolimus, calpain inhibitor). Collectively, our data suggest that we need to prevent the initial cause of the axon damage rather than treat already damaged axons wherein the destructive cascade has started. The drug treatment should be nontoxic and easily administered in the period prior to shunting. We will continue to explore pharmacological approaches that might be used to supplement, not replace, shunt treatment of infantile hydrocephalus.

Table 1. Results of tacrolimus and CsA treatment in hydrocephalic rats

	Control hydrocephalic	Tacrolimus	CsA	Control non-hydrocephalic
Sample size	7	7	8	4
Ventricle area index (pretreatment)	0.194±0.010	0.234±0.021	0.220±0.031	–
Ventricle area index (posttreatment)	0.299±0.035	0.276±0.022	0.247±0.034	0.001±0.0001*
Body weight (pretreatment), g	114±4	117±2	125±14	124±2
Body weight (posttreatment), g	209±9	194±5	184±9	222±6
Swim time for 150 cm (posttreatment), s	14.5±1	20.8±3	13.7±2	10.9±2
Modified water maze test (posttreatment, 1st trial), s	9.4±2.9	13.8±3.1	8.2±1.4	9.5±1.9
Modified water maze test (posttreatment, 3rd trial), s	7.3±3.1	5.8±0.5	9.6±4.0	6.0±0.9
Ambulatory activity (posttreatment), beam breaks in 15 min	1,230±164	1,018±98	1,012±183	982±52
Endurance on roller (continuous speed, posttreatment), s	55.7±13.2	91.0±9.5	49.3±13.2	66.0±20.4
Endurance on roller (accelerating speed, posttreatment), s	28.4±7.8	61.4±10.2	32.6±6.5	43.3±17.7
Corpus callosum thickness, μm	239±40	202±31	268±44	416±38
CGalT activity in corpus callosum, nmol/mg protein/h	29.9±2.0	27.4±1.7	29.4±1.9	34.7±1.5
PNPP activity in corpus callosum, nmol/mg protein/h	73.6±4.3	73.7±2.5	56.8±3.7	98.3±9.6
MBP in posterior cerebrum, arbitrary densitometric units	1.00±0.1	1.46±0.22	1.17±0.17	3.02±1.18
Synaptophysin posterior cerebrum, arbitrary densitometric units	1.00±0.07	1.22±0.12	1.28±0.14	1.46±0.11
GFAP posterior cerebrum, arbitrary densitometric units	1.00±0.18	0.86±0.26	1.08±0.28	0.01±0.00
Serum urea (posttreatment), m*M*	6.4±0.3	12.6±0.7**	6.7±0.3	–
Serum creatinine (posttreatment), μ*M*	23.4±0.5	30.9±2.0	22.9±1.1	–

All data are expressed as mean ± standard error of the mean. * $p < 0.0001$ for normal rats versus both hydrocephalic groups (ANOVA with post hoc Scheffé test for intergroup comparisons). ** $p < 0.002$ for tacrolimus-treated versus control hydrocephalic rats.

Note: This table is from Khan et. al; published in Pediatric Neurosurgery 2003 December; 39 (6):309-313.

Chapter 2.5

Calcium antagonism in neonatal rats with kaolin-induced hydrocephalus

This section was published in: Journal of Child Neurology. 2007 October; 22(10):1161-1166.

Authors: Osaama H. Khan, Lisa C. McPhee, Lisa N. Moddemann and Marc R. Del Bigio

Note: Behavioral and immuno-histological experiments completed by Osaama Khan. Biochemical assays were performed by Terry Enno. Lisa McPhee and Lisa Moddemann helped with animal behavior testing.

ABSTRACT

Juvenile rats with kaolin-induced hydrocephalus have reduced brain injury if treated with nimodipine or magnesium sulfate. Experiments were conducted to determine if the neuroprotective effects could be replicated in neonatal rats with experimental hydrocephalus, at an age comparable to prematurely born humans (26 – 30 weeks gestation). In a blinded and randomized manner, drugs were administered for 14 days, beginning 7 days after induction of hydrocephalus. Nimodipine was given twice daily by subcutaneous injections. Doses greater than 40 mg/kg/day were fatal. Doses of 3.8 – 30 mg/kg/day were not associated with behavioral, structural or biochemical improvements. Magnesium chloride was administered via subcutaneous mini-pump infusion (0.87 mM/kg/day or 1.74 mM/kg/day) along with twice daily injections of 0.74 or 1.48 mM/kg/day. Magnesium sulfate was administered by twice daily subcutaneous doses of 1.54 mM/kg/day and 7.72 mM/kg/day. Sedation occurred, but there was no statistically significant protection in regard to behavior, brain structure or brain composition in any of the magnesium experiments. We speculate that developmental alterations in calcium channels of the neonatal rat brain could account for differences from our prior experiments in young hydrocephalic rats.

INTRODUCTION

Hydrocephalus is a common neurological condition characterized by pathological dilation of the cerebral ventricles. It is usually caused by obstruction of cerebrospinal fluid flow. Enlarging ventricles damage the surrounding brain tissue. The pathophysiology of hydrocephalus-induced brain damage is multifactorial, with contributions made by gradual physical stretching, compression, ischemia and possible accumulation of metabolic waste products [31]. We have previously reported that calcium-activated proteolysis (activated calpain) is associated with the axonal injury in experimental hydrocephalus [8]. The calcium channel blockers, nimodipine and magnesium sulfate reduced the progression of brain damage and neurologic deterioration in young rats when hydrocephalus was induced at three weeks and drug was administered from three to five weeks [39, 41]. At that age, the rat brain is similar to that of a human infant in the first year of life. However, pharmacologic protection for hydrocephalus would be most useful in premature infants who might otherwise suffer complications of shunting procedures. In this study, we assessed the beneficial roles of nimodipine and magnesium therapy in neonatal hydrocephalic rats, an age in which brain maturity is more comparable to that of premature human infants.

There is controversy concerning which magnesium salt, the sulfate or chloride, has more beneficial effects in models of brain injury. Magnesium

chloride might be preferable because there is evidence of reduced toxicity and better absorption and retention [170]. However, in an adult rat brain injury model, magnesium sulfate and magnesium chloride equally improved neurological outcome at one week [171]. Therefore, we independently tested both magnesium salts to evaluate their roles in ameliorating brain and behavior retardation in experimental neonatal hydrocephalus. We have recently described the brain damage in this model in detail [96].

METHODS

Animal preparation

All animals were treated in accordance with guidelines set forth by the Canadian Council on Animal Care, and experiments were approved by the local animal use committee. All efforts were made to minimize suffering and the number of animals used. Sprague-Dawley rats bred locally had kaolin (0.02 ml sterile suspension; 250mg/ml in 0.9% saline) injected percutaneously into the cisterna magna on postnatal day 1, as previously described [96]. Pups were returned to their mothers, which were housed in standard cages and provided with a normal 12-hour day/night lighting schedule with free access to water and pelleted food. The nimodipine experiment utilized 7 litters (11 to 13 pups each), the magnesium chloride experiment 3 litters (11 – 12 pups each), and the magnesium sulfate experiment 8 litters (13 – 18 pups each).

Drug preparation and administration

A variety of treatment doses and regimens were attempted to seek evidence for a beneficial effect. Nimodipine (Research Biochemical International; Natick, MA) was dissolved in 50% dimethyl sulfoxide (DMSO), 30% ethanol, and 20% water by the senior author and provided in coded bottles to ensure blinding. A pilot experiment to assess toxicity was conducted using 18 hydrocephalic rats. They received nimodipine at doses of 38 (n=6), 150 (n=6) and 300 (n=6) mg/kg/day beginning postnatal day 7 (body weight 22.9 g ± 4.1 g). A high level of mortality due to drug toxicity was seen at all doses. After four days, 4/6 rats in the lowest dose group, 5/6 in the medium dose group, and 6/6 in the high dose group had died. Two complete experiments were subsequently conducted. The first experiment included 47 hydrocephalic rats divided into four groups: low dose (3.8 mg/kg/day), medium dose (15 mg/kg/day), high dose (30 mg/kg/day), and vehicle control, along with 4 non-hydrocephalic rats. All drugs were administered by subcutaneous injections twice daily in a volume of 1.5 μl/g bodyweight beginning 7 days after kaolin injection and continuing for 14 days. The second nimodipine trial included 33 hydrocephalic rats and untreated 3 non-hydrocephalic controls. It was conducted in an identical manner to the first trial except for omission of the medium dose of nimodipine.

In the magnesium salt experiments, all drugs were administered by subcutaneous injections twice daily in a volume of 1.5 μl/g bodyweight beginning

7 days after kaolin injection and continuing for 14 days. The daily doses of magnesium chloride were 0.74 (low) and 1.48 mM/kg/day (high). The daily doses of magnesium sulfate were 1.54 (low) and 7.72 (high) mM/kg/day. In our previous publication using magnesium sulfate therapy, we had established that magnesium ion levels in the blood were elevated for 120 minutes and returned to normal by 230 minutes (it should be noted that, in the methods section, our calculations for magnesium concentration were incorrectly reported as μM rather than mM) [41]. Therefore, we hoped to achieve elevated steady state levels by combining continuous infusion of magnesium salt supplemented by bolus injections. For magnesium chloride trials, osmotic minipumps (Alzet model 2004, DURECT Corp., Cupertino CA, U.S.A.) rated at 6 μL/d for 14 days were loaded with 2.46 M or 4.92 M solutions. For magnesium sulfate trials, pumps rated at 12.5 μL/d for 14 days (Alzet model 2002) were loaded with 0.45 M or 2.27 M solutions. Equimolar saline solutions were administered as controls. Osmotic minipumps and syringes were preloaded by the senior author and provided to the animal handlers in a blinded manner. Under aseptic conditions, pumps were placed in a subcutaneous pocket on the back and the skin was closed with staples. The treatment code was not broken until all behavioral, structural, and biochemical analyses were complete. The magnesium sulfate constant infusion trial was discontinued do to complications. The high salt concentration of the infusate caused necrosis and sloughing of the skin over the pumps, and the mothers subsequently removed the pumps or killed the rat pups. Data collected

were not used for statistical analysis. The experiment was repeated with twice daily subcutaneous injections only.

Magnetic resonance imaging

Magnetic resonance imaging studies were performed at 7 and 21 days using a Bruker Biospec/3 MR scanner equipped with a 21-cm bore magnet operating at a field of 7 T (Karlsruhe, Germany) to obtain T_2-weighted images of the brain in the coronal plane. Rats underwent imaging on day 7 to allow stratification into groups. On the brain slice immediately anterior to the third ventricle, frontal horn size was expressed as a ratio determined by dividing the total width of the ventricles by the width of the cerebrum [38]. The ventricles sizes were arranged from largest to smallest and rats were assigned in alternation to different groups so that all had the same average severity of hydrocephalus at the outset. At the end of the trial, the 7 and 21 day magnetic resonance images at that coronal level were used for calculation of the ventricle to cerebrum area. Final imaging of the second nimodipine trial was not possible because of a technical problem with the scanner.

Behavior testing

Rats were weighed three times weekly. Ambulatory behavior, righting response and negative geotactic reactions were tested twice weekly, from 5 days age until 16 days age, to assess acquisition of posture and gait skills. These

tests were described and validated previously [50]. On postnatal days 10, 14, 17, and 20 forelimb grip strength was tested by timing the rats' ability to hang from a 1.5 mm diameter wire, elevated 40 cm above a soft sponge. The maximal time allotted was 120 seconds. In the magnesium sulfate experiment on day 14 quantitative monitoring of spontaneous activity was performed to assess sedative effect of magnesium. Pups were placed in a square enclosure (43 X 43 cm) for 10 min and ambulatory beam breaks were counted (Opto-Varimex; Columbus Instruments, Columbus OH, U.S.A.). On day 20, coordination and agility were assessed by timing endurance on a 10 cm diameter cylinder (Economex, Columbus Instruments) rotating at constant (5 rpm for a maximum of 2 minutes) and accelerating (0.1 rpm per second for a maximum of 2 minutes) speed. Also on day 20, swimming speed was measured in a 20 cm deep, 40 cm wide, and 1.5 meter long channel (average of two trials, separated by a 30 second rest). Learning and memory were then tested in a modified Morris water maze. Water in the pool (90 cm across and 25 cm deep) was made opaque with kaolin and a 10 cm platform was placed 1 cm below water surface in one quadrant. A trial consisted of four attempts to find the platform, each attempt beginning with the rat placed in the center of the pool facing a different quadrant. Room lighting gradient was used as the visual cue. Three trials were performed during the course of the day. The time of the four attempts was averaged for each trial. Further details for these tests and validation can be found in our previous publications [41].

Biochemical assays and Histopathological and Studies:

Rats were euthanized by overdose with pentobarbital, the vasculature was flushed by transcardiac perfusion with ice-cold 0.1M phosphate-buffered saline, and the brains were removed. Samples of the left parietal and frontal cerebrum were dissected and frozen in liquid nitrogen, after which they were stored at –80 °C. Frozen samples were homogenized and processed for quantification of myelin basic protein (MBP), glial fibrillary acidic protein (GFAP), and synaptophysin by enzyme linked immunosorbent assay (ELISA) [96]. Ceramide galactosyltransferase (CGalT), which is most active in oligodendrocytes during the phase of myelin production, was quantified by enzyme activity assay [14]. The right frontal cerebrum was immersion fixed in 10% buffered formalin. Two coronal sections at the level of the optic chiasm were embedded in paraffin. Sections (6 μm thickness) from this level were stained with solochrome cyanin for visualization of myelin. Corpus callosum thickness was measured in the midline and adjacent to the cingulum. The average of these measurements was used for statistical analysis.

At the time of euthanasia, blood samples were taken from heart to measure serum magnesium level (using Hitachi 737 Clinical Chemistry Autoanalyzer). Samples were drawn 30 minutes to 6 hours after the previous magnesium dose. Magnesium levels in hippocampus from the magnesium sulfate experiment (5 high dose, 13 saline, 2 non-hydrocephalic untreated

control) were analyzed by inductively coupled plasma optical emission spectrometry (Varian "Liberty" model 200). Briefly, 0.05 ml of concentrated nitric acid was added to frozen samples, heated to 90 degrees in a heating block to dissolve them and shaken for 24 hours. 1.0 ml water was then added to samples to obtain a total of 1.5 ml and read on spectrometer in parts per million (ppm).

Statistical Analysis

The group treatment codes were revealed after the experiments were completed and all raw data collected. The two nimodipine experiments were pooled. Data are presented as mean + SEM. Quantitative data were analyzed to confirm a normal distribution. Statistical analysis consisted of ANOVA with post-hoc Fisher's protected least square difference calculations for intergroup comparisons (StatView 5.1). P values presented are based on the intergroup comparisons only.

RESULTS

In the nimodipine experiment, rats tolerated the procedures reasonably well. Fifty-five hydrocephalic rats were used for the final analysis (14 low dose, 9 medium dose, 14 high dose, 16 vehicle control). Excluded from the analysis were 7 rats that died during kaolin injection, 5 that failed to develop hydrocephalus, 3 that were euthanized for severe neurologic deficits before assignment to treatment group, and 3 during the drug treatment phase (2 high dose, 1 medium

dose, 2 low dose, 4 vehicle control). All the rats that died during these experiments had very large initial ventricular size (index ≥ 0.30).

Behavior and biochemical data for nimodipine experiments are presented in Table 1. The moderate dose group did not differ statistically from the low or high dose groups, and therefore is not shown. From postnatal day 7 until day 21, there was significant weight difference between the non-hydrocephalic rats and all hydrocephalic groups ($p<0.05$). However, at no time was there a significant weight difference between the nimodipine-treated and untreated hydrocephalus groups. Non-hydrocephalic controls performed better than the hydrocephalic rats on the righting task, the wire hanging, and the swimming speed ($p=0.012$) and final water maze trial ($p = 0.026$). Between hydrocephalic groups, no treatment effect was seen on the rotorod or water maze performance. There was no difference in the magnitude of ventricle enlargement between hydrocephalic groups (Figure 1).

Biochemical analyses of myelin basic protein, glial fibrillary acidic protein and synaptophysin content and ceramide galactosyltransferase activity revealed no statistically significant differences between the control and nimodipine-treated hydrocephalic groups. Content of glial fibrillary acidic protein, a marker of reactive astrocyte change, was greater in the hydrocephalic rats than in the non-hydrocephalic rats as expected. Microscopic observation showed that the corpus callosum of severely hydrocephalic animals was very atrophic and dispersed due to edema.

In the magnesium chloride experiment, among 28 kaolin-induced rats, 2 died shortly after kaolin injection, 2 failed to develop hydrocephalus, and 4 were too sick to be randomized to drug treatment. Twenty hydrocephalic (7 low dose, 7 high dose, 6 control) and 3 non-hydrocephalic control pups survived to the end of the study. There was no obvious adverse effect of magnesium on these rats. Blood samples taken the day of sacrifice showed that control magnesium level was 1.25±0.05 mM/L. In the high and low dose groups, the level 10 minutes after administration was 3.320 mM/L and 1.75 mM/L respectively, but by 60 minutes was <1.5 mM/L. In the magnesium sulfate experiment, 12 rats were excluded because of excessively severe hydrocephalus prior to randomization and 2 were euthanized (2 high dose) because of severe deficit. Twenty-nine hydrocephalic rats (5 high dose, 11 low dose, 13 saline) were used for the final analysis. Control blood magnesium level on day of sacrifice was similar to that in the first experiment at 1.24±0.06 mM/L. In the high and low dose groups, the level 10 minutes after administration was 6.74 mM/L and 2.02 mM/L respectively, but had returned to control values within 90 minutes.

In the magnesium salt experiments there was no statistically significant or trend difference between hydrocephalic groups in weight, wire and water maze behaviors, biochemical or histological parameters (data not shown). However, in the magnesium chloride experiments, the high dose group was impaired in rotorod performance at continuous ($p = 0.0155$) and accelerating ($p=0.0363$) speeds. A sedative effect was also seen in the magnesium sulfate experiment

wherein the high dose rats were less active in the activity monitor (data not shown). Despite elevated peak blood levels, magnesium levels in the brain detected by inductively coupled plasma optical emission spectrometry were similar in the high dose magnesium sulfate (598±30 ppm) and saline control (632±20 ppm) ($P>0.5$).

DISCUSSION

Calcium channels are found in vascular smooth muscle, glia and neurons. Nimodipine blocks L-type voltage dependent calcium channels located on neurons, axons, reactive astrocytes, and vascular smooth muscle [172, 173]. Because it is lipophilic, nimodipine enters the brain well [174]. Like nimodipine, magnesium is neuroprotective in some animal models of brain injury, promotes dilatation of cerebral arteries, and has an established safety profile in the clinical setting of subarachnoid hemorrhage [175]. Magnesium ions noncompetitively antagonize NMDA receptors, and they compete with extracellular calcium ions to reduce calcium entry into cells [176]. Through calcium antagonism, we had hoped to reduce axonal damage and ischemic injury in the neonatal rat model of hydrocephalus.

Our previous study of juvenile hydrocephalic rats showed nimodipine administered 3 – 4 weeks after hydrocephalus induction was protective [39]. No such protection was seen in the current experiment at a range of doses

approaching toxic levels. Similarly, magnesium chloride and magnesium sulfate were of no benefit. Brain magnesium levels were not altered, but an analysis of stored tissues from our previous successful experiment showing mild protective effects of magnesium sulfate in juvenile hydrocephalic rats [41], showed that brain magnesium levels assessed by inductively coupled plasma optical emission spectrometry were not different from controls (unpublished data). Magnesium is likely entering the brain, as seen by the transient sedative, but is not retained. Intermittent drug administration an inability to maintain elevated blood levels is a shortcoming in the magnesium salt experiments. Unfortunately, due to the small size of the young rats, it was not technically possible to implant chronic delivery devices that would ensure constant elevation of magnesium levels.

Do only technical issues explain why these interventions on neonatal rat hydrocephalus failed? Intracellular Ca^{++} concentration is highest in rat brain at 7 days and gradually decreases to adult level by 3 months [177]. Furthermore, messenger RNA (mRNA) expression for C and D alpha 1 subtypes encoding the L-type calcium channels are most highly expressed in the immature brain, declining after postnatal day 14 [178]. N-type voltage dependent calcium channels also change during postnatal development, achieving adult distributions by 14 days [179]. Thus, changing calcium homeostatic mechanisms during the postnatal day 7 - 14 period might help explain why the younger hydrocephalic brains were not protected by nimodipine or magnesium salts. It must also be noted that the safety profile of nimodipine is not clearly defined during fetal and

postnatal brain development. Some studies suggest that nimodipine has no effect on fetal or postnatal development [180]. Others indicate a postnatal acceleration of change among calcium-related proteins in rat brain [181], altered development of vasomotor activity in rat [182], and we have observed that high doses of nimodipine are associated with reduced synaptophysin content in juvenile rat brain [39].

In summary, we found no evidence that nimodipine or magnesium salts are of significant benefit to neonatal rats with kaolin-induced hydrocephalus at doses that reduced brain damage in juvenile rats with hydrocephalus. We speculate that the discrepancy is due to developmental differences in calcium ion channel structure and function. Furthermore, technical aspects of drug delivery in these small animals may have been a limiting factor. Testing in larger animals where continuous delivery, similar to intravenous drip used clinically, is recommended. Continued exploration of pharmacological approaches to supplement the current shunt treatment of hydrocephalus is necessary.

Table 1. Results of nimodipine treatment in neonatal hydrocephalic rats.

	Control hydrocephalic	Low dose nimodipine	High dose nimodipine	Control non-hydrocephalic
Ventricle area index (day 7)	0.29± 0.05	0.28± 0.04	0.24± 0.05	-
Ventricle area index (day 21) (b)	0.21± 0.09	0.30± 0.11	0.21± 0.08	-
Corpus callosum thickness (mm)	0.18± 0.04	0.14± 0.02	0.14± 0.03	0.26± 0.03*
Weight (day 7) g	23.2± 0.9	22.5± 0.7	22.4± 0.8	26.6± 1.9
Weight (day 21) g	53.9± 3.4	56.1± 2.9	55.1± 2.5	65.0± 4.2*
Wire hanging (day 15) sec	10.8± 1.8	24.1± 6.7	24.1± 6.5	11.4± 2.0
Wire hanging (day 18) sec	7.9± 1.4	14.9± 8.1	9.1± 1.7	26.4± 15.8
Swim time 150 cm (day 20) sec	20.7± 2.1	26.8± 4.9	19.2± 2.6	12.2± 2.5 *
Water maze (day 20, 1st trial) sec	27.5± 3.4	32.3± 3.4	29.0± 2.3	24.1± 3.8
Water maze (day 20, 3rd trial) sec	30.6± 4.7	24.2± 4.1	27.7± 4.4	14.1± 1.5 *
Roller endurance (day 20, continuous speed) sec	67.7± 12.6	36.7± 9.9	58.2± 11.6	58.7± 18.0
Roller endurance (day 20, accelerating) sec	25.0± 4.3	25.1± 3.9	21.1± 3.6	24.4± 5.1
CGalT activity, nmol/gm protein/h	0.91± 0.21	0.58± 0.14	0.98± 0.10	0.56± 0.01
GFAP mg/gm protein	1.09± 0.46	0.34± 0.06	0.46± 0.14	0.17± 0.01*
Synaptophysin mg/gm protein	0.13± 0.01	0.13± 0.01	0.13± 0.01	0.12± 0.01

Notes to Table 1

a) All data expressed as mean ± standard error of the mean. Excluded from this table are hydrocephalic animals receiving the moderate dose. "Day" corresponds to postnatal day

b) The apparent decrease in the mean ventricle size index was due to death of most severely hydrocephalic rats during the course of treatment

Abbreviations – GFAP (glial fibrillary acidic protein), CGalT (ceramide galactosyltransferase)

* $p < 0.05$ for hydrocephalic rats versus non-hydrocephalic rats (ANOVA with post-hoc Fisher's test for intergroup comparisons). There were no statistically significant differences between the hydrocephalic groups.

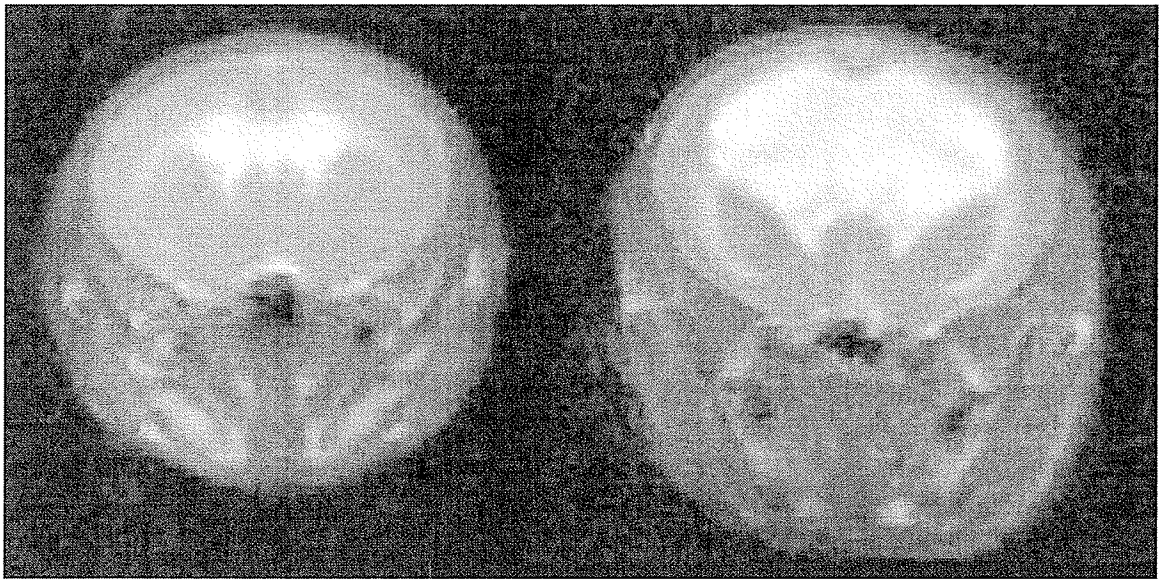

Figure 1. Coronal plane T2-weighted magnetic resonance images of an individual rat from the vehicle control group in the second nimodipine experiment. At one week age, prior to onset of drug treatment (Left panel) the frontal horns of the lateral ventricles are slightly enlarged and the white matter shows increased signal related to edema. At the end of the drug treatment period (Right panel), the ventricles have enlarged considerably and the cerebrum is thinned. However, there was no statistically significant difference in the change when comparing across treatment groups in any of the experiments.

Chapter 3

General Discussion and Conclusions

Hydrocephalus induction of neonatal and juvenile rats via kaolin injection into the cisterna magna created a reproducible hydrocephalus model with ventricles of varying sizes that was observed with MRI and histology at several time points. We accomplished our first goal of describing the behavioral changes and brain injury in neonatal rats. Hydrocephalic rats had developmental delay in spatial memory. Histologically, we illustrated that hydrocephalus in neonatal rats proceeded similarly to young and adult hydrocephalus; however, white matter edema is more extensive in neonatal hydrocephalic rats. The major age related difference in brain damage is that the neonatal brain has a highly proliferative subependymal zone that we showed was affected by increases in ventricle size. The result was decreased cellular proliferation, with fewer mature oligodendrocytes and reduced myelin in the periventricular white matter. This has important implications for human hydrocephalus of early onset, either in utero or after premature birth. Dilating ventricles in fetuses or premature infants could have permanent adverse effects on the developing brain [183, 184].

In addressing our second goal concerning mechanistic issues secondary to hydrocephalus, we had hypothesized that cellular markers of hypoxia would be present in neonatal and juvenile hydrocephalic rats. By using a hypoxia marker, pimonidazole, which irreversibly binds to hypoxic cells, we showed that neurons, glia, and vascular endothelial cells are all affected by hydrocephalus. We further demonstrated that lipid peroxidation, probably caused by free radicals, was increased in hydrocephalic brains. By using HNE and nitrotyrosine

immunohistochemistry, we determined that there was evidence of free radical damage in neurons, glia and endothelial cells predominantly in the cerebral white matter, but also cortical gray matter and striatum. Our data regarding the effects hydrocephalus on HIF – 1α and VEGF expression was not conclusive. We did determine, using immunohistochemistry, that VEGF expression was increased in the cortical gray and white matter of hydrocephalic brains compared to controls, regardless of age of hydrocephalus induction. However, there was not a generalized increase. The role of angiogenesis in hydrocephalus is not well understood [185].

Our final goal was to investigate pharmacological intervention for brain injury in neonatal and juvenile rats with hydrocephalus. By selecting drugs that antagonize calcium in the brain, we hypothesized that brain injury and behavioral abnormalities could be reduced. We showed that $MgSO_4$ treatment, in a dose dependent manner, had a mild protective effect on motor and cognitive behavior in juvenile hydrocephalus, but that high doses were associated with adverse effects, particularly sedation. There was also a statistically significant decrease in white matter gliosis (GFAP) with a trend for treated rats to have a thicker corpus callosum. Using the same outcome measures, we repeated the experiments to test nimodipine or magnesium salts in neonatal rats. There was no significant protective effect on the function, structure or composition of the brain when administered chronically. We speculated that age-related differences in calcium channel structure and function might play a role. We cannot exclude the

possibility that technical aspects related to the small animals limited our ability to deliver drugs reproducibly. Further studies into the pathophysiology of white matter damage are needed develop more effective treatment options for pharmacological intervention in pediatric hydrocephalus.

In summary, the effects of hydrocephalus on brain are age-dependent. Likewise, the protective effects of calcium antagonists are seen in juvenile rats, which correspond to human infants, but not neonatal rats, which correspond to premature human infants or fetuses. This must be considered when developing rationale therapies for hydrocephalus.

REFERENCES

1. Wehby-Grant, M.C., et al., *Metabolic responses of the neonatal rabbit brain to hydrocephalus and shunting.* Pediatr Neurosurg, 1996. **24**: p. 79-91.
2. Stein, S.C. and L. Schut, *Hydrocephalus in myelomeningocele.* Childs Brain, 1979. **5**(4): p. 413-419.
3. Holt, P.J. and W.C. Allan, *The natural history of ventricular dilatation in neonatal intraventricular hemorrhage and its therapeutic implications.* Ann. Neurol., 1981. **10**: p. 293-294.
4. Pudenz, R.H., et al., *Ventriculo-auriculostomy; a technique for shunting cerebrospinal fluid into the right auricle; preliminary report.* J Neurosurg, 1957. **14**(2): p. 171-179.
5. Del Bigio, M.R. and Y.W. Zhang, *Cell death, axonal damage, and cell birth in the immature rat brain following induction of hydrocephalus.* Exp Neurol, 1998. **154**(1): p. 157-169.
6. Hochwald, G.M., et al., *Changes in regional blood-flow and water content of brain and spinal cord in acute and chronic experimental hydrocephalus.* Dev Med Child Neurol Suppl, 1975(35): p. 42-50.
7. Chumas, P.D., et al., *Anaerobic glycolysis preceding white-matter destruction in experimental neonatal hydrocephalus.* J Neurosurg, 1994. **80**(3): p. 491-501.
8. Del Bigio, M.R., *Calcium-mediated proteolytic damage in white matter of hydrocephalic rats?* J Neuropathol Exp Neurol, 2000. **59**(11): p. 946-954.
9. Del Bigio, M.R., M.J. Wilson, and T. Enno, *Chronic hydrocephalus in rats and humans: white matter loss and behavior changes.* Ann Neurol, 2003. **53**(3): p. 337-346.
10. Mangano, F.T., et al., *The microglial response to progressive hydrocephalus in a model of inherited aqueductal stenosis.* Neurol Res, 1998. **20**(8): p. 697-704.
11. Barkovich, A.J. and M.S. Edwards, *Applications of neuroimaging in hydrocephalus.* Pediatr Neurosurg, 1992. **18**(2): p. 65-83.
12. Brody, B.A., et al., *Sequence of central nervous system myelination in human infancy. I. An autopsy study of myelination.* J Neuropathol Exp Neurol, 1987. **46**(3): p. 283-301.
13. Kinney, H.C., et al., *Sequence of central nervous system myelination in human infancy. II. Patterns of myelination in autopsied infants.* J Neuropathol Exp Neurol, 1988. **47**(3): p. 217-234.
14. Del Bigio, M.R., J.N. Kanfer, and Y.W. Zhang, *Myelination delay in the cerebral white matter of immature rats with kaolin-induced hydrocephalus is reversible.* J Neuropathol Exp Neurol, 1997. **56**(9): p. 1053-1066.

15. Taylor, G.A., J.S. Soul, and P.S. Dunning, *Sonographic ventriculography: a new potential use for sonographic contrast agents in neonatal hydrocephalus.* AJNR Am J Neuroradiol, 1998. **19**(10): p. 1931-1934.
16. Nakada, J., et al., *Changes in the cerebral vascular bed in experimental hydrocephalus: an angio-architectural and histological study.* Acta Neurochir (Wien), 1992. **114**(1-2): p. 43-50.
17. Flor, W.J., et al., *Ultrastructure of the ependyma in the lateral ventricles of primates with experimental communicating hydrocephalus.* Scan Electron Microsc, 1979(3): p. 47-54.
18. Hammock, M.K., et al., *Vein of Galen ligation in the primate. Angiographic, gross, and light microscopic evaluation.* J Neurosurg, 1971. **34**(1): p. 77-83.
19. Matsumoto, S., et al., *Comparative study of various models of experimental hydrocephalus.* Childs Brain, 1975. **1**(4): p. 236-242.
20. Del Bigio, M.R., *Future directions for therapy of childhood hydrocephalus: a view from the laboratory.* Pediatr Neurosurg, 2001. **34**(4): p. 172-181.
21. McCullough, D.C., *History of treatment of hydrocephalus.* Hydrocephalus. Volume 3: Concepts in Neurosurgery, ed. R.M. Scott. 1990, Baltimore MD: Williams & Wilkins. 1-10.
22. Elvidge, A.R., C.L. Branch, and G.B. Thompson, *Observations in a case of hydrocephalus treated with diamox.* J Neurosurg, 1957. **14**(6): p. 628-638; discussion 638-639.
23. Shinnar, S., et al., *Management of hydrocephalus in infancy: use of acetazolamide and furosemide to avoid cerebrospinal fluid shunts.* J Pediatr, 1985. **107**(1): p. 31-37.
24. Kennedy, C.R., et al., *Randomized, controlled trial of acetazolamide and furosemide in posthemorrhagic ventricular dilation in infancy: follow-up at 1 year.* Pediatrics, 2001. **108**(3): p. 597-607.
25. Whitelaw, A., C.R. Kennedy, and L.P. Brion, *Diuretic therapy for newborn infants with posthemorrhagic ventricular dilatation.* Cochrane Database Syst Rev, 2001(2): p. CD002270.
26. Becker, B., A.E. Kolker, and T. Krupin, *Isosorbide. An oral hyperosmotic agent.* Arch Ophthalmol, 1967. **78**(2): p. 147-150.
27. Lorber, J., *Isosorbide in the medical treatment of infantile hydrocephalus.* J Neurosurg, 1973. **39**(6): p. 702-711.
28. Davson, H., K. Welch, and M.B. Segal, *The Physiology and Pathophysiology of the Cerebrospinal Fluid.* 1987, Edinburgh: Churchill Livingstone.
29. Del Bigio, M.R., *Neuropathological changes caused by hydrocephalus.* Acta Neuropathol (Berl), 1993. **85**(6): p. 573-585.
30. Del Bigio, M.R., *Cellular damage and prevention in childhood hydrocephalus.* Brain Pathol, 2004. **14**(3): p. 317-324.
31. McAllister, J.P., II and P. Chovan, *Neonatal hydrocephalus. Mechanisms and consequences.* Neurosurg Clin N Am, 1998. **9**(1): p. 73-93.

32. Jones, H.C. and R.M. Bucknall, *Inherited prenatal hydrocephalus in the H-Tx rat: a morphological study.* Neuropathol Appl Neurobiol, 1988. **14**(4): p. 263-274.
33. Bruni, J.E., et al., *Hereditary hydrocephalus in laboratory animals and humans.* Exp Pathol, 1988. **35**(4): p. 239-246.
34. Cherian, S.S., et al., *Posthemorrhagic ventricular dilation in the neonate: development and characterization of a rat model.* J Neuropathol Exp Neurol, 2003. **62**(3): p. 292-303.
35. Balasubramaniam, J., et al., *Persistent motor deficit following infusion of autologous blood into the periventricular region of neonatal rats.* Exp Neurol, 2006. **197**(1): p. 122-132.
36. Jacobson, S., *Sequence of Myelinization in the Brain of the Albino Rat. A. Cerebral Cortex, Thalamus and Related Structures.* J Comp Neurol, 1963. **121**: p. 5-29.
37. Romijn, H.J., M.A. Hofman, and A. Gramsbergen, *At what age is the developing cerebral cortex of the rat comparable to that of the full-term newborn human baby?* Early Hum Dev, 1991. **26**(1): p. 61-67.
38. Del Bigio, M.R., C.R. Crook, and R. Buist, *Magnetic resonance imaging and behavioral analysis of immature rats with kaolin-induced hydrocephalus: pre- and postshunting observations.* Exp Neurol, 1997. **148**(1): p. 256-264.
39. Del Bigio, M.R. and E.M. Massicotte, *Protective effect of nimodipine on behavior and white matter of rats with hydrocephalus.* J Neurosurg, 2001. **94**(5): p. 788-794.
40. Khan, O.H., T. Enno, and M.R. Del Bigio, *Tacrolimus and cyclosporine A are of no benefit to young rats with kaolin-induced hydrocephalus.* Pediatr Neurosurg, 2003. **39**(6): p. 309-13.
41. Khan, O.H., T. Enno, and M.R. Del Bigio, *Magnesium sulfate therapy is of mild benefit to young rats with kaolin-induced hydrocephalus.* Pediatr Res, 2003. **53**(6): p. 970-6.
42. Boillat, C.A., et al., *Ultrastructural changes in the deep cortical pyramidal cells of infant rats with inherited hydrocephalus and the effect of shunt treatment.* Exp Neurol, 1997. **147**(2): p. 377-388.
43. Jones, H.C., et al., *Breeding characteristics and genetic analysis of the H-Tx rat strain.* Eur J Pediatr Surg, 1999. **9 Suppl 1**: p. 42-43.
44. Jones, H.C., et al., *Chromosomal linkage associated with disease severity in the hydrocephalic H-Tx rat.* Behav Genet, 2001. **31**(1): p. 101-111.
45. Jones, H.C., et al., *Genetic analysis of inherited hydrocephalus in a rat model.* Exp Neurol, 2004. **190**(1): p. 79-90.
46. Chovanes, G.I., et al., *Monoamine alterations during experimental hydrocephalus in neonatal rats.* Neurosurgery, 1988. **22**(1 Pt 1): p. 86-91.
47. Cosan, T.E., et al., *Cerebral blood flow alterations in progressive communicating hydrocephalus: transcranial Doppler ultrasonography*

assessment in an experimental model. Journal Of Neurosurgery. Feb, 2001. **94**(2): p. 265-269.
48. Ishizaki, R., et al., *Acute and subacute hydrocephalus in a rat neonatal model: Correlation with functional injury of neurotransmitter systems.* Pediatr. Neurosurg., 2000. **33**(6): p. 298-305.
49. McAllister, J.P., 2nd, et al., *Neuronal effects of experimentally induced hydrocephalus in newborn rats.* J Neurosurg, 1985. **63**(5): p. 776-783.
50. Altman, J. and K. Sudarshan, *Postnatal development of locomotion in the laboratory rat.* Anim Behav, 1975. **23**(4): p. 896-920.
51. Kraemer, P.J., et al., *Validation of a single-day Morris water maze procedure used to assess cognitive deficits associated with brain damage.* Brain Res. Bull., 1996. **39**: p. 17-22.
52. Barradas, P.C., et al., *2'3'Cyclic nucleotide 3'phosphodiesterase immunohistochemistry shows an impairment on myelin compaction in hypothyroid rats.* Int J Dev Neurosci, 2000. **18**(8): p. 887-892.
53. Kanfer, J.N. and D. McCartney, *An unusual phosphodiesterase activity towards p-nitrophenylphosphorylcholine present in rat brain membranes.* Neurochem Res, 1990. **15**(10): p. 987-992.
54. Monge, M., et al., *Glycerophosphorylcholine phosphocholine phosphodiesterase activity during the differentiation of glial progenitor cells.* J Neurosci Res, 1993. **36**(4): p. 441-445.
55. Schaeren-Wiemers, N., P. van der Bijl, and M.E. Schwab, *The UDP-galactose:ceramide galactosyltransferase: expression pattern in oligodendrocytes and Schwann cells during myelination and substrate preference for hydroxyceramide.* J Neurochem, 1995. **65**(5): p. 2267-2278.
56. Sprong, H., et al., *UDP-galactose:ceramide galactosyltransferase is a class I integral membrane protein of the endoplasmic reticulum.* J Biol Chem, 1998. **273**(40): p. 25880-25888.
57. White, C.L.I., et al., *Production and characterization of a recombinant synaptophysin fragment suitable for use as a standard in immunoassays.* J Neuropathol Exp Neurol, 1997. **56**: p. 608 (abstract).
58. Schmued, L.C. and K.J. Hopkins, *Fluoro-Jade B: a high affinity fluorescent marker for the localization of neuronal degeneration.* Brain Res, 2000. **874**(2): p. 123-130.
59. Bayer, S.A., et al., *Embryology*, in *Pediatric Neuropathology*, S. Duckett, Editor. 1995, Williams and Wilkins: Baltimore. p. 54-107.
60. Dobbing, J. and J. Sands, *Comparative aspects of the brain growth spurt.* Early Hum Dev, 1979. **3**(1): p. 79-83.
61. Mashayekhi, F., et al., *Deficient cortical development in the hydrocephalic Texas (H-Tx) rat: a role for CSF.* Brain, 2002. **125**(Pt 8): p. 1859-1874.
62. Owen-Lynch, P.J., et al., *Defective cell cycle control underlies abnormal cortical development in the hydrocephalic Texas rat.* Brain, 2003. **126**(Pt 3): p. 623-631.

63. Levison, S.W. and J.E. Goldman, *Both oligodendrocytes and astrocytes develop from progenitors in the subventricular zone of postnatal rat forebrain.* Neuron, 1993. **10**(2): p. 201-212.
64. Zerlin, M., S.W. Levison, and J.E. Goldman, *Early patterns of migration, morphogenesis, and intermediate filament expression of subventricular zone cells in the postnatal rat forebrain.* J Neurosci, 1995. **15**(11): p. 7238-7249.
65. Csillik, A.E., et al., *Expression of kynurenine aminotransferase in the subplate of the rat and its possible role in the regulation of programmed cell death.* Cereb Cortex, 2002. **12**(11): p. 1193-1201.
66. Robertson, R.T., et al., *Do subplate neurons comprise a transient population of cells in developing neocortex of rats?* J Comp Neurol, 2000. **426**(4): p. 632-650.
67. Ulfig, N., A. Szabo, and J. Bohl, *Effect of fetal hydrocephalus on the distribution patterns of calcium-binding proteins in the human occipital cortex.* Pediatr Neurosurg, 2001. **34**(1): p. 20-32.
68. Mori, F., et al., *Thalamic retrograde degeneration in the congenitally hydrocephalic rat is attributable to apoptotic cell death.* Neuropathology, 2002. **22**(3): p. 186-193.
69. Oka, A., et al., *Vulnerability of oligodendroglia to glutamate: pharmacology, mechanisms, and prevention.* J Neurosci, 1993. **13**(4): p. 1441-1453.
70. Castejon, O.J., H.V. Castejon, and A. Castellano, *Oligodendroglial cell damage and demyelination in infant hydrocephalus. An electron microscopic study.* J Submicrosc Cytol Pathol, 2001. **33**(1-2): p. 33-40.
71. Ulfig, N., et al., *Brain macrophages and microglia in human fetal hydrocephalus.* Brain Dev, 2004. **26**(5): p. 307-315.
72. Jones, H.C., K.M. Rivera, and N.G. Harris, *Learning deficits in congenitally hydrocephalic rats and prevention by early shunt treatment.* Childs Nerv Syst, 1995. **11**(11): p. 655-660.
73. Jones, H.C., et al., *Shunt treatment at two postnatal ages in hydrocephalic H-Tx rats quantified using MR imaging.* Exp Neurol, 1995. **133**(2): p. 144-152.
74. Jones, H.C., R.M. Bucknall, and N.G. Harris, *The cerebral cortex in congenital hydrocephalus in the H-Tx rat: a quantitative light microscopy study.* Acta Neuropathol (Berl), 1991. **82**(3): p. 217-224.
75. Jones, H.C., et al., *Progressive changes in cortical metabolites at three stages of infantile hydrocephalus studied by in vitro NMR spectroscopy.* J Neurotrauma, 1997. **14**(9): p. 587-602.
76. Hawkins, D., et al., *The functional outcome of shunting H-Tx rat pups at different ages.* Eur J Pediatr Surg, 1997. **7 Suppl 1**: p. 31-34.
77. Cosan, T.E., et al., *Progressive ventricular enlargement in the absence of high ventricular pressure in an experimental neonatal rat model.* Childs Nerv Syst, 2002. **18**(1-2): p. 10-14.

78. Del Bigio, M.R. and J.E. Bruni, *Changes in periventricular vasculature of rabbit brain following induction of hydrocephalus and after shunting.* J Neurosurg, 1988. **69**(1): p. 115-120.
79. Momjian, S., et al., *Pattern of white matter regional cerebral blood flow and autoregulation in normal pressure hydrocephalus.* Brain, 2004. **127**(Pt 5): p. 965-972.
80. da Silva, M.C., et al., *Reduced local cerebral blood flow in periventricular white matter in experimental neonatal hydrocephalus-restoration with CSF shunting.* J Cereb Blood Flow Metab, 1995. **15**(6): p. 1057-1065.
81. Soul, J.S., et al., *Noninvasive detection of changes in cerebral blood flow by near-infrared spectroscopy in a piglet model of hydrocephalus.* Pediatr Res, 2000. **48**(4): p. 445-449.
82. Smith, K.J., R. Kapoor, and P.A. Felts, *Demyelination: the role of reactive oxygen and nitrogen species.* Brain Pathol, 1999. **9**(1): p. 69-92.
83. Keynes, R.G. and J. Garthwaite, *Nitric oxide and its role in ischaemic brain injury.* Curr Mol Med, 2004. **4**(2): p. 179-191.
84. van der Vliet, A., et al., *Nitrotyrosine as biomarker for reactive nitrogen species.* Methods Enzymol, 1996. **269**: p. 175-184.
85. Zarkovic, K., *4-hydroxynonenal and neurodegenerative diseases.* Mol Aspects Med, 2003. **24**(4-5): p. 293-303.
86. Arteel, G.E., et al., *Evidence that hypoxia markers detect oxygen gradients in liver: pimonidazole and retrograde perfusion of rat liver.* Br J Cancer, 1995. **72**(4): p. 889-895.
87. Halliwell, B., *Reactive oxygen species and the central nervous system.* J Neurochem, 1992. **59**(5): p. 1609-1623.
88. Jakeman, L.B., et al., *Developmental expression of binding sites and messenger ribonucleic acid for vascular endothelial growth factor suggests a role for this protein in vasculogenesis and angiogenesis.* Endocrinology, 1993. **133**(2): p. 848-859.
89. Ferrara, N. and T. Davis-Smyth, *The biology of vascular endothelial growth factor.* Endocr Rev, 1997. **18**(1): p. 4-25.
90. Chavez, J.C., et al., *Expression of hypoxia-inducible factor-1alpha in the brain of rats during chronic hypoxia.* J Appl Physiol, 2000. **89**(5): p. 1937-1942.
91. Ohkawa, H., N. Ohishi, and K. Yagi, *Assay for lipid peroxides in animal tissues by thiobarbituric acid reaction.* Anal Biochem, 1979. **95**(2): p. 351-358.
92. Janero, D.R., *Malondialdehyde and thiobarbituric acid-reactivity as diagnostic indices of lipid peroxidation and peroxidative tissue injury.* Free Radic Biol Med, 1990. **9**(6): p. 515-540.
93. Sinha, A.K., *Colorimetric assay of catalase.* Anal Biochem, 1972. **47**(2): p. 389-394.
94. Rotruck, J.T., et al., *Selenium: biochemical role as a component of glutathione peroxidase.* Science, 1973. **179**(73): p. 588-590.

95. Zarkovic, N., *4-hydroxynonenal as a bioactive marker of pathophysiological processes.* Mol Aspects Med, 2003. **24**(4-5): p. 281-291.
96. Khan, O.H., T.L. Enno, and M.R. Del Bigio, *Brain damage in neonatal rats following kaolin induction of hydrocephalus.* Exp Neurol, 2006. **200**(2): p. 311-320.
97. Zhang, Y.W. and M.R. Del Bigio, *Growth-associated protein-43 is increased in cerebrum of immature rats following induction of hydrocephalus.* Neuroscience, 1998. **86**(3): p. 847-854.
98. Soul, J.S., et al., *CSF removal in infantile posthemorrhagic hydrocephalus results in significant improvement in cerebral hemodynamics.* Pediatr Res, 2004. **55**(5): p. 872-876.
99. McCracken, E., et al., *The lipid peroxidation by-product 4-hydroxynonenal is toxic to axons and oligodendrocytes.* J Cereb Blood Flow Metab, 2000. **20**(11): p. 1529-1536.
100. Neely, M.D., et al., *The lipid peroxidation product 4-hydroxynonenal inhibits neurite outgrowth, disrupts neuronal microtubules, and modifies cellular tubulin.* J Neurochem, 1999. **72**(6): p. 2323-2333.
101. Tanaka, K., et al., *Immunohistochemical detection of nitrotyrosine in postischemic cerebral cortex in gerbil.* Neurosci Lett, 1997. **235**(1-2): p. 85-88.
102. Morgan, F.W., et al., *Differential expression of stress response genes in the H-Tx rat model of congenital hydrocephalus.* Brain Res Mol Brain Res, 2005. **138**(2): p. 273-290.
103. Fontana, G., et al., *Activation of brain nitric oxide synthase in depolarized human temporal cortex slices: differential role of voltage-sensitive calcium channels.* Br J Pharmacol, 1997. **122**(5): p. 930-934.
104. Watanabe, Y., et al., *Post-synaptic density-95 promotes calcium/calmodulin-dependent protein kinase II-mediated Ser847 phosphorylation of neuronal nitric oxide synthase.* Biochem J, 2003. **372**(Pt 2): p. 465-471.
105. Miyan, J.A., et al., *Effects of hydrocephalus on nitric oxide neurones in the brain of the HTx rat.* Eur J Pediatr Surg, 1997. **7 Suppl 1**: p. 23-27.
106. Klinge, P., et al., *Temporal and regional profile of neuronal and glial cellular injury after induction of kaolin hydrocephalus.* Acta Neurochir Suppl, 2002. **81**: p. 275-277.
107. Klinge, P.M., et al., *Cerebral hypoperfusion and delayed hippocampal response after induction of adult kaolin hydrocephalus.* Stroke, 2003. **34**(1): p. 193-199.
108. Balasubramaniam, J. and M.R. Del Bigio, *Analysis of age-dependant alteration in the brain gene expression profile following induction of hydrocephalus in rats.* Exp Neurol, 2002. **173**(1): p. 105-113.

109. Mori, K., et al., *Immunohistochemical localization of superoxide dismutase in congenital hydrocephalic rat brain.* Childs Nerv Syst, 1993. **9**(3): p. 136-141.
110. Conway, E.M., D. Collen, and P. Carmeliet, *Molecular mechanisms of blood vessel growth.* Cardiovasc Res, 2001. **49**(3): p. 507-521.
111. Lahiri, S., et al., *Oxygen sensing in the body.* Prog Biophys Mol Biol, 2006. **91**(3): p. 249-286.
112. Marti, H.H. and W. Risau, *Systemic hypoxia changes the organ-specific distribution of vascular endothelial growth factor and its receptors.* Proc Natl Acad Sci U S A, 1998. **95**(26): p. 15809-15814.
113. Rosenstein, J.M. and J.M. Krum, *New roles for VEGF in nervous tissue--beyond blood vessels.* Exp Neurol, 2004. **187**(2): p. 246-253.
114. Heep, A., et al., *Vascular endothelial growth factor and transforming growth factor-beta1 are highly expressed in the cerebrospinal fluid of premature infants with posthemorrhagic hydrocephalus.* Pediatr Res, 2004. **56**(5): p. 768-774.
115. Koehne, P., et al., *Vascular endothelial growth factor and erythropoietin concentrations in cerebrospinal fluid of children with hydrocephalus.* Childs Nerv Syst, 2002. **18**(3-4): p. 137-141.
116. Luciano, M.G., et al., *Cerebrovascular adaptation in chronic hydrocephalus.* J Cereb Blood Flow Metab, 2001. **21**(3): p. 285-294.
117. Edwards, R.J., et al., *Chronic hydrocephalus in adults.* Brain Pathol, 2004. **14**(3): p. 325-336.
118. Dombrowski, S.M., et al., *Chronic hydrocephalus-induced changes in cerebral blood flow: mediation through cardiac effects.* J Cereb Blood Flow Metab, 2006. **26**(10): p. 1298-1310.
119. Ladomery, M.R., S.J. Harper, and D.O. Bates, *Alternative splicing in angiogenesis: the vascular endothelial growth factor paradigm.* Cancer Lett, 2007. **249**(2): p. 133-142.
120. Etus, V., et al., *Green tea polyphenol (-)-epigallocatechin gallate prevents oxidative damage on periventricular white matter of infantile rats with hydrocephalus.* Tohoku J Exp Med, 2003. **200**(4): p. 203-209.
121. Etus, V., G. N., and A. Belce, *N-acetylcystein reduces cerebral lipid peroxidation in a rat model of infantile hydrocephalus.* J. Neurol. Sci. (Turk.) (online) 18:#2, 2001.
122. Simpson, J.I., et al., *Intrathecal magnesium sulfate protects the spinal cord from ischemic injury during thoracic aortic cross-clamping.* Anesthesiology, 1994. **81**(6): p. 1493-1499; discussion 26A-27A.
123. Marinov, M.B., et al., *Neuroprotective effects of preischemia intraarterial magnesium sulfate in reversible focal cerebral ischemia.* J Neurosurg, 1996. **85**(1): p. 117-124.
124. Suzer, T., et al., *Neuroprotective effect of magnesium on lipid peroxidation and axonal function after experimental spinal cord injury.* Spinal Cord, 1999. **37**(7): p. 480-484.

125. Sameshima, H. and T. Ikenoue, *Long-term magnesium sulfate treatment as protection against hypoxic-ischemic brain injury in seven-day-old rats.* Am J Obstet Gynecol, 2001. **184**(2): p. 185-190.
126. Vink, R., A.J. Nimmo, and I. Cernak, *An overview of new and novel pharmacotherapies for use in traumatic brain injury.* Clin Exp Pharmacol Physiol, 2001. **28**(11): p. 919-921.
127. Hoane, M.R. and T.M. Barth, *The behavioral and anatomical effects of MgCl2 therapy in an electrolytic lesion model of cortical injury in the rat.* Magnes Res, 2001. **14**(1-2): p. 51-63.
128. Brewer, R.P., et al., *Cerebral blood flow velocity response to magnesium sulfate in patients after subarachnoid hemorrhage.* J Neurosurg Anesthesiol, 2001. **13**(3): p. 202-206.
129. Nelson, K.B. and J.K. Grether, *Can magnesium sulfate reduce the risk of cerebral palsy in very low birthweight infants?* Pediatrics, 1995. **95**(2): p. 263-269.
130. Massicotte, E.M., R. Buist, and M.R. Del Bigio, *Altered diffusion and perfusion in hydrocephalic rat brain: a magnetic resonance imaging analysis.* J Neurosurg, 2000. **92**(3): p. 442-447.
131. Galvin, K.A. and D.E. Oorschot, *Postinjury magnesium sulfate treatment is not markedly neuroprotective for striatal medium spiny neurons after perinatal hypoxia/ischemia in the rat.* Pediatr Res, 1998. **44**(5): p. 740-745.
132. Hallak, M., et al., *Magnesium sulfate treatment decreases N-methyl-D-aspartate receptor binding in the rat brain: an autoradiographic study.* J Soc Gynecol Investig, 1994. **1**(1): p. 25-30.
133. Kaya, M., et al., *Magnesium sulfate attenuates increased blood-brain barrier permeability during insulin-induced hypoglycemia in rats.* Can J Physiol Pharmacol, 2001. **79**(9): p. 793-798.
134. Wolf, G., et al., *Subcutaneously applied magnesium protects reliably against quinolinate-induced N-methyl-D-aspartate (NMDA)-mediated neurodegeneration and convulsions in rats: are there therapeutical implications.* Neurosci Lett, 1990. **117**(1-2): p. 207-211.
135. Moser, V.C., et al., *The IPCS Collaborative Study on Neurobehavioral Screening Methods: II. Protocol design and testing procedures.* NeuroToxicology, 1997. **18**(4): p. 929-938.
136. Hallak, M., et al., *Peripheral magnesium sulfate enters the brain and increases the threshold for hippocampal seizures in rats.* Am J Obstet Gynecol, 1992. **167**(6): p. 1605-1610.
137. Ustun, M.E., et al., *Effects of nimodipine and magnesium sulfate on endogenous antioxidant levels in brain tissue after experimental head trauma.* J Neurosurg Anesthesiol, 2001. **13**(3): p. 227-232.
138. Heath, D.L. and R. Vink, *Optimization of magnesium therapy after severe diffuse axonal brain injury in rats.* J Pharmacol Exp Ther, 1999. **288**(3): p. 1311-1316.

139. Heath, D.L. and R. Vink, *Improved motor outcome in response to magnesium therapy received up to 24 hours after traumatic diffuse axonal brain injury in rats.* J Neurosurg, 1999. **90**(3): p. 504-509.
140. Krueger, R.C., Jr., et al., *Increased extracellular magnesium modulates proliferation in fetal neural cells in culture.* Brain Res Dev Brain Res, 2001. **127**(2): p. 99-109.
141. Philibert, R.A., et al., *Dose-dependent, K+-stimulated efflux of endogenous taurine from primary astrocyte cultures is Ca2+-dependent.* J Neurochem, 1988. **51**(1): p. 122-126.
142. Mittendorf, R., et al., *Association between the use of antenatal magnesium sulfate in preterm labor and adverse health outcomes in infants.* Am J Obstet Gynecol, 2002. **186**(6): p. 1111-1118.
143. Snyder, S.H., M.M. Lai, and P.E. Burnett, *Immunophilins in the nervous system.* Neuron, 1998. **21**(2): p. 283-294.
144. Kim, M.J., et al., *Calpain-dependent cleavage of cain/cabin1 activates calcineurin to mediate calcium-triggered cell death.* Proc Natl Acad Sci U S A, 2002. **99**(15): p. 9870-9875.
145. Wakita, H., et al., *Protective effect of cyclosporin A on white matter changes in the rat brain after chronic cerebral hypoperfusion.* Stroke, 1995. **26**(8): p. 1415-1422.
146. Wakita, H., et al., *Dose-dependent, protective effect of FK506 against white matter changes in the rat brain after chronic cerebral ischemia.* Brain Res, 1998. **792**(1): p. 105-113.
147. Singleton, R.H., et al., *The immunophilin ligand FK506 attenuates axonal injury in an impact-acceleration model of traumatic brain injury.* J Neurotrauma, 2001. **18**(6): p. 607-614.
148. Drake, M., et al., *The immunosuppressant FK506 ameliorates ischaemic damage in the rat brain.* Acta Physiol Scand, 1996. **158**(2): p. 155-159.
149. Sharkey, J. and S.P. Butcher, *Immunophilins mediate the neuroprotective effects of FK506 in focal cerebral ischaemia.* Nature, 1994. **371**(6495): p. 336-339.
150. Bavetta, S., et al., *The effects of FK506 on dorsal column axons following spinal cord injury in adult rats: neuroprotection and local regeneration.* Exp Neurol, 1999. **158**(2): p. 382-393.
151. Hansson, M.J., et al., *Powerful cyclosporin inhibition of calcium-induced permeability transition in brain mitochondria.* Brain Res, 2003. **960**(1-2): p. 99-111.
152. Uchino, H., et al., *Differential neuroprotection by cyclosporin A and FK506 following ischemia corresponds with differing abilities to inhibit calcineurin and the mitochondrial permeability transition.* Neurobiol Dis, 2002. **10**(3): p. 219-233.
153. Okonkwo, D.O. and J.T. Povlishock, *An intrathecal bolus of cyclosporin A before injury preserves mitochondrial integrity and attenuates axonal*

disruption in traumatic brain injury. J Cereb Blood Flow Metab, 1999. **19**(4): p. 443-451.
154. Buki, A., et al., *The role of calpain-mediated spectrin proteolysis in traumatically induced axonal injury.* J Neuropathol Exp Neurol, 1999. **58**(4): p. 365-375.
155. Wells, G.J. and R. Bihovsky, *Calpain inhibitors as potential treatment for stroke and other neurodegenerative diseases: Recent trends and developments.* Exp Opin Therapeutic Patents, 1998. **8**: p. 1707–1727.
156. Rami, A. and J. Krieglstein, *Protective effects of calpain inhibitors against neuronal damage caused by cytotoxic hypoxia in vitro and ischemia in vivo.* Brain Res, 1993. **609**(1-2): p. 67-70.
157. Koedel, U., et al., *Pharmacologic interference with NF-kappaB activation attenuates central nervous system complications in experimental Pneumococcal meningitis.* J Infect Dis, 2000. **182**(5): p. 1437-1445.
158. Del Bigio, M.R., X. Wang, and M.J. Wilson, *Sodium channel-blocking agents are not of benefit to rats with kaolin-induced hydrocephalus.* Neurosurgery, 2002. **51**(2): p. 460-466; discussion 466-467.
159. Liu, X.D., et al., *Cyclosporin A enhanced protection of nimodipine against brain damage induced by hypoxia-ischemia in mice and rats.* Acta Pharmacol Sin, 2002. **23**(3): p. 225-229.
160. Shibazaki, Y., et al., *Effect of the immunosuppressant drug FK506 on neonatal cerebral mitochondrial function and energy metabolism after transient intrauterine ischemia in rats.* Brain Res, 2001. **892**(2): p. 351-358.
161. Araki, T., et al., *Age-related changes of sodium-dependent D-[3H]aspartate and [3H]FK506 binding in rat brain.* J Neural Transm, 1997. **104**(2-3): p. 259-267.
162. Campbell, G., et al., *Spontaneous axonal regeneration after optic nerve injury in adult rat.* Neuroreport, 1999. **10**(18): p. 3955-3960.
163. Donkor, I.O., *A survey of calpain inhibitors.* Curr Med Chem, 2000. **7**(12): p. 1171-1188.
164. Wang, K.K. and P.W. Yuen, *Calpain inhibition: an overview of its therapeutic potential.* Trends Pharmacol Sci, 1994. **15**(11): p. 412-419.
165. Vachon, P., et al., *Cyclosporin A in blood and brain tissue following intra-carotid injections in normal and stroke-induced rats.* Brain Res, 2002. **943**(1): p. 1-8.
166. Sullivan, P.G., et al., *Dose-response curve and optimal dosing regimen of cyclosporin A after traumatic brain injury in rats.* Neuroscience, 2000. **101**(2): p. 289-295.
167. Li, P.A., et al., *Postischemic treatment with calpain inhibitor MDL 28170 ameliorates brain damage in a gerbil model of global ischemia.* Neurosci Lett, 1998. **247**(1): p. 17-20.

168. Mollison, K.W., et al., *Nephrotoxicity studies of the immunosuppressants tacrolimus (FK506) and ascomycin in rat models.* Toxicology, 1998. **125**(2-3): p. 169-181.
169. Wijdicks, E.F., *Neurotoxicity of immunosuppressive drugs.* Liver Transpl, 2001. **7**(11): p. 937-942.
170. Durlach, J., M. Bara, and T. Theophanides, *A hint on pharmacological and toxicological differences between magnesium chloride and magnesium sulphate, or of scallops and men.* Magnes Res, 1996. **9**(3): p. 217-219.
171. Heath, D.L. and R. Vink, *Neuroprotective effects of MgSO4 and MgCl2 in closed head injury: a comparative phosphorus NMR study.* J Neurotrauma, 1998. **15**(3): p. 183-189.
172. Fern, R., B.R. Ransom, and S.G. Waxman, *Voltage-gated calcium channels in CNS white matter: role in anoxic injury.* J Neurophysiol, 1995. **74**(1): p. 369-377.
173. Westenbroek, R.E., et al., *Upregulation of L-type Ca2+ channels in reactive astrocytes after brain injury, hypomyelination, and ischemia.* J Neurosci, 1998. **18**(7): p. 2321-2334.
174. Scriabine, A. and W. van den Kerckhoff, *Pharmacology of nimodipine. A review.* Ann N Y Acad Sci, 1988. **522**: p. 698-706.
175. Rinkel, G.J., et al., *Calcium antagonists for aneurysmal subarachnoid haemorrhage.* Cochrane Database Syst Rev, 2005(1): p. CD000277.
176. Iseri, L.T. and J.H. French, *Magnesium: nature's physiologic calcium blocker.* Am Heart J, 1984. **108**(1): p. 188-193.
177. Bahar, M., et al., *Intracellular Ca++/Mg++ homeostasis during postnatal growth of experimental rats. Multiple time-point study.* Growth Dev Aging, 2002. **66**(2): p. 55-62.
178. Tanaka, O., H. Sakagami, and H. Kondo, *Localization of mRNAs of voltage-dependent Ca(2+)-channels: four subtypes of alpha 1- and beta-subunits in developing and mature rat brain.* Brain Res Mol Brain Res, 1995. **30**(1): p. 1-16.
179. Vance, C.L., et al., *Differential expression and association of calcium channel alpha1B and beta subunits during rat brain ontogeny.* J Biol Chem, 1998. **273**(23): p. 14495-14502.
180. Schluter, G., *Toxicological investigations with nimodipine. Summary of relevant studies.* Arzneimittelforschung, 1986. **36**(12): p. 1733-1735.
181. Buwalda, B., et al., *Nimodipine accelerates the postnatal development of parvalbumin and S-100 beta immunoreactivity in the rat brain.* Brain Res Dev Brain Res, 1994. **78**(2): p. 210-216.
182. Angrisani, M., et al., *Interference of prenatal and postnatal exposure to Ca2+-antagonist agents on rat functional development of vascular system.* Teratog Carcinog Mutagen, 1989. **9**(1): p. 39-49.
183. Futagi, Y., et al., *Neurodevelopmental outcome in children with fetal hydrocephalus.* Pediatr Neurol, 2002. **27**(2): p. 111-116.

184. Hanlo, P.W., et al., *The effect of intracranial pressure on myelination and the relationship with neurodevelopment in infantile hydrocephalus.* Dev Med Child Neurol, 1997. **39**(5): p. 286-291.
185. Begg, A.C., *Is HIF-1alpha a good marker for tumor hypoxia?* Int J Radiat Oncol Biol Phys, 2003. **56**(4): p. 917-919.

APPENDIX

Experimental Models of Hydrocephalus

This was published in: Handbook of Experimental Neurology: Methods and Techniques in Animal Research. Editors: Turgut Tatlisumak and Marc Fisher. Cambridge University Press; 2006: 457 – 471; ISBN: 0-521-83814-2.

Authors: Osaama H. Khan and Marc R. Del Bigio

I INTRODUCTION

Hydrocephalus is a common neurological condition characterized by impairment of cerebrospinal fluid (CSF) flow with subsequent enlargement of CSF-containing ventricular cavities in the brain. CSF absorption occurs through arachnoid villi into venous sinuses and along cranial and spinal nerves into lymphatics (1). Enlarging ventricles damage the surrounding brain tissue. In children, hydrocephalus is associated with mental retardation, physical disability, and impaired growth. The pathogenesis of brain dysfunction includes alterations in the chemical environment of brain, chronic ischemia in white matter, and physical damage to axons with ultimate disconnection of neurons (2-4). Hydrocephalus is the second most frequent congenital malformation (after spina bifida) of the nervous system, occurring in 5-6/10,000 live births (5). It also develops in 80% of patients with spina bifida (6), and 15% of premature (<30 weeks) infants following intraventricular hemorrhage (7). Hydrocephalus can develop later in childhood or adulthood as a consequence of brain tumors, meningitis, brain injury, or subarachnoid hemorrhage.

For detailed discussions of the pathology of hydrocephalus see previous reviews (2, 3). Briefly summarized, the ependyma lining the ventricles is damaged. In the subependymal layer, reactive gliosis is almost always observed and mitotic activity occurs among subependymal cells (8). Hydrocephalus can cause reduction in cerebral blood flow and alterations in oxidative metabolism in subcortical regions (9, 10) where white matter axons and myelin are the main target of damage in hydrocephalus (11, 12). Imaging studies indicate that the brain is edematous in the periventricular region (13). Severe hydrocephalus can cause thinning of the cerebral cortex and atrophy of the basal ganglia (2). Age of the animal and mode of induction of hydrocephalus are important factors in determining the pathology (14).

II Animal Models

Hochwald (15) categorized methods for inducing hydrocephalus: 1. Obstruction to CSF flow through the aqueduct of Sylvius and foramen of Monro, or the basilar cisterns and the cisterna magna, 2. Interference with the flow of blood through the great vein of Galen, 3. Creation of primary congenital malformations of the neural tube or neurological anomalies secondary to axial skeletal dysraphic states caused by exogenous insults with teratogens directed at pregnant mammals. To study the pathophysiology of hydrocephalic brain damage (in contrast to the causes of hydrocephalus), the method of induction should cause the ventricles to enlarge but should not directly affect the brain, which chemical, radiation and viral induction methods can do. The range of species used includes mouse, rat, guinea pig, rabbit, cat, dog, pig (16), fetal lamb (17), and primates such as Macaca mulatta (18) and Rhesus monkey (19).

When choosing a model, several factors need to be addressed such as animal availability, the pathological aspects one wishes to explore, age, time-course of hydrocephalus, and methods for assessing physical, behavioral, and/or biochemical changes (14, 20). Unlike humans, rodents have only narrow layers of periventricular white matter and their brains are lissencephalic (i.e. no gyri), therefore there are limitations in the applicability.

Hereditary Models of Hydrocephalus

hy3 Mouse

The spontaneous hydrocephalus murine mutant model (hy3) was identified in 1943 (21). Perinatal onset is associated with alterations in periventricular tissues and eventually the cerebral cortex (22). The underlying pathological mechanisms are not completely understood. It is an autosomal recessive trait (23). More recently a random transgenic insertion on chromosome 8 led unexpectedly to hydrocephalus in mice and genetic crosses between hemizygous OVE459 mice and mice heterozygous for hy3 produced hydrocephalic offspring with a frequency of 22%, demonstrating that these two mutations are allelic (24-26).

hyh Mouse

A lethal recessive mutation in the C57BL/10J mouse strain was labeled hydrocephalus with hop gait (hyh). Morphological changes are evident between 4 and 10 weeks of age with enlargement of lateral and third ventricles, and narrowing of the cerebral aqueduct. Hyh has been mapped to the proximal end of chromosome 7 (27). The soluble *N*-ethylmalemide-sensitive factor (NSF) attachment protein alpha-S-nitroso-N-acetylpenicillamine (alpha-SNAP) has been identified as the only mutated protein (28, 29). The mutation causes a smaller cerebral cortex due to reduced progenitor pool of late-born upper-layer cortical neurons (30). Obliteration of distal end of aqueduct and severe hydrocephalus has been observed (31).

L1 CAM

L1 cell adhesion molecule (L1 CAM) is a member of the superfamily of immunoglobulin (Ig)-related cell adhesion molecules. It plays a pivotal role in growth and guidance of particular axon tracts in the developing nervous system (32). In humans, mutations in L1 are associated with a neurological syndrome termed CRASH, which includes corpus callosum agenesis, mental retardation, adducted thumbs, spasticity, and X-linked hydrocephalus (33, 34). The L1-CAM gene is located at Xq28 in humans (35) and pathological human mutations are believed to eliminate exon 2 (36). In the mouse model, the size of the corticospinal tract corpus callosum is reduced and, depending on genetic background, the lateral ventricles are often enlarged. In vitro, neurite outgrowth is impaired (37) and surface ligand interactions are altered (38). In the cerebral cortex, many pyramidal neurons in layer V exhibit undulating apical dendrites that do not reach layer I. The hippocampus is small, with fewer pyramidal and granule cells (39).

Transforming Growth Factor- $_1$

Mice that overexpress transforming growth factor-$_1$ (TGF_1) were generated in an attempt to study astrocytic response to injury. The unexpected result was severe ventricle enlargement, spasticity, limb tremors and ataxia with death by three weeks of age (40-42). Injection of human TGF_1 into the subarachnoid space of 10-day-old mice results in hydrocephalus (43). In all cases, the cause appears to be obliteration of CSF pathways in the subarachnoid space. This cytokine may play a role in post-meningitis and subarachnoid hemorrhage meningeal scarring.

H-Tx Rat

The Hydrocephalus Texas (H-Tx) rat has been extremely well studied. H-Tx was described in 1981 (44) and probably arose from the Lewis strain of Sprague-Dawley rats (45). The H-Tx rat is a homozygous carrier of an autosomal recessive gene with incomplete penetrance (46-50). There is an epigenetic factor that increases in fetuses if suckling pups are present during gestation (51). Strong linkages to the trait are on loci of chromosomes 10, 11, and 17 with weaker linkages on 4, 9, and 19 (47). Jones's group and others have published morphological (45, 52, 53), metabolic (54), and behavioral (55) descriptions. The rats have fetal-onset associated with the closure of the cerebral aqueduct. The precise mechanisms through which narrowing occurs is not clear. Even non-hydrocephalic H-Tx rats have abnormal behavior (56).

LEW/Jms Rat

The LEW/Jms rat strain, described in 1983 (57), was derived from an inbred strain of Wistar-Lewis rats at the University of Tokyo. In most respects, the phenotype for LEW/Jms is similar in onset and pathophysiology to that of H-Tx (58).

Mechanical Models of Hydrocephalus

Injections into the cisterna magna

Dandy and Blackfan described induction of hydrocephalus by injecting lampblack (i.e. charcoal soot) into the cisterna magna of dogs (59). Injections of many substances can be done percutaneously or with surgical exposure of the skull base. CSF of an equal volume may be withdrawn, but this is not always necessary because spontaneous leakage of CSF around the needle tends to occur. A sufficiently small needle must be used to avoid reflux (e.g. 28 gauge in the rat). Proper flexion of the neck (Figure 1) is necessary so that the substance is delivered into the foramen magnum and/or fourth ventricle while avoiding injury to the brainstem. In the case of the rodent, this flexion can be achieved by placing the chest on a sponge support with application of gentle pressure on the snout and mid-back. Larger animals (rabbits, dogs, etc.) usually require more rigid fixation, for example with a maxillary clamp. In rodents the foramen magnum can be palpated after the neck is shaved and cleansed with iodine or 70% ethanol. The needle should enter the dorsal foramen magnum, and be almost parallel to the cervical spine. In mature rodents and larger animals, as the needle passes through the dura a sudden loss of resistance is felt. In small animals the needle should be advanced no more than 1 – 2 mm beyond this point. If the foramen magnum is surgically exposed through a midline suboccipital / cervical incision, a pad of surgical hemostasis material (e.g. Gelfoam) can be placed over the puncture site. A retention suture can be used to approximate the cervical muscles in the midline to help retain this material.

We have used many types of anesthesia including cooling for neonatal rodents, ketamine-xylazine delivered parenterally, and inhalation of halothane or isoflurane by nose cone. The latter has the advantage of rapid recovery, but it is sometimes difficult to keep the nose cone in place during neck flexion. After recovery, the animal should be closely observed for head tilt, leaning to one side, circling, or hemiparesis, which indicate injury to brain stem or spinal cord. Some recovery of head tilt may occur but paretic animals should be euthanized. Seizures, presumably the result of a more general irritative phenomenon, may occasionally occur. Most animals exhibit signs of lethargy, weakness, and ataxia

for a few days post-induction. Delayed gain of weight is often the earliest indicator of successful induction of hydrocephalus.

Kaolin

Kaolin-induced subarachnoid space occlusion is among the most commonly used models (60). Kaolin is a whitish, clay-like substance (aluminum silicate) that is placed in suspension (250mg/ml kaolin in 0.9% saline) before injection. It mimics post-meningitis or post-subarachnoid hemorrhage hydrocephalus with scarring in the subarachnoid space. It is simple, reproducible, inexpensive, and is not species dependent. The optimum volume depends on size of the animal. The severity can be titrated according to dose. Neonatal (less than a week old) rats receive 0.02 ml, while 0.05 ml is given to young and adult rats (61). During injection into neonatal rodents, kaolin can be seen spreading beneath the translucent occipital bone. Other authors report effectiveness of 0.2 – 0.5 ml in young rabbits (62) and 3 ml in adult dogs (63). Kaolin spreads with CSF flow and following sacrifice it can be identified on the ventral surface of the brainstem and as far as the olfactory tracts or middle cerebral arteries (Figure 2). In addition to ventricle enlargement, syrinx formation can occur in the cervical and thoracic spinal cord. Microscopically, kaolin engulfed by macrophages can be identified as small black refractive granules. The inflammatory cells are embedded in a delicate collagen web in the subarachnoid space. Although we have observed no astroglial or microglial reaction in adjacent brain matter (8), T lymphocytes have been reported to appear early in the subarachnoid compartment and adjacent to brain tissue following kaolin injections (64).

Fibroblast growth factor

Fibroblast growth factor (FGF-2) or basic FGF can induce proliferation of fibroblasts, endothelial cells, smooth muscle cells, as well as other cells (65). Hydrocephalus was induced in adult Sprague-Dawley rats by infusing recombinant FGF-2 at 1 microgram/day into the lateral ventricle for 2-12 days

(66). High doses of FGF in mice resulted in enlargement of the ventricles and thinning of the cortex (67). Exogenous FGF can affect brain cell survival and differentiation directly without causing hydrocephalus (68)

Silastic oil

Silastic oil injected into the cisterna magna produces a pure mechanical obstruction without inflammatory changes in the subarachnoid compartment (69-71). This transparent substance is available in different viscosities; typically a viscosity of 5000 – 10,000 centistokes is optimal. The oil sits in the fourth ventricle and subarachnoid space. The injection method is essentially the same as kaolin, however, because the viscosity is greater a larger needle (>23 gauge) must be used. Severe ventriculomegaly and high pressures are not possible. In an attempt to increase the success rate, 5ml of Silastic elastomer solution, which hardens after injection, has been used in dogs (72, 73).

Cyanoacrylic gel

Luciano and coworkers described a model applicable to large animals (74, 75). Cyanoacrylic gel glue is injected into adult dogs to create surgical occlusion of the fourth ventricle. The large size of the canine brain enables implementation and testing of novel diagnostic and treatment modalities. Surgeries are performed with the dog in the prone position in a stereotaxic head frame. A suboccipital craniectomy exposes the fourth ventricle floor. Obstructions are produced by placing flexible silicone tubing (1.5 mm o.d.) connected to an 18-gauge catheter in the fourth ventricle. Through this catheter 0.25–0.35 ml of surgical grade cyanoacrylic gel glue (Loctite Corp., Newington, CT) is delivered. The rapidly curing glue does not significantly compress or deform surrounding tissues, while it adheres to the ependymal and pial membranes of the brainstem and cerebellum. Therefore potential for CSF leakage is minimal. The catheter remains in place. Postoperatively, animals receive anti-inflammatory, antibiotic,

and analgesic drugs. Histologically, multinucleate foreign body giant cells can be seen at sites of contact between glue and tissue.

Plugs

Dandy and Blackfan used a piece of cotton to surgically occlude the aqueduct of Sylvius via the fourth ventricle (59). Cellophane cylinders have also been used in dogs with a success rate of 75% (76). The major disadvantage of this model is that it is a major surgical procedure with a high likelihood of damage to brain stem structures. Therefore, this model should probably be only used for acute experiments.

Venous occlusion

Dandy also described ligation of the vena magna galeni or sinus rectus as a way of creating hydrocephalus in dogs (77). The rationale is that some CSF is absorbed through the venous system. Hydrocephalus due to elevated venous pressure certainly occurs in human infants (78, 79), but seldom in older children or adults (80). Obliteration of the internal and external jugular veins at the base of the skull of adult dogs results in moderate hydrocephalus (81). A similar result can be achieved in adult rabbits (82).

III Methods of Assessment

Behavior

Hydrocephalus in immature animals whose skull sutures are not fused is associated with a dome-shaped head and/or persistent fontanel (Figure 3). However, the correlation between head width and ventricle size is not accurate. In mature animals the head does not enlarge and the degree of lethargy or retardation of weight gain may be more valid indicators. We and others have used behavioral methods to study hydrocephalic rats. In neonatal rats we have observed that acquisition of early motor behaviors such as righting reflex,

pivoting, negative geotaxis, and wire-hanging (83) are delayed. In young and adult rats, deficits in memory can be assessed using a water maze (55, 56) or radial arm maze (84). Posture, movement, and gait can be assessed using treadmills, rotorods, automated activity monitoring, and open field test to assess lethargy (12, 85).

Imaging

There is inherent variability in the models therefore it is important to image the brain in vivo. Barkovich has compared the range of imaging techniques used on humans (13); similar methods can be used in animals. Ultrasonography has been used for kittens (86), dogs (72), and piglets (16). However, it cannot be used when the skull sutures are fused because ultrasound does not penetrate bone. Furthermore, the resolution is not very good. Computerized tomography (CT) scanning has been used to image hydrocephalic cats, dogs, etc. (87, 88). A new bench-top CT (SkyScan, Aartselaar Belgium) could be conveniently used for rodents. Many labs now use magnetic resonance (MR) imaging which provides superb anatomical resolution as well as metabolic imaging capability in any species (Figure 4) (53, 85, 89, 90). Ventricle size can be measured quickly with Evans ratios (ventricle width / brain width) or complete image sets can be assessed by planimetry to calculate the brain and ventricle volumes (12).

Histology

After sacrifice and opening of the skull, the expansion and thinning of the cerebrum can be assessed. If the brain is very thin, it will tend to collapse as CSF leaks out. Fixed brains are slightly more rigid. If sectioned in the coronal plane, the ventricle width or area can be determined in the fresh state or after sectioning for histologic preparation. In vivo imaging, however, is inherently more accurate.

IV Summary

Many animal models are available for studies of hydrocephalus (Table 1). Genetic models might have associated brain changes not directly due to hydrocephalus, but they are predictable and they mimic some types of human fetal-onset hydrocephalus. Artificial induction models vary in the invasiveness, expense, and the extent to which they mimic human situations. The investigator must choose the model that will allow proper study of the topic in question. Imaging of animals is expensive but critical for linking animal studies to the human disorder, for studying the dynamics of ventricle enlargement, and for neuroprotective studies which require assignment to treatment groups prior to sacrifice. Recognizing the applicability and limitations of these models is critical to understanding human hydrocephalus.

Table 1. Summary of Hydrocephalic Animal Models

Experimental Model	Advantages	Disadvantages
Mouse mutant models	Resurgence of interest because genetic exploration/understanding feasible; relatively inexpensive, reproducible	Cost of maintaining breeding colony; applicability awaits understanding of underlying cause of hydrocephalus; too small for surgical interventions
Rat mutant models	Spontaneous neonatal hydrocephalus; predictable; surgical intervention possible	Genetic explanation unknown; possible brain abnormalities in unaffected animals of same strain; cost of maintaining breeding colony
Kaolin injection into cisterna magna	Easy; inexpensive; titratable severity; any age and any animal possible	Possible broader effect of inflammation
Silicone oil injection into cisterna magna	Easy; inexpensive; pure mechanical obstruction	Severe ventriculomegaly and high pressures not possible
Cyanoacrylate glue injection into cisterna magna of dogs	Large animal therefore modeling of complex surgical systems possible	Technically complicated and expensive
FGF injection into cisterna magna	Easy; fibrotic obstruction in subarachnoid space	Expensive; FGF might affect brain cells directly

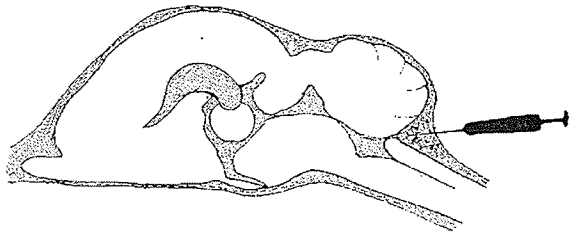

Figure 1. Diagram showing position of needle entry for cisternal injection in rodents.

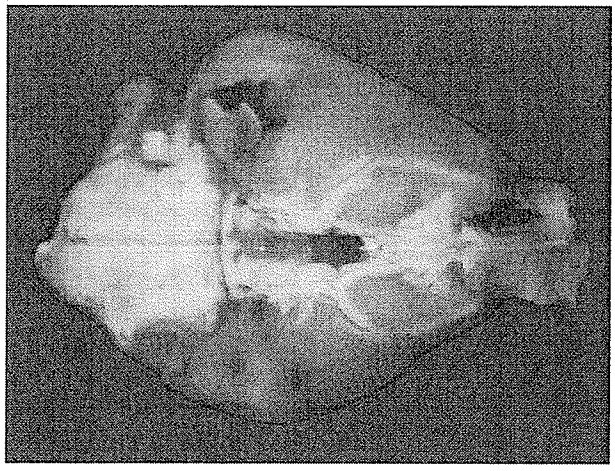

Figure 2. Photograph showing base of adult rat brain with severe hydrocephalus, 9 months after kaolin injection into the cisterna magna. The kaolin appears as a white layer on the surface of the brainstem, around the hypothalamus, and along the middle cerebral arteries.

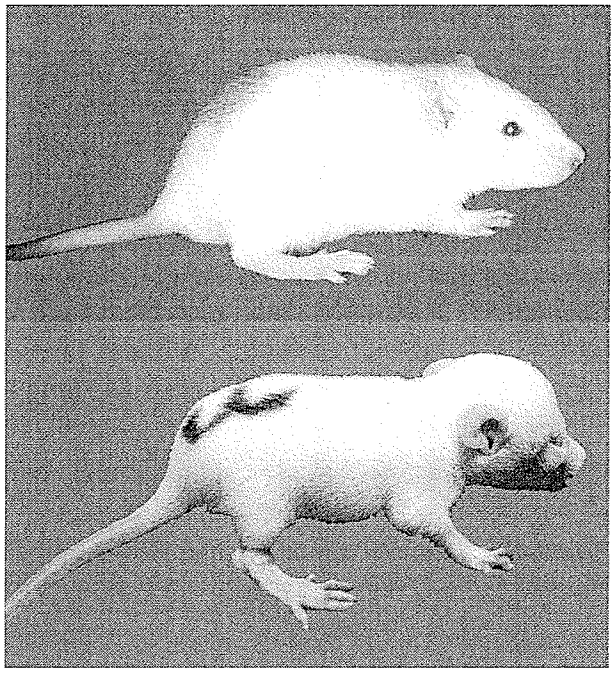

Figure 3. Photographs showing a normal 17-day old rat (A) and a hydrocephalic rat (B) of the same age that received kaolin injection on day 1. The body is smaller, the head is domed, and the legs are positioned abnormally.

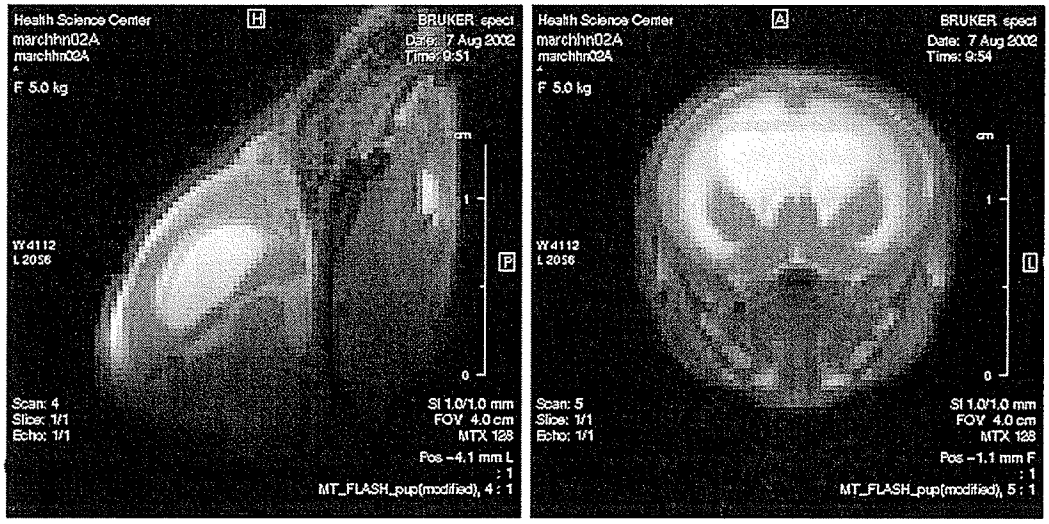

Figure 4. T2-weighted MR images showing sagittal (left) and coronal (right) views of brain of 7-day old hydrocephalic rat that received kaolin injection on day 1. The

ventricles are enlarged and the external capsule white matter is edematous (bright signal).

REFERENCES

1. Papaiconomou C, Bozanovic-Sosic R, Zakharov A, Johnston M. Does neonatal cerebrospinal fluid absorption occur via arachnoid projections or extracranial lymphatics? Am J Physiol Regul Integr Comp Physiol 2002;283(4):R869-R876.
2. Del Bigio MR. Neuropathological changes caused by hydrocephalus. Acta Neuropathol (Berl) 1993;85(6):573-585.
3. Del Bigio MR. Pathophysiologic consequences of hydrocephalus. Neurosurg Clin N Am 2001;12(4):639-649.
4. Del Bigio MR, McAllister JP, II. Hydrocephalus - Pathology. In: Choux M, Di Rocco C, Hockley AD, Walker ML, editors. Pediatric Neurosurgery. London: Churchill Livingstone; 1999. p. 217-236.
5. Wiswell TE, Tuttle DJ, Northam RS, Simonds GR. Major congenital neurologic malformations. A 17-year survey. Am. J. Dis. Child. 1990;144:61-67.
6. Stein SC, Schut L. Hydrocephalus in myelomeningocele. Child's Brain 1979;5:413-419.
7. Holt PJ, Allan WC. The natural history of ventricular dilatation in neonatal intraventricular hemorrhage and its therapeutic implications. Ann. Neurol. 1981;10:293-294.
8. Del Bigio MR, Zhang YW. Cell death, axonal damage, and cell birth in the immature rat brain following induction of hydrocephalus. Exp Neurol 1998;154(1):157-169.
9. Hochwald GM, Boal RD, Marlin AE, Kumar AJ. Changes in regional blood-flow and water content of brain and spinal cord in acute and chronic experimental hydrocephalus. Dev Med Child Neurol Suppl 1975;35:42-50.
10. Chumas PD, Drake JM, Del Bigio MR, Da Silva M, Tuor UI. Anaerobic glycolysis preceding white-matter destruction in experimental neonatal hydrocephalus. J Neurosurg 1994;80(3):491-501.
11. Del Bigio MR. Calcium-mediated proteolytic damage in white matter of hydrocephalic rats? J Neuropathol Exp Neurol 2000;59(11):946-954.
12. Del Bigio MR, Wilson MJ, Enno T. Chronic hydrocephalus in rats and humans: white matter loss and behavior changes. Ann Neurol 2003;53(3):337-346.
13. Barkovich AJ, Edwards MS. Applications of neuroimaging in hydrocephalus. Pediatr Neurosurg 1992;18(2):65-83.
14. Matsumoto S, Hirayama A, Yamasaki S, Shirataki K, Fujiwara K. Comparative study of various models of experimental hydrocephalus. Childs Brain 1975;1(4):236-242.
15. Hochwald GM. Animal models of hydrocephalus: recent developments. Proc. Soc. Exp. Biol. Med. 1985;178:1-11.

16. Taylor GA, Soul JS, Dunning PS. Sonographic ventriculography: a new potential use for sonographic contrast agents in neonatal hydrocephalus. AJNR Am J Neuroradiol 1998;19(10):1931-1934.
17. Nakayama DK, Harrison MR, Berger MS, Chinn DH, Halks-Miller M, Edwards MS. Correction of congenital hydrocephalus in utero I. The model: intracisternal kaolin produces hydrocephalus in fetal lambs and rhesus monkeys. J Pediatr Surg 1983;18(4):331-338.
18. Flor WJ, James AE, Jr., Ribas JL, Parker JL, Sickel WL. Ultrastructure of the ependyma in the lateral ventricles of primates with experimental communicating hydrocephalus. Scan Electron Microsc 1979;III:47-54.
19. Hammock MK, Milhorat TH, Earle K, Di Chiro G. Vein of Galen ligation in the primate. Angiographic, gross, and light microscopic evaluation. J Neurosurg 1971;34(1):77-83.
20. Del Bigio MR. Future directions for therapy of childhood hydrocephalus: a view from the laboratory. Pediatr. Neurosurg. 2001;34(4):172-181.
21. Gruneberg H. Congenital hydrocephalus in the mouse; a case of spurious pleiotropism. J. Genet. 1943;45:1-21.
22. McLone DG, Bondareff W, Raimondi AJ. Brain edema in the hydrocephalic hy-3 mouse: submicroscopic morphology. J. Neuropathol. Exp. Neurol. 1971;30:627-637.
23. Berry RJ. The inheritance and pathogenesis of hydrocephalus-3 in the mouse. J. Pathol. Bacteriol. 1961;81:157-167.
24. Robinson ML, Davy.B.E., Elliot C, Rizo CM, Harrison WR, Elder FF, et al. A new allele of an old mutation: genetic mapping of an autosomal recessive, hydrocephalus-inducing mutation in mice. In: Society for Research into Hydrocephalus and Spina Bifida, 44th Annual Scientific Meeting; 2000; Atlanta GA, June 21-24; 2000.
25. Robinson ML, Allen CE, Davy BE, Durfee WJ, Elder FF, Elliott CS, et al. Genetic mapping of an insertional hydrocephalus-inducing mutation allelic to hy3. Mamm Genome 2002;13(11):625-632.
26. Davy BE, Robinson ML. Congenital hydrocephalus in hy3 mice is caused by a frameshift mutation in Hydin, a large novel gene. Hum Mol Genet 2003;12(10):1163-1170.
27. Bronson RT, Lane PW. Hydrocephalus with hop gait (hyh): a new mutation on chromosome 7 in the mouse. Brain Res Dev Brain Res 1990;54(1):131-136.
28. Hong HK, Chakravarti A, Takahashi JS. The gene for soluble N-ethylmaleimide sensitive factor attachment protein alpha is mutated in hydrocephaly with hop gait (hyh) mice. Proc Natl Acad Sci U S A 2004;101(6):1748-1753.
29. Chae TH, Allen KM, Davisson MT, Sweet HO, Walsh CA. Mapping of the mouse hyh gene to a YAC/BAC contig on proximal Chromosome 7. Mamm Genome 2002;13(5):239-244.

30. Chae TH, Kim S, Marz KE, Hanson PI, Walsh CA. The hyh mutation uncovers roles for alpha Snap in apical protein localization and control of neural cell fate. Nat Genet 2004;36(3):264-270.
31. Wagner C, Batiz LF, Rodriguez S, Jimenez AJ, Paez P, Tome M, et al. Cellular mechanisms involved in the stenosis and obliteration of the cerebral aqueduct of hyh mutant mice developing congenital hydrocephalus. J Neuropathol Exp Neurol 2003;62(10):1019-1040.
32. Kenwrick S, Watkins A, De Angelis E. Neural cell recognition molecule L1: relating biological complexity to human disease mutations. Hum Mol Genet 2000;9(6):879-886.
33. Kenwrick S, Jouet M, Donnai D. X linked hydrocephalus and MASA syndrome. J Med Genet 1996;33(1):59-65.
34. Itoh K, Cheng L, Kamei Y, Fushiki S, Kamiguchi H, Gutwein P, et al. Brain development in mice lacking L1-L1 homophilic adhesion. J Cell Biol 2004;165(1):145-154.
35. Van Camp G, Vits L, Coucke P, Lyonnet S, Schrander-Stumpel C, Darby J, et al. A duplication in the L1CAM gene associated with X-linked hydrocephalus. Nat Genet 1993;4(4):421-425.
36. Jacob J, Haspel J, Kane-Goldsmith N, Grumet M. L1 mediated homophilic binding and neurite outgrowth are modulated by alternative splicing of exon 2. J Neurobiol 2002;51(3):177-189.
37. Dahme M, Bartsch U, Martini R, Anliker B, Schachner M, Mantei N. Disruption of the mouse L1 gene leads to malformations of the nervous system. Nat Genet 1997;17(3):346-349.
38. De Angelis E, Watkins A, Schafer M, Brummendorf T, Kenwrick S. Disease-associated mutations in L1 CAM interfere with ligand interactions and cell-surface expression. Hum Mol Genet 2002;11(1):1-12.
39. Demyanenko GP, Tsai AY, Maness PF. Abnormalities in neuronal process extension, hippocampal development, and the ventricular system of L1 knockout mice. J Neurosci 1999;19(12):4907-4920.
40. Galbreath E, Kim SJ, Park K, Brenner M, Messing A. Overexpression of TGF-beta 1 in the central nervous system of transgenic mice results in hydrocephalus. J Neuropathol Exp Neurol 1995;54(3):339-349.
41. Wyss-Coray T, Feng L, Masliah E, Ruppe MD, Lee HS, Toggas SM, et al. Increased central nervous system production of extracellular matrix components and development of hydrocephalus in transgenic mice overexpressing transforming growth factor-beta 1. Am J Pathol 1995;147(1):53-67.
42. Cohen AR, Leifer DW, Zechel M, Flaningan DP, Lewin JS, Lust WD. Characterization of a model of hydrocephalus in transgenic mice. J Neurosurg 1999;91(6):978-988.
43. Tada T, Kanaji M, Kobayashi S. Induction of communicating hydrocephalus in mice by intrathecal injection of human recombinant transforming growth factor-beta 1. J Neuroimmunol 1994;50(2):153-158.

44. Kohn DF, Chinookoswong N, Chou SM. A new model of congenital hydrocephalus in the rat. Acta Neuropathol (Berl) 1981;54(3):211-218.
45. Jones HC, Bucknall RM. Inherited prenatal hydrocephalus in the H-Tx rat: a morphological study. Neuropathol Appl Neurobiol 1988;14(4):263-274.
46. Cai X, McGraw G, Pattisapu JV, von Kalm L, Willingham S, Socci D, et al. Hydrocephalus in the H-Tx rat: a monogenic disease? Exp Neurol 2000;163(1):131-135.
47. Jones HC, Carter BJ, Depelteau JS, Roman M, Morel L. Chromosomal linkage associated with disease severity in the hydrocephalic H-Tx rat. Behav Genet 2001;31(1):101-111.
48. Jones HC, Lopman BA, Jones TW, Carter BJ, Depelteau JS, Morel L. The expression of inherited hydrocephalus in H-Tx rats. Childs Nerv Syst 2000;16(9):578-584.
49. Jones HC, Lopman BA, Jones TW, Morel LM. Breeding characteristics and genetic analysis of the H-Tx rat strain. Eur J Pediatr Surg 1999;9 Suppl 1:42-43.
50. Jones HC, Depelteau JS, Carter BJ, Lopman BA, Morel L. Genome-wide linkage analysis of inherited hydrocephalus in the H-Tx rat. Mamm Genome 2001;12(1):22-26.
51. Jones HC, Depelteau JS, Carter BJ, Somera KC. The frequency of inherited hydrocephalus is influenced by intrauterine factors in H-Tx rats. Exp Neurol 2002;176(1):213-220.
52. Boillat CA, Jones HC, Kaiser GL, Harris NG. Ultrastructural changes in the deep cortical pyramidal cells of infant rats with inherited hydrocephalus and the effect of shunt treatment. Exp Neurol 1997;147(2):377-388.
53. Jones HC, Harris NG, Briggs RW, Williams SC. Shunt treatment at two postnatal ages in hydrocephalic H-Tx rats quantified using MR imaging. Exp Neurol 1995;133(2):144-152.
54. Jones HC, Harris NG, Rocca JR, Andersohn RW. Progressive changes in cortical metabolites at three stages of infantile hydrocephalus studied by in vitro NMR spectroscopy. J Neurotrauma 1997;14(9):587-602.
55. Jones HC, Rivera KM, Harris NG. Learning deficits in congenitally hydrocephalic rats and prevention by early shunt treatment. Childs Nerv Syst 1995;11(11):655-660.
56. Hawkins D, Bowers TM, Bannister CM, Miyan JA. The functional outcome of shunting H-Tx rat pups at different ages. Eur J Pediatr Surg 1997;7 Suppl 1:31-34.
57. Sasaki S, Goto H, Nagano H, Furuya K, Omata Y, Kanazawa K, et al. Congenital hydrocephalus revealed in the inbred rat, LEW/Jms. Neurosurgery 1983;13(5):548-554.
58. Jones HC, Carter BJ, Morel L. Characteristics of hydrocephalus expression in the LEW/Jms rat strain with inherited disease. Childs Nerv Syst 2003;19(1):11-18.

59. Dandy WE, Blackfan KD. An experimental and clinical study of internal hydrocephalus. JAMA 1913;61:2216-2217.
60. Dixon WE, Heller H. Experimentelle Hypertonie durch Eröhung des intrakaniellen Druckes. Arch. Exp. Pathol. Pharmakol. 1932;166:265-275.
61. Khan OH, Enno T, Del Bigio MR. Magnesium sulfate therapy is of mild benefit to young rats with kaolin-induced hydrocephalus. Pediatr Res 2003;53(6):970-976.
62. Gopinath G, Bhatia R, Gopinath PG. Ultrastructural observations in experimental hydrocephalus in the rabbit. J Neurol Sci 1979;43(3):333-334.
63. Gonzalez-Darder J, Barbera J, Cerda-Nicolas M, Segura D, Broseta J, Barcia-Salorio JL. Sequential morphological and functional changes in kaolin-induced hydrocephalus. J Neurosurg 1984;61(5):918-924.
64. Shinoda M, Olson L. Immunological aspects of kaolin-induced hydrocephalus. Int J Neurosci 1997;92(1-2):9-28.
65. Burgess WH, Maciag T. The heparin-binding (fibroblast) growth factor family of proteins. Annu Rev Biochem 1989;58:575-606.
66. Johanson CE, Szmydynger Chodobska J, Chodobski A, Baird A, McMillan P, Stopa EG. Altered formation and bulk absorption of cerebrospinal fluid in FGF-2-induced hydrocephalus. Am. J. Physiol. 1999;277(1):R263-R271.
67. Ohmiya M, Fukumitsu H, Nitta A, Nomoto H, Furukawa Y, Furukawa S. Administration of FGF-2 to embryonic mouse brain induces hydrocephalic brain morphology and aberrant differentiation of neurons in the postnatal cerebral cortex. J Neurosci Res 2001;65(3):228-235.
68. Alzheimer C, Werner S. Fibroblast growth factors and neuroprotection. Adv Exp Med Biol 2002;513:335-351.
69. Wisniewski H, Weller RO, Terry RD. Experimental hydrocephalus produced by the subarachnoid infusion of silicone oil. J Neurosurg 1969;31(1):10-14.
70. James AE, Jr., Strecker E-P. Use of silastic to produce communicating hydrocephalus. Invest Radiol 1973;8(2):105-110.
71. Del Bigio MR, Bruni JE. Periventricular pathology in hydrocephalic rabbits before and after shunting. Acta Neuropathol (Berl) 1988;77(2):186-195.
72. Brown JA, Rachlin J, Rubin JM, Wollmann RL. Ultrasound evaluation of experimental hydrocephalus in dogs. Surg Neurol 1984;22(3):273-276.
73. Page LK, White WP. Transsphenoidal injection of silicone for the production of communicating or obstructive hydrocephalus in dogs. Surg Neurol 1982;17(4):247-250.
74. Johnson MJ, Ayzman I, Wood AS, Tkach JA, Klauschie J, Skarupa DJ, et al. Development and characterization of an adult model of obstructive hydrocephalus. J. Neurosci. Meth. 1999;91(1-2):55-65.
75. Luciano MG, Skarupa DJ, Booth AM, Wood AS, Brant CL, Gdowski MJ. Cerebrovascular adaptation in chronic hydrocephalus. J Cereb Blood Flow Metab 2001;21(3):285-294.

76. Schurr PH, McLaurin RL, Ingraham FD. Experimental studies on the circulation of the cerebrospinal fluid and methods of producing communicating hydrocephalus in the dog. J Neurosurg 1953;10(5):515-525.
77. Dandy WE. Experimental hydrocephalus. Ann. Surg. 1919;70(2):129-142.
78. Sainte-Rose C, LaCombe J, Pierre-Kahn A, Renier D, Hirsch JF. Intracranial venous sinus hypertension: cause or consequence of hydrocephalus in infants? J Neurosurg 1984;60(4):727-736.
79. Karahalios DG, Rekate HL, Khayata MH, Apostolides PJ. Elevated intracranial venous pressure as a universal mechanism in pseudotumor cerebri of varying etiologies. Neurology 1996;46(1):198-202.
80. Gil Z, Specter-Himberg G, Gomori MJ, Matot I, Rein AJ, Nir A, et al. Association between increased central venous pressure and hydrocephalus in children undergoing cardiac catheterization. A prospective study. Childs Nerv Syst 2001;17(8):478-482.
81. Bering EA, Jr., Salibi B. Production of hydrocephalus by increased cephalic-venous pressure. AMA Arch Neurol Psychiatry 1959;81(6):693-698.
82. Hasan M, Srimal RC, Maitra SC. Bilateral jugular vein ligation-induced alterations in the ventricular ependyma: scanning electron microscopy. Int Surg 1980;65(6):533-540.
83. Altman J, Sudarshan K. Postnatal development of locomotion in the laboratory rat. Animal Behav. 1975;23:896-920.
84. Egawa T, Mishima K, Egashira N, Fukuzawa M, Abe K, Yae T, et al. Impairment of spatial memory in kaolin-induced hydrocephalic rats is associated with changes in the hippocampal cholinergic and noradrenergic contents. Behav Brain Res 2002;129(1-2):31-39.
85. Del Bigio MR, Crook CR, Buist R. Magnetic resonance imaging and behavioral analysis of immature rats with kaolin-induced hydrocephalus: pre- and postshunting observations. Exp Neurol 1997;148(1):256-264.
86. Wolfson BJ, McAllister JP, II, Lovely TJ, Wright LC, Miller DW, Salotto AG. Sonographic evaluation of experimental hydrocephalus in kittens. Am J Neuroradiol 1989;10(5):1065-1067.
87. Donauer E, Wussow W, Rascher K. Experimental hydrocephalus and hydrosyringomyelia. Computertomographic studies. Neurosurg Rev 1988;11(1):87-94.
88. Yamada H, Yokota A, Furuta A, Horie A. Reconstitution of shunted mantle in experimental hydrocephalus. J Neurosurg 1992;76(5):856-862.
89. Drake JM, Potts DG, Lemaire C. Magnetic resonance imaging of silastic-induced canine hydrocephalus. Surg Neurol 1989;31(1):28-40.
90. Braun KPJ, de Graaf RA, Vandertop WP, Gooskens RHJM, Tulleken KAF, Nicolay K. In vivo H-1 MR spectroscopic imaging and diffusion weighted MRI in experimental hydrocephalus. Mag. Res. Med. 1998;40(6):832-839.